AD_____

Award Number: W81XWH-11-C-0095

TITLE: Development of an Ocular and Craniofacial Trauma Treatment Training System

PRINCIPAL INVESTIGATOR: Mark P. Ottensmeyer, Ph.D.

CONTRACTING ORGANIZATION: Massachusetts General Hospital
Boston, MA 02114

REPORT DATE: August 2013

TYPE OF REPORT: Annual

PREPARED FOR: U.S. Army Medical Research and Materiel Command
Fort Detrick, Maryland 21702-5012

DISTRIBUTION STATEMENT: Approved for Public Release;
Distribution Unlimited

The views, opinions and/or findings contained in this report are those of the author(s) and should not be construed as an official Department of the Army position, policy or decision unless so designated by other documentation.

REPORT DOCUMENTATION PAGE

Form Approved
OMB No. 0704-0188

1. REPORT DATE	2. REPORT TYPE	3. DATES COVERED
August 2013	Annual	11 July 2012 – 10 July 2013

4. TITLE AND SUBTITLE
Development of an Ocular and Craniofacial Trauma Treatment Training System

5a. CONTRACT NUMBER
W81XWH-11-C-0095

5b. GRANT NUMBER
W81XWH-11-C-0095

5c. PROGRAM ELEMENT NUMBER

6. AUTHOR(S)
Mark P. Ottensmeyer, Ph.D.,
Bummo Ahn, Ph.D., Ryan S. Bardsley, Gianluca De Novi, Ph.D., Martina Festi, Stefano Iorino, John Cho Moore, Federico Pifferi, Rajesh J. Shah, Simone Zivieri

E-Mail: mottensmeyer@partners.org

5d. PROJECT NUMBER

5e. TASK NUMBER

5f. WORK UNIT NUMBER

7. PERFORMING ORGANIZATION NAME(S) AND ADDRESS(ES)

Massachusetts General Hospital
55 Fruit St., LND-209
Boston, MA 02114

8. PERFORMING ORGANIZATION REPORT NUMBER

9. SPONSORING / MONITORING AGENCY NAME(S) AND ADDRESS(ES)
U.S. Army Medical Research and Materiel Command
Fort Detrick, Maryland 21702-5012

10. SPONSOR/MONITOR'S ACRONYM(S)

11. SPONSOR/MONITOR'S REPORT NUMBER(S)

12. DISTRIBUTION / AVAILABILITY STATEMENT
Approved for Public Release; Distribution Unlimited

13. SUPPLEMENTARY NOTES

14. ABSTRACT
A novel simulator of ocular and facial trauma is being developed to support the training and skills maintenance of eye surgeons and first responders who are likely to face injuries to the face and eyes. It combines physical anatomical modules with instrument tracking sensors and a data acquisition, scoring and feedback system. During the second year of the program, the standalone version of the simulator reached a nearly complete state, with a new physical structure, upgraded surgical instrument interfaces, an augmented reality surgical microscope, and substantial improvements to the software architecture. The software includes revised content for teaching eyelid laceration repair, includes state machine structure for detecting surgical gestures and evaluating progress through the training scenario. The system was demoed again at the annual USUHS ocular trauma course, at which performance data from an additional cohort of participants was collected. A commercial mannequin-based simulator was acquired and modifications of software and hardware have begun to attach an eye/face trauma head to the mannequin for medic training. Posters and oral presentations about the system have been given in local and national conferences/workshops. Options for commercialization continue to be investigated.

15. SUBJECT TERMS
Medical modeling and simulation; ophthalmic surgical training; ocular trauma; facial trauma

16. SECURITY CLASSIFICATION OF:			17. LIMITATION OF ABSTRACT	18. NUMBER OF PAGES	19a. NAME OF RESPONSIBLE PERSON
a. REPORT	b. ABSTRACT	c. THIS PAGE			USAMRMC
U	U	U	UU	86	19b. TELEPHONE NUMBER *(include area code)*

Table of Contents

Page

Table of Contents 3
1. Introduction 5
2. Body 5
2.1. Project background: proof-of-principle simulator development 5
2.2. Quarterly Report Administrative Details 7
2.3. Research Accomplishments by Milestone 13
2.3.1. "Month 1" - Review of craniofacial trauma training needs with Subject Matter Experts (SMEs), creation of specifications, limitations, detailed analysis for trauma cases. 14
2.3.2. "Month 2" - 15
2.3.2.a. Review of treatment modes and potential error modes to be detected 15
2.3.2.b. Implement improvements for upgraded proof-of-concept stand-alone eye trauma simulator based on feedback from preliminary user testing by CIMIT project advisors. 15
2.3.3. "Month 4" - 15
2.3.3.a. Perform user evaluation at USUHS TriService Ophthalmology courses. 15
2.3.3.b. Locate and coordinate commercial partner to manufacture first version of the stand-alone eye trauma simulator. 16
2.3.4. "Month 6" - Revise design and fabricate improvements based upon USUHS Spring evaluation. 17
2.3.4.a. Stand-alone simulator structure finalization 17
2.3.4.b. Force sensing strain gages for scissors and needle holders, characterization of sensing 21
2.3.4.c. Polhemus sensor evaluation completion 27
2.3.5. "Month 7" – 28
2.3.5.a. Design of skeletal structure, docking points, sensor/actuator interfaces with ocular and craniofacial trauma modules. 28
2.3.5.b. Start developing augmented reality training guidance system for enhanced eye trauma simulator. 48
2.3.6. "Month 8" - Design of mandibular/maxillary trauma modules, upper airway model for use of airway devices, new cricothyroidotomy portal. 51
2.3.6.a. Cricothyroidotomy module cut sensing 51

2.3.6.b. Hemorrhage control sensing system 52
2.3.7. “Month 10” – 54
2.3.7.a. User testing of enhanced eye trauma simulator at USUHS or Madigan Army Medical Center. 54
2.3.7.b. Pass upgraded proof-of-concept simulator specifications onto commercial partner. 59
2.3.7.c. Continue working on augmented reality guidance system for enhanced eye trauma simulator. 59
2.3.8. “Month 11” - Completion of prototype stand-alone ocular and craniofacial trauma training module, control software supporting sensing and response functionality. 70
2.3.9. “Month 12” - Testing of fit, function of sensors, actuators, replaceable components. 70
2.3.10. “Month 14” - Design of modifications to trauma mannequin for integration of ocular and craniofacial simulator structure module. 74
2.3.11. “Month 16” - Revision of physiology model software. 77
2.3.12. “Month 18” – 79
2.3.12.a. Completion of prototype integrated ocular and craniofacial trauma system with mannequin. 79
2.3.12.b. Completion of augmented reality system supporting stand-alone simulator. 79
2.3.13. “Month 20” - User testing of combined system. 79
2.3.14. “Month 23” - Completion of revisions based on user testing. 79
2.3.15. “Month 24” - Final report submission. 79
3. Key Research Accomplishments 80
4. Reportable Outcomes 82
5. Conclusion 84

1. Introduction

This research program addresses an unmet need in the training for treatment of head trauma, focusing on ocular, peri-ocular and facial trauma. While improvements in armor systems have reduced injuries to the trunk and extremities, the face and head remain relatively vulnerable. Opportunities for medics to learn the treatment of facial and head trauma are limited due to the lack of realistic training simulators for this area of the body. For military ophthalmologists, critical trauma skills such as microsurgical suturing are no longer routinely taught in US residencies. Consequently, the burden of developing and maintaining these essential trauma skills is on the ophthalmologists themselves. We are addressing these dual needs by creating a new prototype training system to simulate injuries of the orbit and peri-orbital tissues, followed by the mandible, maxilla, and upper airway. The system will function as a procedural training system and will also be designed for integration into a mannequin-based trauma simulator for advanced, multiple trauma scenarios. It is being designed to incorporate performance measurement sensors and algorithms with physical mannequin components, conventional displays and augmented presentations of teaching content, and provide meaningful feedback to enhance learning. The research is being performed in three overlapping phases: improvement of an earlier proof-of-principle eye trauma system for preliminary user testing; substantial revision and expansion of the eye trauma system to form a full face/neck trauma system with additional eye trauma and face trauma components; and development and integration of a mannequin-compatible version of relevant components to enable more comprehensive trauma scenarios.

This program was originally conceived as a two year research and development effort; a no cost extension request was submitted to enable completion of the work which has been subject to various delays.

This report presents the accomplishments of the second year of the program.

2. Body

2.1. Project background: proof-of-principle simulator development

The origin of this research program is in proof-of-principle system developed in our laboratory in response to training needs expressed by our subject matter expert, Dr. Robert Mazzoli, now of the Vision Center of Excellence. In that earlier research, Dr. Paul Neumann and colleagues created a physical silicone head form with a replaceable left eye module, and coupled it to a pair of magnetic position tracking sensors attached with Velcro straps to the surgeon's index fingers. In performing lid laceration repair, the index figure motions were measured, with performance statistics previously employed in a laparoscopy trainer that we developed **Error! Reference source not found.**, including total exercise duration, instrument path length, an indication of motion smoothness, and a measure of amount of hand reorientation. The original project included demonstrations for the subject matter experts and others, but did not extend to the level of collecting expert and novice performance data to create a means for distinguishing the groups and determining when a novice reached some threshold of acceptable performance.

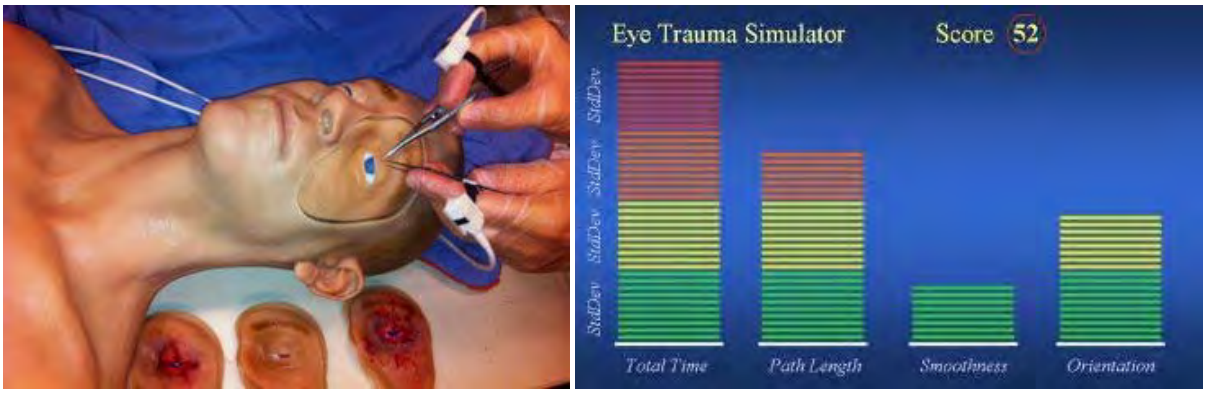

Figure 1. Proof-of-principle physical mannequin, motion tracking system, sample results plot, circa 2010.

While a strong beginning, numerous desirable changes were identified by Dr. Mazzoli and others. Anatomically, the eye lid consisted of only one layer of silicone; real lids have two major layers of differing biomechanical character and additional structures and landmarks important to correct surgical repair. A hollow eye globe was filled with a simulated vitreous humor substitute, however the cornea was opaque and the anterior chamber was a solid structure; for realism and to allow simulated injury of the globe, a transparent, thin cornea is necessary, together with an iris/pupil, which should indicate light response or pathology. The lid lacerations were manually created, with limitations on how repeatable the simulated injury could be generated; a training system with standardized, replicable scenarios would be more useful and reliable as a measurement/testing system. The tracking sensors were attached to the user's fingers, providing at best a poor approximation of the motions of the instrument tips; revision of this and the expansion of the instrument suite were requested. Lastly, while the laparoscopy simulator-based scoring system used has been shown to be able to distinguish expert from novice laparoscopic surgeons (on a suitable simulator), it is a post-performance score and cannot easily be used to make detailed recommendations for improvement – a more detailed evaluation and feedback system is desirable.

In addition to addressing these system improvements, the original vision was to create a larger suite of scenarios, to be supported by a series of replaceable eye trauma modules: globe laceration (scleral and/or corneal), more complex lid lacerations, and retrobulbar hemorrhage.

The current research also extends the simulator to create a system that supports training of first responders in management of eye trauma as well. As ocular injuries are typically addressed surgically only after life threatening conditions are managed, it is essential that first responders properly protect the injured eye prior to transport, avoid causing additional damage (typically by applying inappropriate pressure), and in the case of retrobulbar hemorrhage, quickly identify the condition and take appropriate steps to relieve pressure on the optic nerve to avoid permanent loss of vision. For this reason, developing capabilities to present eye injuries to medics and detect interventions was deemed to be important for ongoing development. Because eye trauma is often accompanied by face trauma, including additional facial trauma elements and airway management features were also considered,

together with integration of a revised/improved simulator with a full-body mannequin-based simulator for combined head/body trauma capabilities.

These needs lead to the current research effort, which seeks to address them in three overlapping phases:

- Revision and evaluation of the proof-of-principle eye trauma system, including user testing
- Expansion of the eye trauma system to include additional ocular elements, facial trauma components and upper airway management elements
- Integration of the procedural trainer components into a mannequin system

The second year progress towards these areas, described by the various milestones related to these phases, is detailed in the sections below.

2.2. Quarterly Report Administrative Details

As this report includes all required elements of the Q8 quarterly report, items 1 – 10 are included here. Items 11 and 12 (Scientific Progress, and Plans/Milestones statement) are reported in the remainder of the body (section 2.3 and its subsections) and the key research accomplishments (section 3) and reportable outcomes (section 4), corresponding with the Annual Report format.

1. Contract No. __ W81XWH-11-C-0095 _____
2. Report Date _8/10/2013_____
3. Reporting period from __4/11/2013_____ to ____7/10/2013_____
4. PI _Mark P. Ottensmeyer, Ph.D._____
5. Telephone No. _617-768-8783__
6. Institution__Massachusetts General Hospital_____
7. Project Title_Development of an Ocular and Craniofacial Trauma Treatment Training System__
8. Current staff, with percent effort of each on project:

Mark P. Ottensmeyer, Ph.D.	P.I.	89%
Steven L. Dawson, M.D.	co-I, SME	20%
Gianluca De Novi, Ph.D.	Computer Scientist, Post-Doc	100%
Gregory J. Loan	Clinical Engineer, Fabrication Lead	90%
Maria J. Troulis, D.D.S.	SME	10%[1]

1. Dr. Troulis will be continuing to serve as an SME during the period of the requested no-cost extension, with no further salary component requested.

9. Contract expenditures to date (as applicable):

	This Qtr	/	Cumulative
Personnel:	$92,131.66	/	$816,841.77
Fringe Benefits:	35,173.55	/	292,586.08
Travel:	5,253.32	/	22,410.73
Equipment:	0.00	/	139,858.50

Non-capital equipment:	11.98	/	27,702.70
Supplies:	3,227.08	/	66,350.28
Consultants:	0.00	/	15,346.40
Other:	10,946.47	/	36,430.90
Subtotal:	146,744.06	/	$1,449,307.84
Indirect Costs:	108,590.68	/	490,832.80
Fee:	0.00	/	0.00
Total:	255,334.74	/	$2,427,748.03

10. Comments on administrative and logistical matters.

A summary of all of the quarterly report logistics/administration sections is summarized here, and the new elements that were relevant to Q8 are described, with **bold** indicating the quarter.

From an overall perspective, as has been previously reported, personnel availability limitations have lead to lags behind the originally anticipated progress schedule. While performance is consistent with expenditure levels, completion of the program's planned deliverables will require an extension of the performance period of this effort. Pursuant to this, in Q7, a no-cost extension request was submitted (29 March 2013), to extend the period of performance by a total of 12 months, to July 10, 2014. This extension anticipates that the research and development components of the work will be completed early in 2013. Following this, we expect a reduction of effort level and salary expenditures for the remainder of the period, as remaining work is expected to focus mainly on publications, conference presentations, and potentially a third user trial/demo at the 2014 USUHS eye trauma course in May 2014.

At the close of Q8, the response to the NCE request remained pending.

Personnel updates:

Over the course of Year 2, we have seen turnover in some of our permanent staff, primarily due to outside opportunities, counteracted in part by the recruitment of new personnel, and we have benefited from the contributions of an ongoing series of graduate student interns.

In Q5, Mr Raj Shah, clinical engineer, who had been working part time between our group and the Volpe Center of the Department of Transport, took on full time status with the DOT. In the same quarter, Mr. Simone Zivieri, mechanical engineering intern, began work to learn design and fabrication techniques with application to developing the eye motion and blinking mechanisms for the system.

During Q6, Dr. Bummo Ahn, our post-doctoral research fellow in mechanical engineering, completed his training with us and returned to his home country to a position in industry. His work on the neck

mechanism and various sensing systems was picked up by Dr. Ottensmeyer. In the same quarter, Mr. John Moore took a permanent position as a director of product design for a commercial entity. Mr. Ryan Bardsley took on the anatomical modeling and fabrication duties of Mr. Moore. Ms. Martina Festi, master's student intern in computer science began her work with us, learning coding techniques in C# and C++ as applied to communications between our simulation system and the operation of the Laerdal SimMan Essential mannequin, assembly code to update the data acquisition system for the stand-alone simulator (developed by year 1 intern, Evgheni Munteanu), and basic statistical tools.

In Q7, we completed the hiring process for Mr. Gregory Loan, with experience in molding and model making, as well as interfacing and control of robotic systems using microcontrollers similar to the ones we are using. In addition, he has brought the concepts and some of the techniques of the Scrum/Agile software development methods to our overall project management toolset. Also in this period, our post-doc Dr. Gianluca De Novi was recommended for and received promotion to full time Assistant in Research/Instructor status. Intern Zivieri completed his work term with us successfully and returned to his studies to complete his degree requirements, graduating cum laude. Dr. Ottensmeyer and Mr. Bardsley obtained training in the use of laser cutting at a local service shop, to expand the range of fabrication capabilities within the group.

Q8 saw the departure of one of the group's longest serving members, Mr. Ryan Bardsley, who left to take a position with a pharmaceutical firm, who had been working with us part-time since the outset of the program. At the close of the quarter, we have not yet identified a replacement for him. A new mechanical engineering intern, Mr. Federico Pifferi, began his work term with us, focusing on development of the neck mechanisms, in support of his exposure to CAD, rapid prototyping and fabrication techniques, and developing control code for neck motion.

Review of significant non-personnel expenses during Year 2

Equipment/Supplies:

During Q6, we acquired a Laerdal SimMan Essential mannequin system (equipment), to which we will be attaching the mannequin-compatible version of the trauma head/neck. In addition, we extended the 1-year license to a perpetual license for the Materialise Mimics/3-Matic software tools for segmentation of CT anatomical scans and conversion of that data into computer aided design formats. The annual maintenance fee for the Objet Eden 260V 3D printing system was incurred, as was the fee for our Solidworks CAD software. In addition, after a year of good service, one of the print heads on the Objet system had to be replaced to ensure ongoing good quality parts fabrication.

During Q7, Dr. Ottensmeyer's main laptop computer failed permanently, requiring replacement, and the annual maintenance fee for the Stratasys FDM 3D printing system was incurred.

Consultants:

In Q8, we again turned to our consultant Mr. Daniel Langston, who has previously fabricated copies of our trauma modules, to create the modules that were used by trainees and staff at the 2013 USUHS Ocular Trauma course user testing exercise of our simulator.

Travel:

During Q5, Dr. Ottensmeyer, and now-former team members Mr. Bardsley and Mr. Shah attended the 2012 MHSRS/ATACCC meeting in Ft. Lauderdale, FL (13-16 August 2012), to present a research poster on the project, perform demonstrations to TATRC personnel and our SME Dr. Mazzoli and colleagues of his.

During Q6, Dr. Ottensmeyer, Dr. De Novi and Mr. Bardsley attended, gave an oral presentation and demonstrated the simulator system at the TATRC booth at the 2013 MMVR conference (20-23 February 2013).

In Q8, Dr. Ottensmeyer, Dr. De Novi and Mr. Loan traveled to USUHS to conduct the second user testing exercise at the 2013 Ocular Trauma course (20-23 May 2013), and Dr. Ottensmeyer traveled to TATRC to present a progress report before the JPC1 committee members (19 June 2013).

IRB/Human use protocol status:

During Q6, the Biosafety committee protocol covering the use of the human tissue acquired for our early work towards obtaining anatomical models from CT and MR scanning and molding methods was concluded. As we are using the high resolution CT imagery from our earlier neuroendovascular simulator project, we did not renew the biosafety protocol. In addition, in the context of developing additional research topics, we made contact with Dr. Mannudeep Kalra of MGH Imaging, who has a project to develop a virtual reality cadaver/anatomy visualization system. He has acquired high resolution data sets of over 100 deceased patients. We requested permission to examine these data sets, and were added to his protocol towards the end of the quarter. Other element of the effort have had higher priority than this examination, however we retain the opportunity to examine these data going forward.

In Q7, pursuant to a return to the USUHS ocular trauma course, we submitted the continuing review documentation to our IRB and submitted an amendment to cover the extended period, additional cohort of participants, change in the context of the human study (simulator session vs. independent event), and a request to collect additional demographic data regarding prior medical and simulator training. Our IRB issued its approval without request for any changes. We forwarded these documents to the ORP HRPO for their review, which also issued its approval for the ongoing work. The vendor agreement that was prepared between MGH and USUHS to permit bringing our simulator to the course was also completed during this quarter.

In Q8, following the second user trial, we submitted a minor amendment to our IRB to confirm that we may merge certain demographic details collected as part of the user testing, with the responses obtained from a user feedback survey that was developed to aid the Ocular Trauma course organizers in evaluating the use of simulators for future programs; responses to the survey could therefore be

stratified between responses from residents and those from ophthalmologists, rather than lumping all of those responses together. The HRPO expressed the opinion that they did not require review of minor amendments such as this one, however minor amendments will still be sent to TATRC regulatory personnel for their review and awareness. Also related to the USUHS user testing, Mr. Loan completed his CITI training to permit him to participate in human studies work, and an amendment was approved to add him to the study staff. Another minor amendment was approved by our IRB to permit statistical analysis to be performed by Dr. Paul Latkany at the Vision Center for Excellence and his colleagues, who have background in this area beyond the capabilities of the Simulation Group team. Lastly, with TATRC regulatory personnel, we confirmed that the use of the deidentified, anonymized CT data set being used to derive the anatomy for the revised version of the head/neck anatomy (to replace the original life-cast silicone head), is considered no-human-use.

SME and other expert interactions:

We have continued to maintain ongoing contact with our primary SMEs, Dr. Robert Mazzoli (Vision Center of Excellence), Dr. Maria Troulis (Massachusetts General Hospital), Dr. Suzanne Freitag (Massachusetts Eye and Ear Infirmary), and re-establish and cultivate new contacts to provide expertise, feedback and additional motivation for the work.

We have had in-person discussions with Dr. Mazzoli at events including the Military Vision Research Symposium (18-20 Sept 2012) and workshop on Developing a Roadmap for Simulation in Eye Care (17-19 Oct 2012), as well as having him review the status of the system at the 2013 USUHS Ocular Trauma course (20-23 May 2013) and maintaining periodic e-mail contact. We have approximately quarterly meetings with Dr. Freitag, including discussions to develop step-by-step outlines of surgical procedures and reviews of the simulator development and anatomical material behavior, including a visit **at the end of Q8** to aid in calibration of the force sensing systems of the surgical instruments. We continue to discuss plans for facial fracture scenarios with Dr. Troulis, and will increase our contact with her during the NCE period as we shift focus to the facial components of the simulator. Her current recommendation is to develop a bilateral mandibular fracture module, which would contribute to collapse of the oral cavity, leading to the requirement to perform a surgical airway.

Additional interactions over year 2 have included:

- Dr. Paul Latkany, Vision Center of Excellence, who has interests in developing an eye trauma registry, and also the statistical analysis of data related to training for eye surgery. At the USUHS Ocular Trauma course, we met with colleagues of his with statistical analysis backgrounds, who may be able to provide advice in development tools for validation of the gesture detection algorithms and of scoring methods for distinguishing experts from novice users of the simulator.
- COL Robert Hale, ISR, **in Q8,** as recommended by TATRC personnel following the JPC1 presentation in June 2013, to follow up on our early discussions regarding the training needs for facial trauma. In this conversation, it was reiterated that there is a strong need for a realistic simulation of facial trauma, including elements such as VR atlases of trauma and physical simulators that could enable the teaching of wiring techniques, and that physicians outside of

level 1 trauma centers need simulators as they have limited exposure to facial trauma otherwise.

- COL Patrick Storms, USAF, who was developing a training program for physicians in the reserves, scheduled for summer 2013 and inquired regarding whether our simulator could be used, however that event was scaled back due to funding limitations, so we did not participate
- CDR Chris Cornelissen, USN, at NAVMEDWEST, with whom we discussed his training programs involving cadaver use. While we could not coordinate a visit by him to view our system at the MMVR 2013 TATRC booth, we will attempt to reestablish that contact for a demo at MMVR2014, to be held near Los Angeles.
- Dr. Mannudeep Kalra, Radiology, MGH, who has established a research program to study high resolution CT image sets of cadavers, with over 100 subjects in his archives. We have discussed exploration of his data for potential guidance on developing the facial fracture and airway components, as well as development of a spin-off technology from the gesture recognition work in the form of a virtual autopsy table with a natural motion user interface. A proposal for a small grant was submitted to support this project, however in a large field of applicants, it was not selected for funding.
- Dr. Diane Wright and Dr. Timothy Toth, MGH Fertility center, who have expressed interest in the concept of a VR simulator, based on our augmented reality surgical microscope work, to teach their staff and those of other centers techniques for micromanipulation of egg and sperm cells, without need for tissue-based training and use of the expensive, real manipulator. In Q7, we visited their facility to observe the procedure, **and in Q8** followed up with a demonstration of our system and capabilities.
- Neil Schell, Director, Business Development, Polhemus, who we met at MMVR 2013, and who provided us with an evaluation loan of their sensor technology so that we could compare it with the existing Ascension hardware **in Q8**. We found their sensor cable flexibility to be superior, however the sensors themselves were very large compared with the smaller surgical instruments) and there appeared to be no price advantage. In the course of the testing, we did uncover that the Ascension sensors should not necessarily be used by people with pacemakers and similar life-saving devices; we have amended the IRB protocol for user studies to exclude people in this class.
- At MMVR2013, we met with Ken Gracey, president of Parallax, Inc., in reference to the MicroMedic program sponsored by TATRC. We acquired one of the kits, and expect to make use of the technology in the following year. Also at MMVR2013, we met with COL Lenhart and Mr. Magee to gage interest in a number of potential project ideas, including the AR autopsy table, and investigating whether physical therapy might benefit from the development of a training mannequin system.
- Dr. Pamela Andreatta, who Dr. Ottensmeyer met at the JPC1a in-progress review meeting on June 19, and her colleagues who had interest in the simulator for use in emergency medicine training. Conversations have been scheduled for 12 July 2013.
- Beth Pettit and Jack Norfleet of ARL, following on from inquiries at the JPC1a meeting regarding whether the system could be attached to other mannequin systems. This conversation also lead

to an invitation to ARL to participate in a Massachusetts General Hospital proposal in response to the USAMRMC solicitation for the Advanced Modular Mannequin project.

Funding Proposals:

During this year, we have been working to prepare two proposals related to this program, namely, a response to the solicitation for the Advance Modular Manikin program (W81XWH-13-R-0032), and a response to a call for proposals issued by CIMIT towards a combined program addressing the Joint Warfighter Medical Research Program. As the year ended, we had initiated discussions towards a sponsored research agreement to develop a modular ear anatomy simulator that will adopt a number of the features of the eye trauma sim.

For the AMM program, we are proposing to adapt the mannequin-compatible version of the eye trauma head/neck system for use as one of the peripheral units that would be compatible with and demonstrated as a part of a new modular manikin. The concept of adapting the head-neck component for use on additional mannequin systems was brought following the presentation given at the JPC1a In-Progress Review on 19 June 2013, at which point we confirmed that adaptation of the system to mannequins other than the Laerdal SimMan Essential, which we are using for our mannequin platform, was feasible.

For the JWMRP proposal, we are preparing a submission with three elements of work, namely creation of a surgical, mid-face fracture module, creation of an enucleation module, and adaptation of the head-neck system for compatibility with another modular mannequin system currently under development at the Massachusetts General Hospital Learning Laboratory. This latter mannequin system is aimed at a low-cost market, without many of the advanced features called for in the AMM solicitation, however the architecture under development would be compatible with the creation of physical, power and data adapters to allow attachment of our head.

The ear anatomy simulator is in response to inquiries from a local company developing a 3D scanning technology for ear canals. Our anatomical modeling work and data acquisition tools for the eye trauma sim are expected to form elements of a new system. The sponsored research agreement is expected to support development of a prototype that will be replicated by a third party vendor.

Further details on these proposals will be reported in future reports.

2.3. Research Accomplishments by Milestone

For each of the individual milestone tasks, a review of the work over the relevant periods of the program (previously described in quarterly reports 5 - 7 and monthly technical reports 6 - 9) is presented. Where new work has been performed, it follows the review and its significance relative to the earlier work is presented.

The “Month #” reference follows the language of the contract, although progress proceeds in parallel across multiple milestones and completion of the milestones varies from that calendar.

In the proposal, certain separate milestones were listed for completion in the same month, but were combined in the contract language. In this overview, such items are separated as parts a, b, etc. where relevant.

2.3.1. "Month 1" - Review of craniofacial trauma training needs with Subject Matter Experts (SMEs), creation of specifications, limitations, detailed analysis for trauma cases.

This milestone, relevant to the Phase I work, was completed in year 1. As the Phase II and Phase III work continues, ongoing feedback from SMEs and user testing will influence ongoing design decisions, as in milestones 2.3.7 (completed) and 2.3.13 (pending for year 3). As a whole, no changes have been made to the plans for the types of injuries to be simulated by the system. Corresponding with preliminary discussions that lead to the original project scope, the scope of injury scenarios that the system should address include:

For surgical scenarios:

- Full thickness lid lacerations
- Lid laceration with canalicular damage
- Intact globe with retrobulbar hemorrhage
- Globe laceration (scleral and corneal)
- Combinations of the above

For first responders:

- Protection of the eye using an eye shield and stabilization of penetrating objects
- Intact globe with retrobulbar hemorrhage
- Removal of non-penetrating foreign bodies
- Facial hemorrhage control
- Management of airway with severe damage to the lower face
- Surgical airway

Retrobulbar hemorrhage appears in both lists as this is a condition that requires recognition and urgent response whether in the field or at a medical facility, namely lateral canthotomy and cantholysis, is included both in surgical training and also in the SOF Medical Handbook.

While facial fractures should be included as part of the damage calling for hemorrhage control and management of complicated airway, surgical repair and/or stabilization of the bone fragments is outside of the scope of this simulation system program. Similarly, enucleation has been recommended as a valuable scenario. **In Q8, as was described earlier in this report**, a proposal for funding to create modules for both of these scenarios is in preparation, as part of a call-for-proposals issued by the CIMIT organization, towards programs supporting the Joint Warfighter Medical Research Program.

2.3.2. "Month 2" -

2.3.2.a. Review of treatment modes and potential error modes to be detected

This milestone, relevant to the Phase I work, was completed in Year 1. As the Phase II work continues, ongoing feedback from SMEs and user testing will influence ongoing design decisions. These are discussed further in relation to reporting on the results from the second USUHS Ocular Trauma Course user testing event.

2.3.2.b. Implement improvements for upgraded proof-of-concept stand-alone eye trauma simulator based on feedback from preliminary user testing by CIMIT project advisors.

This milestone, relevant to the Phase I work, was completed in Year 1. The improvements to the system have incorporated the feedback and lead to the system that was used at the first USUHS Ocular Trauma Course user trials, 22-24 May 2012. Improvements beyond these fall under revisions based on experience at USUHS and into the development of the Phase II system.

2.3.3. "Month 4" -

2.3.3.a. Perform user evaluation at USUHS TriService Ophthalmology courses.

The user evaluation element of this milestone was completed in Year 1.

The data collected during this event continues to be analyzed during Year 2. During Q5, we reviewed the USUHS results with our SME, Dr. Freitag, to identify features of user performance that would warrant feedback to the user. We also created a photographic record of the sutured modules that could be used to evaluate final performance, using expert review. This effort has served as inspiration for a more comprehensive set of photographs to be created from the second USUHS trial modules, including additional view angles, as recommended by Dr. Mazzoli. This is anticipated for Q9 or Q10.

A second round of user testing at the 2013 USUHS Ocular Trauma course is described below in section 2.3.7.

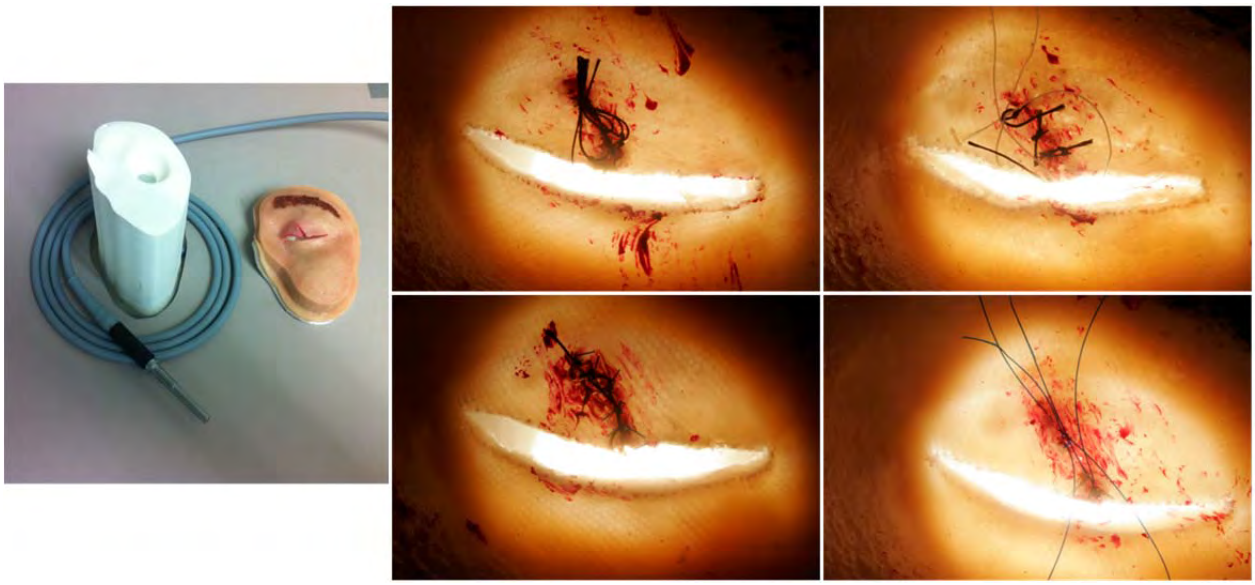

Figure 2: Alignment rig and light source for photographing sutured portals. Examples of different suture types, all addressing the same injury.

2.3.3.b. Locate and coordinate commercial partner to manufacture first version of the stand-alone eye trauma simulator.

Work to investigate commercialization is ongoing.

During Q6, we established a confidentiality agreement with Laeral and began to hold technical discussions regarding how our system can be combined with the SimMan Essential mannequin. The SimMan Essential was chosen as a platform for use in this project as it is representative of relatively high fidelity mannequin systems (i.e. computer controlled physiology, internal breathing, physiological systems) that would be able to support the electronic and fluidic systems of our system. The contact with Laerdal has also supported our work towards integrating our software systems with the Laerdal SDK used to communicate with and control the Laerdal mannequin.

In Q7, following introductions made by TATRC at MMVR 2013, we established a confidentiality agreement with Polhemus, a provider of magnetic position tracking sensors. This allowed us to evaluate the Polhemus sensor set as an alternative to the Ascension tracking system currently in use in the stand-alone system for measurement of instrument positions. Our findings were that the larger size of the Polhemus sensors and the higher cost did not justify switching to the new system. One desirable feature is the highly flexible cabling system that they use, which would help to avoid cable twisting/tangling that we observe in some users of the existing system.

In Q8, we held discussions with Ascension Technologies regarding modifications of their sensors systems to improve their sensors. Particular areas for enhancement include more flexible cables and integration of additional signal wires into the cable, supporting the strain gage and identification circuits we developed for the instruments. These are features that could be custom developed for a future,

commercial version of the system, however our immediate research and development needs do not justify the non-recurring engineering costs that would be involved in custom sensors at this time.

Also in Q8 we were approached by a local start-up company, Lantos Technologies, who are commercializing 3D scanning technology developed at MIT for use in ear canal measurement. They became aware of the quality of the head form developed for our simulator and inquired whether the technology could be adapted for use to train otolaryngologists on their device. We are drafting a new sponsored research agreement towards development of a commercial prototype that would be replicated to at least the level of dozens of units. This system would be a commercial application of the data acquisition and motion/gesture evaluation methods developed through this current program.

2.3.4. "Month 6" - Revise design and fabricate improvements based upon USUHS Spring evaluation.

This milestone is in progress. Based on lessons learned and reported in the Year 1 annual report, the design of the stand-alone system has undergone substantial improvement over Year 2.

This section will review the progress in the design of the simulator structure and the instruments. The anatomical elements of the head and eye trauma modules will be discussed in later sections.

2.3.4.a. Stand-alone simulator structure finalization

At the close of Q5, we presented a series of concept drawings that began to address limitations of the system used at the first user testing exercise.

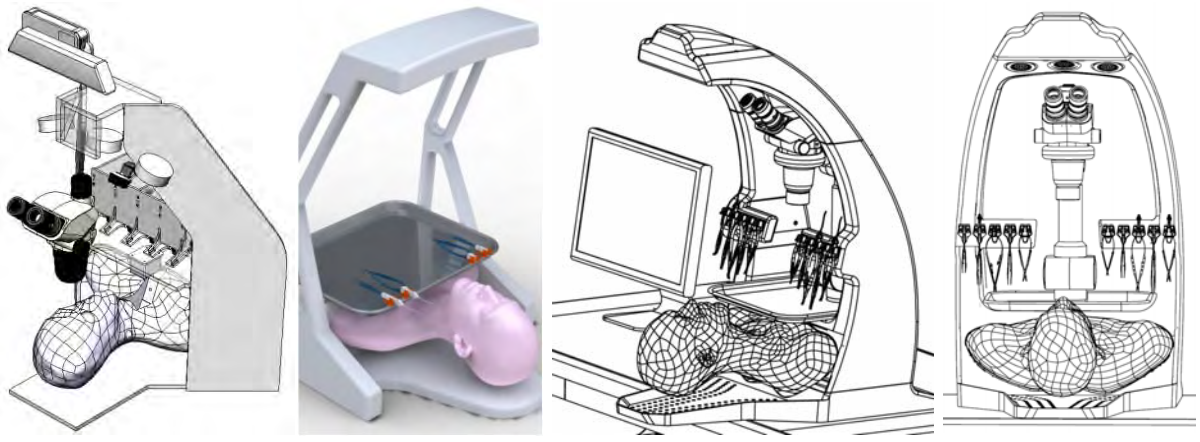

Figure 3: Design concepts for revised stand-alone system. Preliminary concept for blocking out system components; early revision for instrument tray and integrated overhead lighting system by Mr. Iorino; views of more advanced concepts including mobile arm to support microscope head, also Iorino.

Elements of these designs were adopted through further concept development that lead to a new instrument rack system shown at MMVR2013, and an entirely revised system that was used at the 2013 USUHS Ocular Trauma course. Evolution of the design concepts was reported in Q7 and is summarized below. These designs integrate new means for mounting the surgical instruments, optimize the

positioning of the magnetic and optical tracking systems, optimize the display field of the projector system, and notably support ease of assembly/packing/shipping.

Figure 4: Evolution of stand-alone simulator: modification of original proof-of-principle system integrating overhead display and lighting capability; addition of broadened suite of instruments, instrument rack and early augmented reality microscope; revision prior to MMVR 2013 including suture/instrument rack fabricated using laser-cut panel construction and the more robust, user friendly instrument connectors

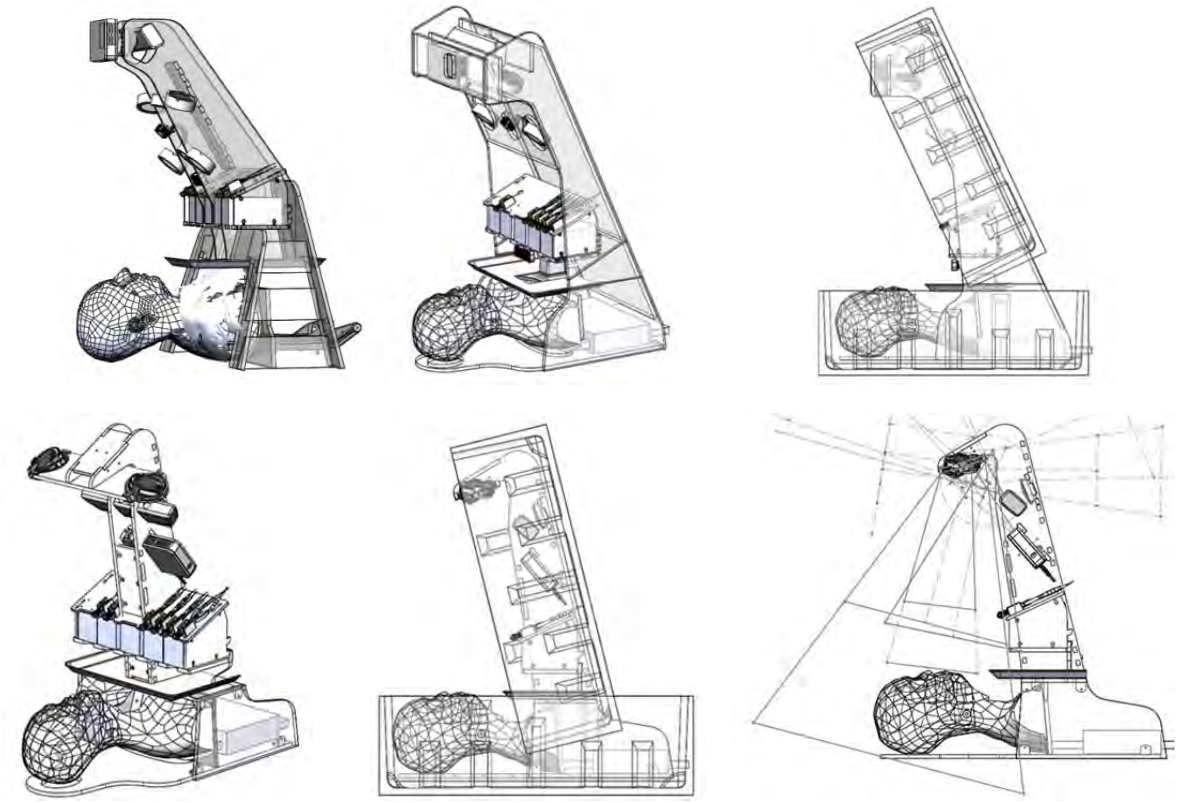

Figure 5: Evolution of design concepts for standalone system, as described in Q7 report

During Q8, the design shown in schematic form above was reduced to practice and fabricated in time for the 2013 USUHS Ocular Trauma course. With minor ongoing revisions, we expect that this represents the essentially final version of the structural frame and main component placement of the stand-alone simulator. The head-form and trauma modules will continue to be developed in tandem with development of the mannequin-mounted version, with the new head-form being a drop-in replacement for the version shown below.

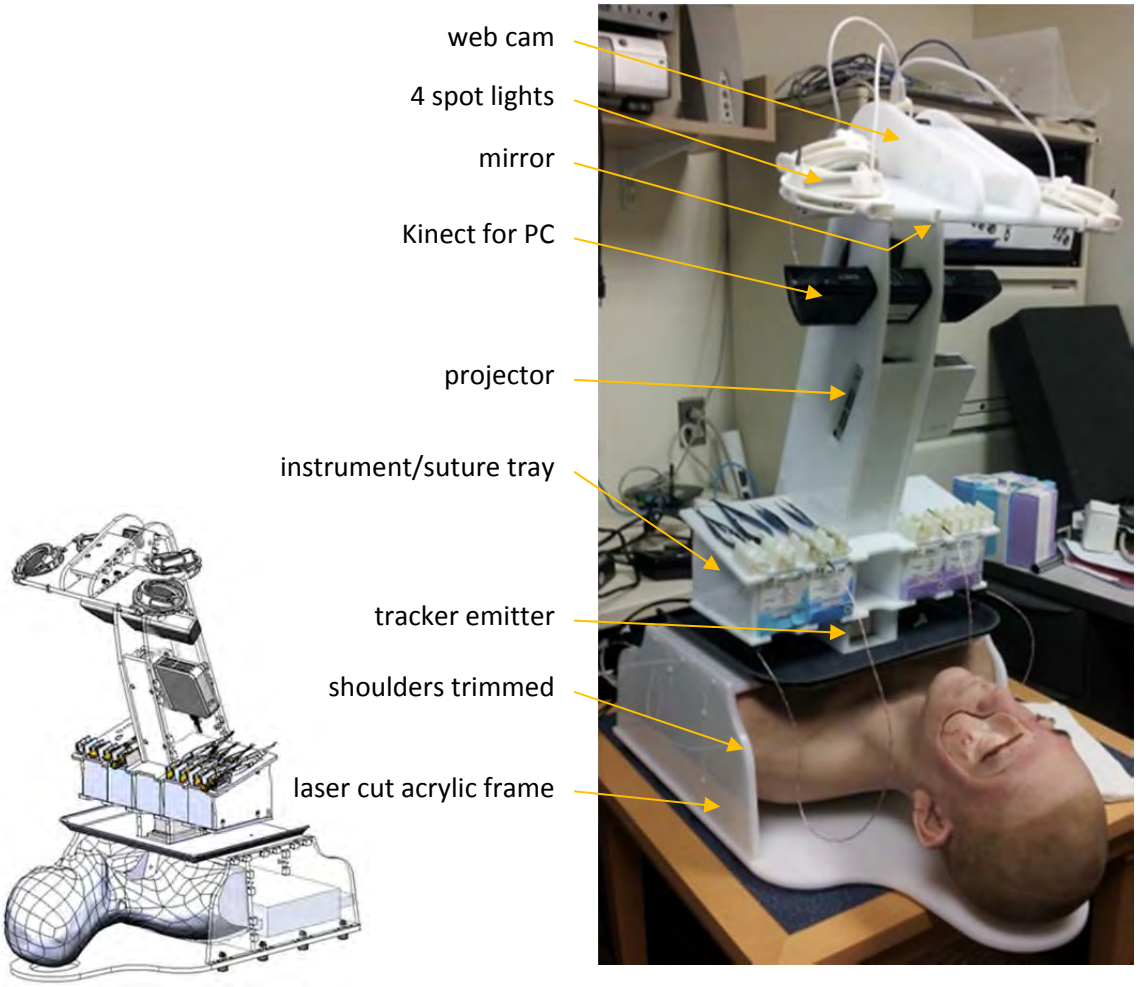

Figure 6: (Left Lower) Detailed design of USUHS2013 version of system, complete with all assembly/mating features, additional lights, optimal arrangement of imaging and projector components, revised instrument/suture holder rack, revised placement of magnetic field emitter. (Right) Fully assembled system ready for packing for transport to Ocular Trauma Course.

This iteration of the system implemented the following:

- Arrangement of optical component arrangements to optimize overlap between fields of view of projector, Kinect, web cam and lighting system
- Added additional light source to increase operating field brightness

- Added data acquisition interface control of lighting system brightness using the “Mind Board” developed in Year 1 for sampling surgical instrument force/grasp position signals
- Detailed design of panel components including interlocking t-slot joining features
- Finalization of mating features between base and upper stand for separation and shipping with minimal disassembly of subcomponents
- Trimmed the shoulders of the head form core and silicone skin covering to permit fit within structure, in turn designed to fit within standard Pelican cases
- Modified instrument holder seats
- Laser cut acrylic panels, learned to perform mirror/glass cutting, cut mirror to size
- 3D printed lighting fixtures, instrument holder seats
- Full assembly & testing of system for optical alignment

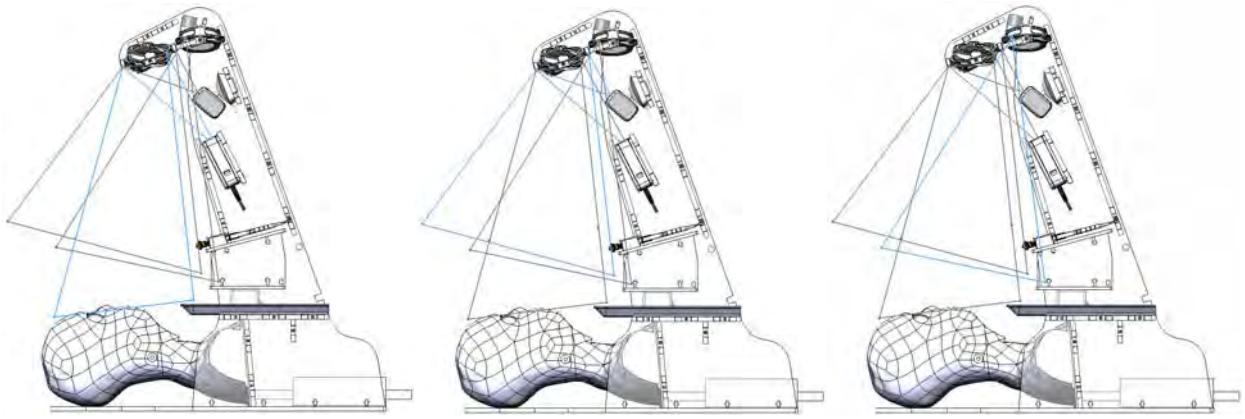

Figure 7: Fields of view of projection/imaging components. Highlighted in blue are: (left) video projection, (center) Kinect motion tracking, (right) web-cam. Use of a first-surface mirror mounted near the top of the system allows for reduced overall height; minimum focal distance for Kinect and projector would otherwise add 12” or more vertically.

Observations made and comments generated at the 2013 USUHS Ocular Trauma course and in a meeting with Dr. Frietag in **late Q8** were fewer than in Year 1, a promising change, signaling that the system is close to being fully acceptable by trainers for these procedures. Requests for future modifications, likely to be made outside the scope of this program include:

- Increase size of storage tray over mannequin chest
- Move suture boxes out of the “sterile field” of the simulator
- Lower the tool rack, which will be possible with the removal of the suture box storage space
- Possible inclusion of a “swing-out” tray for suture storage
- Modification of the use model, such that trainees would withdraw the desired set of sutures in advance, not interacting with the storage boxes during a scenario

Lastly for the standalone system, in reviewing the magnetic tracker documentation, we found a warning for pacemaker wearers and users of similar technology against use of the sensor technology without

consultation with their physician. To avoid potential risk to end users of the current system, we have altered the IRB protocol to exclude pacemaker users, and added warning labels supplied by Ascension to the exterior of the system.

2.3.4.b. Force sensing strain gages for scissors and needle holders, characterization of sensing

In the Q6 report, we described the need to add additional strain gages to the scissors and needle holder instruments, for use in better detecting contact and interaction with tissue and with needles. The previously installed gages only detected open/closing action, without the capacity to determine when and what type of object was in contact with the instrument. Cutting tissue presents a different force profile from cutting through suture. We presented finite element analysis plots showing optimal locations for gaging. Examples of curved scissors and needle holders are shown below.

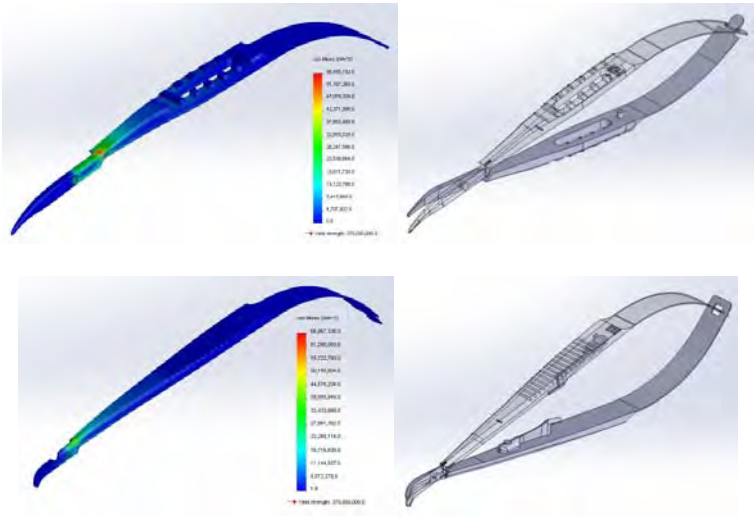

Figure 8: FEA of scissors and needle holders showing optimal placement for strain gages; instruments showing design positions of gages for force sensing and inactive gage for temperature compensation. Top to bottom: curved Westcott scissors and Castroviejo needle holder.

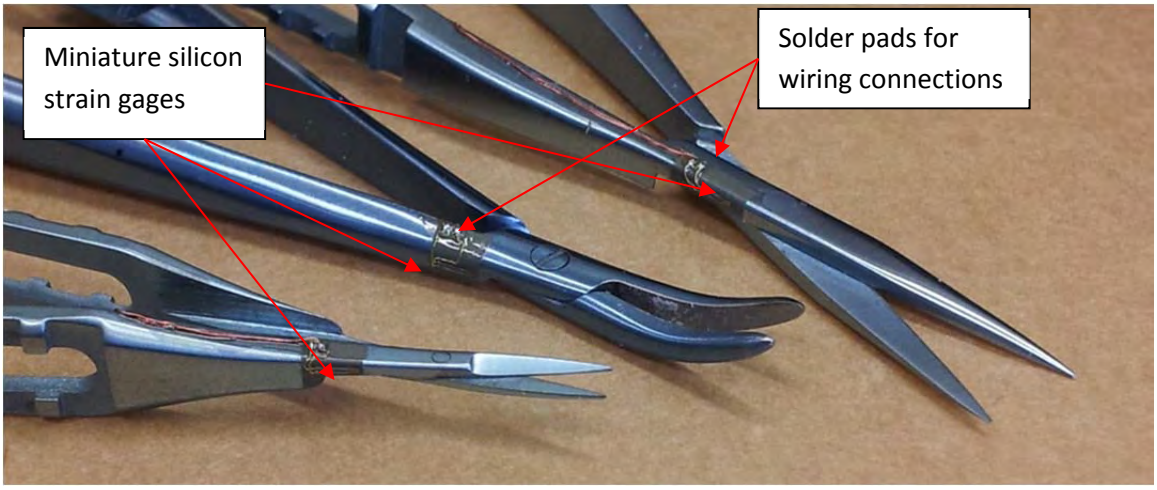

Figure 9: Detail of scissors and needle holder with silicon strain gages installed.

Described in the Q7 report, additional metal foil and silicone strain gages were added to the scissors and needle holder instruments to allow detection of relative stiffness of grasped/cut objects, for example to discriminate between grasping of tissue vs. grasping of a suture needle vs. closure on empty space. This distinction can be recognized by the event-based gesture recognition system, as the force-displacement response of the instrument changes.

In empty space, the position sensing gage registers the user squeezing the instrument closed, without an intial response from the force sensing gage, located close to the instrument tip. Once the tips come together, the force sensing gage begins to respond, and the two responses plotted against each other generate a curve that is related to the instrument's own spring stiffness. If an object is grasped, the position at which the force response begins occurs earlier than for the empty instrument, giving information about approximate size of the object grasped. This shifts the break-point in the force-displacement curve accordingly. The slope of the characteristic curve also changes, as the response is now a combination of the stiffness of the instrument and the object grasped.

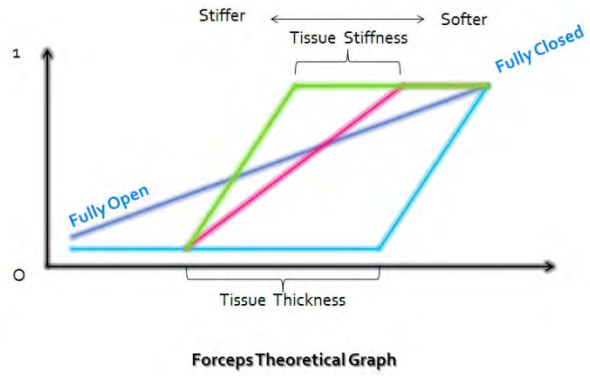

Figure 10: Schematic of force-displacement curves for use of grasping instruments in open space and grasping different stiffness tissues.

A simple jig was designed to repeatably close the forceps, shown below. In testing, strain gage outputs were collected for each full turn of the lead screw. For scissors and the needle holder, digital calipers were locked at a series of closure positions.

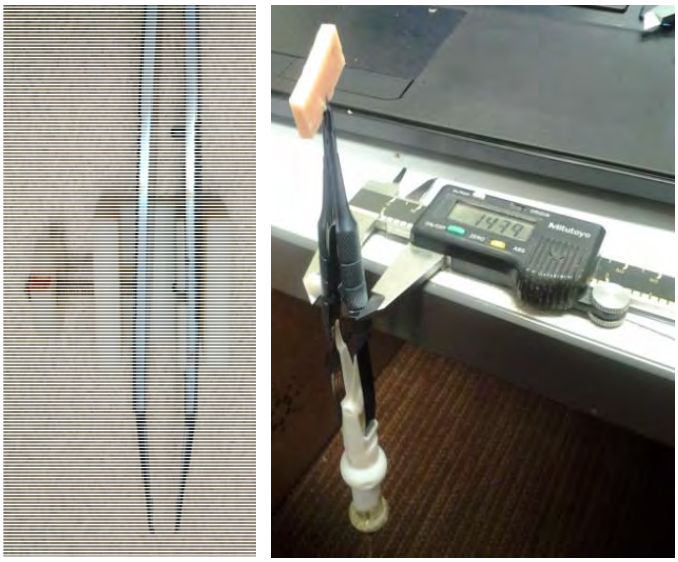

Figure 11: Forceps force-displacement test rig.

In the graphs below, taken using the forceps, the shifts in break point and overall slope are clearly shown.

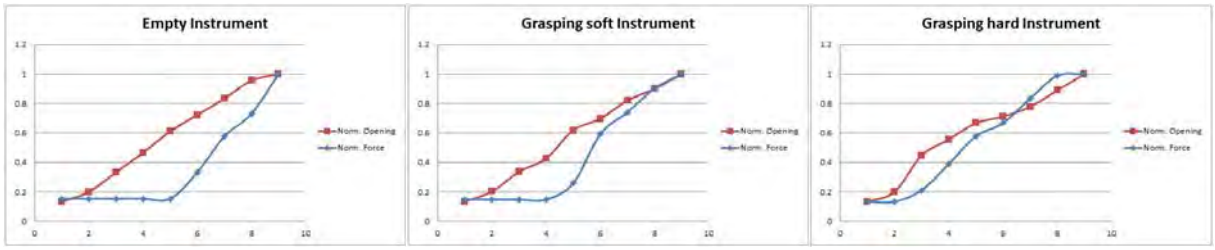

Figure 12:Normalized strain gage output vs. instrument closure: red curve – closure sensor, blue curve – grasp force sensor. (Left) Closing instrument, with tips coming together at 5mm displacement of lead screw, with force increasing as forceps are squeezed further. (Center) Grasping soft object, with initial deviation from baseline curve at 4mm displacement, difference in force slope with additional squeezing. (Right) Large, hard object, with contact detected at 2mm.

These same data sets were collected for each of the instruments planned for use at the USUHS test. Plots showing force strain gage output (normalized with respect to maximum output over all instruments) vs. normalized grasping displacement (using lead screw jig or digital calipers) are shown below.

Different instrument types also show different characteristic responses. The needle holders are of a locking variety, with a spring-loaded mechanism that holds the jaws closed after the user has squeezed the instrument far enough. This results in a momentary reversal of the force curve at the locking point. This locking action also appears in the pure closure position sensing response described in earlier reports. Similarly, the scissors show almost no output force in empty space until complete closure is achieved, while force increases during cutting, as the shearing forces generated by the scissors increase while cutting through an object. In the cutting case, as the scissors close the cutting point shifts away

from the scissor axis, increasing the bending moment on the scissors (force x distance increases), and the angle between the cutting edges becomes smaller, so a larger section of the material is being sheared. This results in the non-linear increase in the response observed.

Described below, these curves are being built into the gesture recognition architecture, however have not been thoroughly tested as of our design freeze point for the USUHS testing, so the earlier, position-based event detection algorithms will be used to ensure reliability.

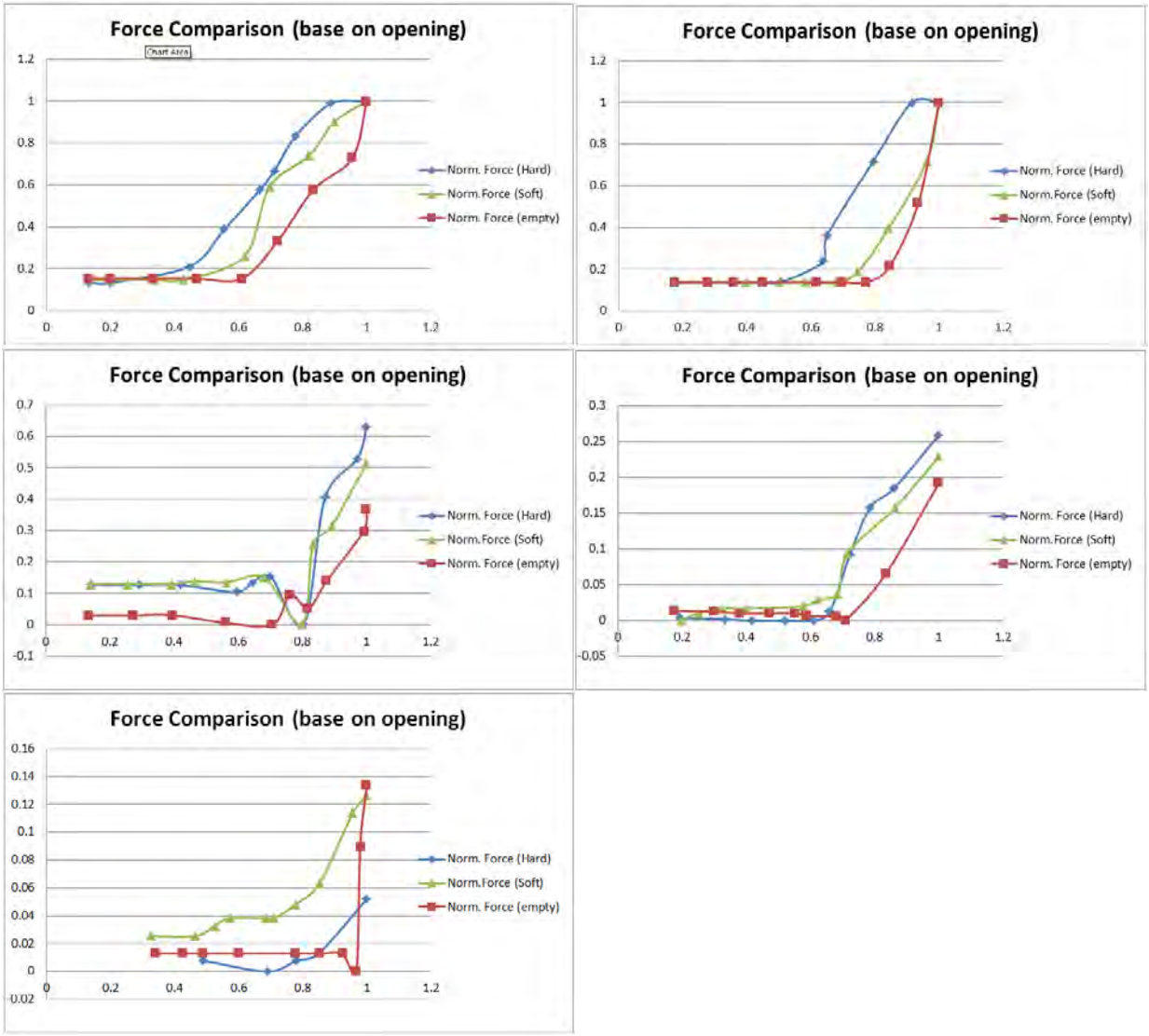

Figure 13: Strain gage response curves: (upper left) 0.5mm jaw grasping forceps; (upper right) 0.3mm jaw grasping forceps; (center left) large jaw needle holder; (center right) small jaw needle holder; (lower left) curved scissors.

Revision of instrument connector shells, stabilization of instrument/sensor orientation

In Q7 we began work to replace the earlier iteration of the housing that connects the Ascension sensor, the strain gage amplifiers and the instruments together. This version, used at the 2012 USUHS eye trauma course data collection exercise, was subject to accidental misalignment of the connector, which

prevented proper mating and distraction to the surgeon/trainee. The new design includes spiral "ramp" features to guarantee that during plug insertion, the instrument and plug rotate with respect to each other in the correct direction towards the correct connector alignment. In addition, spherical features allow for mating with the instrument holding rack in any orientation rotated around the instrument's axis.

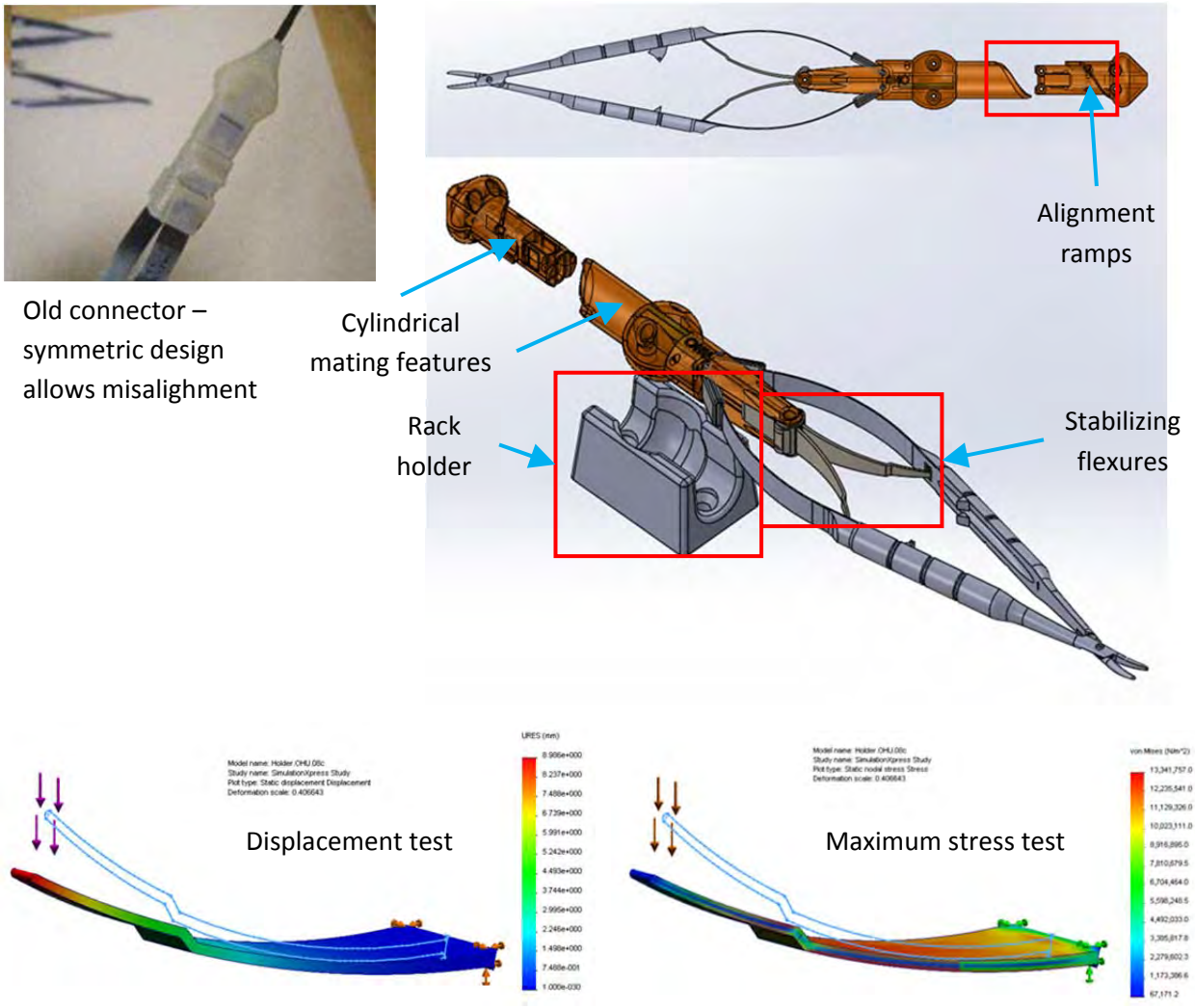

Figure 14: New design for instrument/sensor interconnect format with features to make insertion/removal intuitive and resistant to misalignment. For scissor/needle holder instruments, FEA of concepts for flexural beams for holding connector/sensor housing aligned with long axis of each instrument. Not necessary for forceps.

These housings were customized for all of the available instruments. For the scissors and needle holders, the pivoting action of the proximal ends allowed the housing to rotate away from the axis of the instrument, causing position sensing to miscalculate the tip location. To prevent this, stabilizing cantilever flexures were designed into the housings to hold the scissor/needle holder arms apart. Early versions were printed as part of the housing using the Polyjet process of our Objet rapid prototyping system. This material suffers from creep deformation when held under continuous load (e.g. needle holder locked closed); a solution was found in the form of combining parts from both of our RP systems

– the high resolution Polyjet parts for the rigid elements of the housing, with a flexible cantilever fabricated using our FDM system, which uses a different plastic that appears to be substantially less subject to creep.

Over the course of Q7, variations of the flexure were designed for use on both needle holders and the two large scissors used for the lid laceration scenario. Versions of the housing/flexure combinations for the corneo-scleral scissors are pending and will be complete by the time the globe surgery modules are complete.

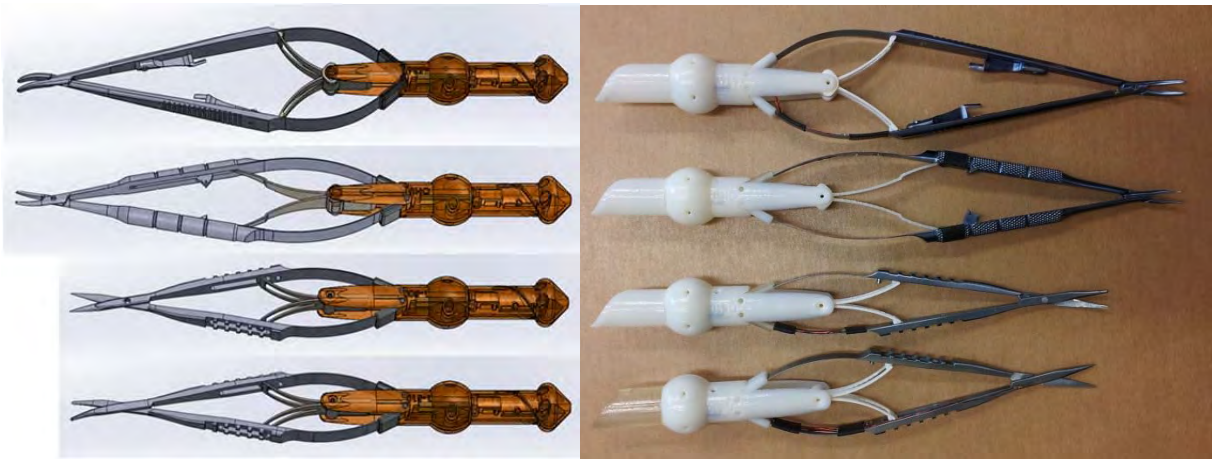

Figure 15: Design and completed versions of housings with stabilizing flexures on needle holder and scissor instruments.

In Q8, in advance of the USUHS testing, we tested the instruments through normal use and calibration to determine if there were any failure modes that could be identified and resolved before the testing. We found that the scissor flexure design is robust, as is that of the small-jaw needle holder. One of the flexures of the large jaw needle holder (upper instrument in figure above) split off at the base, so the cantilever design was revised to reduce strain generated at that point. Spares of all of the flexures were prepared in advance of user testing, in case of unexpected failures.

The attachment clips that mate the needle holders and scissors to the miniPCB housing/connector shells were modified for all of the instruments to improve alignment of the tool tip to the axis of the housing – when the jaws are closed, slight differences in the arm lengths of the instruments can cause the jaws to deviate to one side or the other of the housing axis. Adjusting the design of the attachment clips, attaching to slightly more or less of the end of the arms, allows correction of this deviation.

During testing of the large jaw needle holder, we found that grasping a needle at the throat of the jaws generates substantial strain in the arm where the silicon strain gages that we had ordered. This resulted in the failure of one of those gages. We identified normal strain gages small enough for mounting on the inside surfaces of the needle holder arms, near the pivot point and installed a replacement. We also

added these same small strain gages to the equivalent surfaces of the scissors to detect cut forces. Calibration is described above, and interfacing with the software is described below.

Following the USUHS trials, based on real-world use observations, we began to change gain values in the force sensor amplifier boards to match the range of sensitivity of the instruments to the force range actually used by physicians, which was much smaller than what we employed during our testing.

2.3.4.c. Polhemus sensor evaluation completion

The Q7 report described the fabrication and initial testing of alternate position/orientation tracking systems from Polhemus, which resulted from contact established with the company at the TATRC booth at MMVR earlier this year. **During Q8**, we completed testing of the sensors and returned the loaned system back to the vendor. We found the increased cable flexibility to be a desirable feature, vs. the Ascension Technologies system that we currently use, however the sensor size is too large for the ophthalmic instruments and we observed additional noise added to the strain gage sensor signals. We held discussions with Ascension and evaluated material samples in regards to the possibility of creating cabling with enhanced flexibility and with integrated conductors to support our force/grasp strain gages, however at this time we have not pursued desirable modifications as the expense of the engineering work is not justified for a relatively small improvement to our prototype. We will recommend reexamination of this feature in any commercialization discussions.

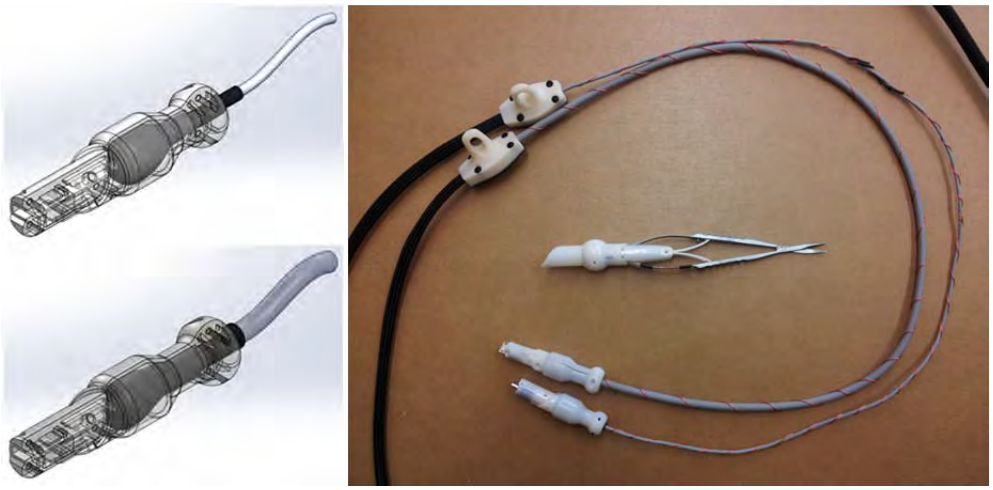

Figure 16: (left) designs for Polhemus sensor holders for teardrop sensor style, with standard and thin cable implementations. (right) Sensor cabling implemented for physical testing.

The Augmented Reality microscope design, described in detail in later sections, was modified to support use of Polhemus sensors, such that designs would be available should commercialization discussions result in a shift from the Ascension to the Polhemus sensor system.

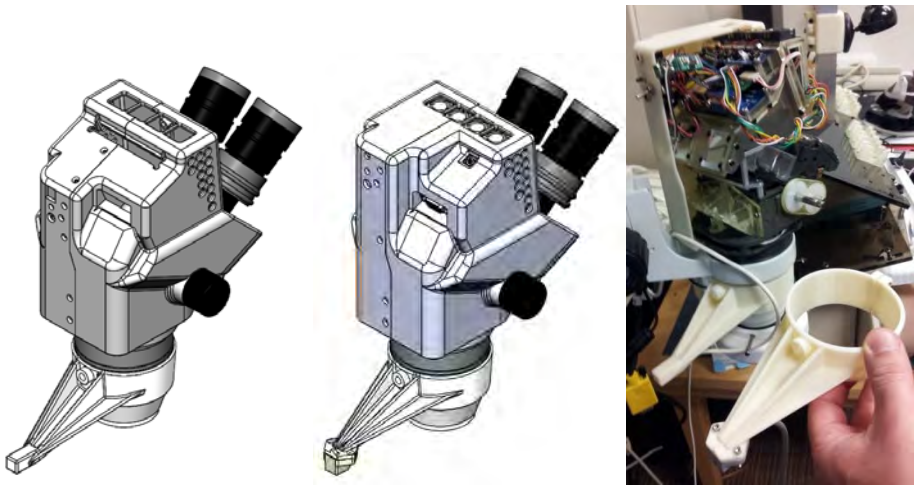

Figure 17:Designs for original Ascension sensor for microscope position tracking, design revision for Polhemus sensor and modified shell design

2.3.5. "Month 7" –

2.3.5.a. Design of skeletal structure, docking points, sensor/actuator interfaces with ocular and craniofacial trauma modules.

Eye motion mechanism

During Q5, building on earlier design concepts, masters student intern, Simone Zivieri designed and prototyped a mechanism that includes all of the globe motion features that will be included in the eye modules: eye pitch and yaw, proptosis, backdriveability in pitch and yaw (to allow the surgeon to manipulate the eye) and applied force sensing to detect pressure/load applied to the globe and the reduction of force on the eye expected on successful canthotomy/cantholysis.

The mechanism shown below is the first iteration which supports the mechanical m otions and compliance features analogous to normal eye motions, and relative sizes of the components in reference to our CT-derived skull model.

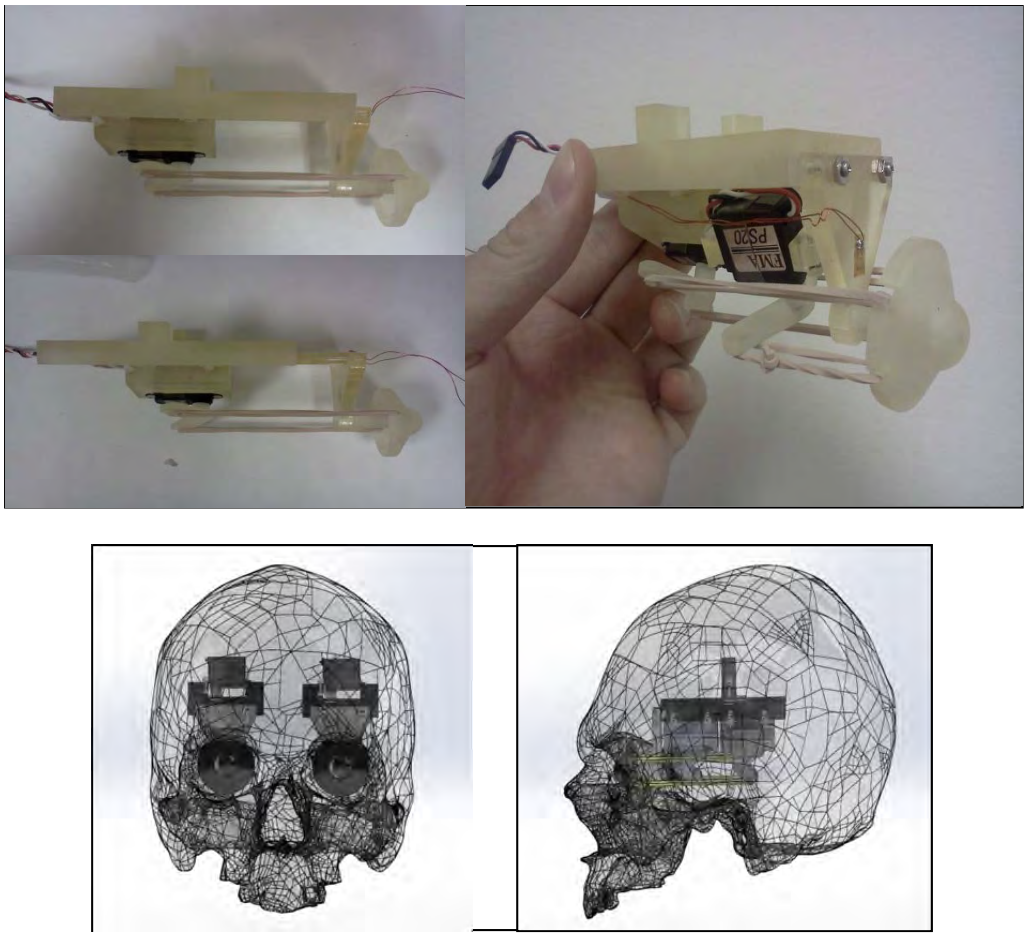

Figure 18: Eye motion module for pitch, yaw and proptosis, with backdriveability in globe motion. Sizing of components relative to skull model.

Eyeball baseplate redesign

To allow for attachment of our replaceable eye globe models and provide fluid and signal connectivity, we have included fluid channels that protrude into the space of the globe. These serve the dual purpose of providing mechanical connection through a tight friction fit. The fluid channels will connect the globe to a fake blood supply for simulation of bleeding and/or hemorrhagic chemosis – bleeding behind the conjunctiva creating a red zone around the cornea, one of the common signs of retrobulbar hemorrhage. They will further provide the fluid source for testing for suture watertightness and likely control of the pupil mechanism. Shown below are modifications, including reduction in thickness (to accommodate large angular motion without collision between fluid connections and the supporting post), the fluid channels with connection points front and back and corrections to the central spherical joint design from the earlier version. It also integrates a first test at a revision to the elastic member connection, replacing the latex rubber bands with neoprene o-ring material for improved reliability. This is expected to increase the lifetime of the mechanism (the neoprene is expected to have a longer lifespan than latex, which rapidly dries and fractures). The attachment mechanism is no longer subject to the possibility of the elastic member becoming dislodged, as set screws maintain the connections.

Figure 19: base plate modifications, rapid prototyped test versions of plate and globe showing plate and globe segment separately and assembled. Features include bosses for neoprene cords to replace latex rubber bands. Modified elastic transmission components: o-ring cord threaded through servo arm, initial baseplate attachment.

During Q6, examination of sections through the model of the skull was done to verify mechanism fit within the skull model, and maintain a reasonable thickness of skull structure external to the motion mechanism. The initial orthogonal arrangements of eye motion mechanisms would violate the outer section of the skull, so they were angled inwards and the servo/cord arrangements and contour of the globe base plates modified to retain the normal forward looking orientation of the globe.

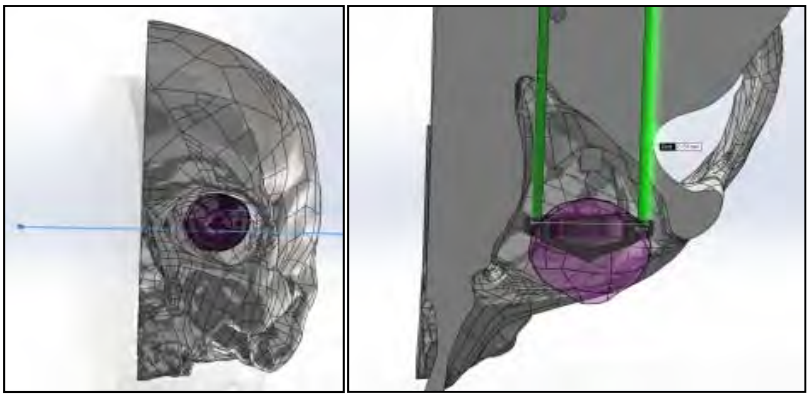

Figure 20: Sectioning of skull with prototype motion mechanism showing excursion of elastic cords from surface of skull in zygomatic/sphenoid region.

Proptosis mechanism

The proptosis mechanism designed early in Q5 reached a functional test model by the end of the quarter, demonstrating a range of motion of approximately 10mm, more than sufficient to generate the protrusion of the globe necessary to indicate retrobulbar hemorrhage. Shown below is proof of principle design, and the sliding carriage shown in the extended configuration.

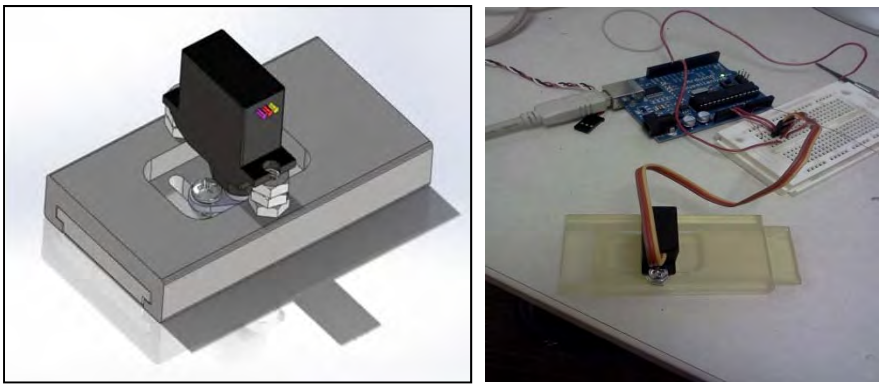

Figure 21: Proptosis mechanism (separate from pitch/yaw components)

The upper part of the mechanism, the components that drive proptosis, remains in a straight direction, in order to keep the translation of the eye the same as before. Changing from FMA PS20 servos to smaller Hitech HS-5035HD models allowed unification of multiple components of the servo support frame into one part. Flipping the orientation of one servo of each pair further reduces size of the mechanism and continues to prevent collision between the control arms. This change enables mechanism rotation of 15 degrees from the original position to align with the orbit axis and preserve the orbital wall thickness. A prototype of the compact version of the eye motion system was built, shown below. The system has been tested with positive results.

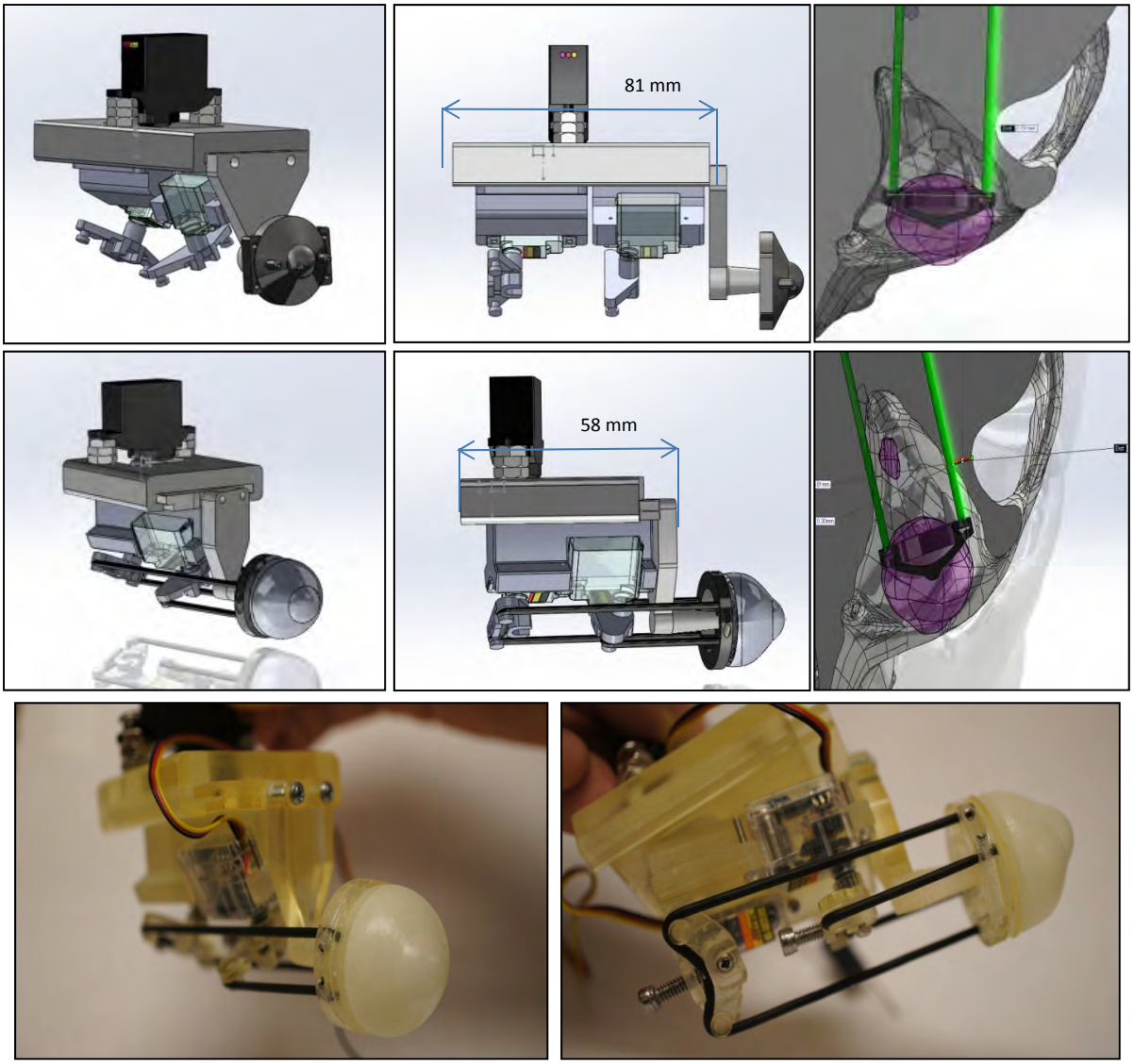

Figure 22: comparison of initial and modified orientations of eye motion mechanisms, preserving orbital wall thickness and reducing overall mechanism size. Assembled, compact motion module.

Blinking mechanism

In Q6, the final main actuated component of the eye motion system, the blinking mechanism was prototyped, so that the mannequin-mounted version of the system will provide a sense of presence and indication of level of consciousness, and help to provide indications of eye trauma; blinking would be prevented, for example, during a retrobulbar hemorrhage scenario, for example.

The eyelid is made of silicone soft layers (see also below for portal design), mounted to an orbital rim structure. A silicone protrusion of the eyelid, corresponding roughly with the levator and Muller's muscles, will pass through a gap created in the upper part of the orbital rim of the portal. This protrusion will link with a retraction mechanism, part of the eye motion assembly. Shown below is Q6 iteration of the design of the bony components of the system, with protrusion slots.

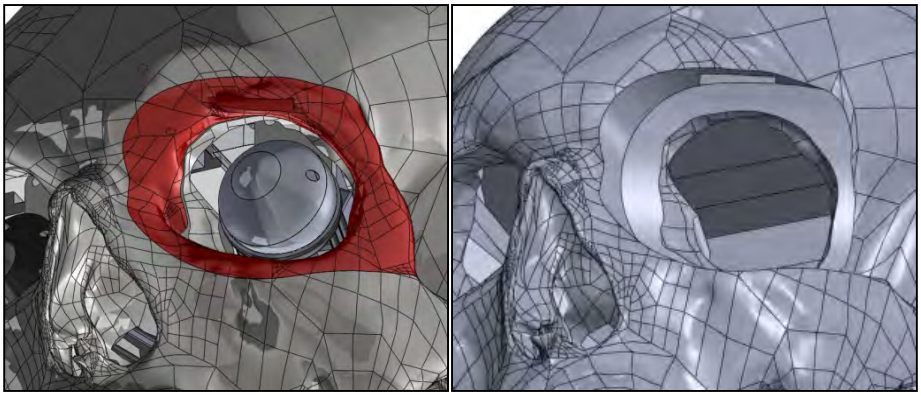

Figure 23: Orbital rim installed in skull, with slot for "levator muscle" protrusion of eye lid; orbital rim removed with slot for access to blinking mechanism behind forehead.

The blinking mechanism is a servo-actuated crank-slider, with an end-hook which will mate with the eye lid protrusion. A crank-slider linkage is necessary to orient the pulling direction of the eyelid and to avoid collision with the internal wall in the skull. The final hook shape will be determined as we develop the removable portal in more detail.

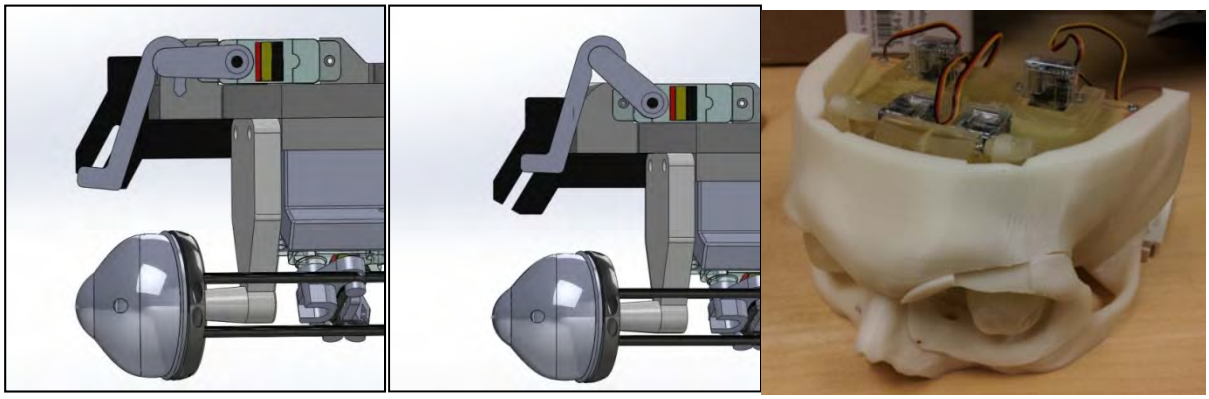

Figure 24: Blink motion eyelid retraction mechanism. Skull segment with motion mechanism for testing of assembly and fit. Also shown is partially seated bony orbital rim which will support the trauma portal soft tissue.

Replication for left and right sides

Also in Q6, the bilateral system was designed. A simple reflection of the mechanism across the sagittal plane results in collision between the servo control arms of the posterior servo. Instead, keeping the same servo mounting frame and rotating its placement prevents collisions and reduces part count. This can be seen in the detail of Figure 25.

The slide mechanisms for proptosis have been lengthened, their anterior ends modified to support the angled orientation of the mechanism, and the main frame that supports the assembly widened with mounting features for attachment to the skull. To further unify the design, the same, smaller servo used for eye motion is now used for the proptosis motion. This design decision simplifies the bill of materials, also reduces mechanism size and simplifies software control of the system.

Two additional servos are shown, which will be used for the blinking mechanism, described below.

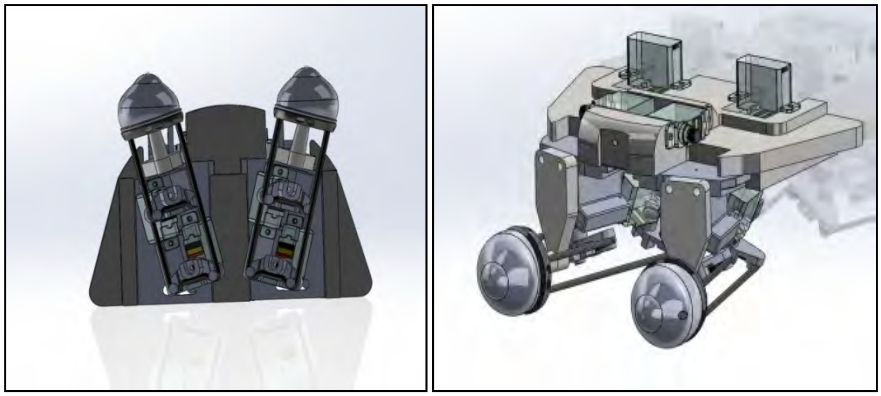

Figure 25: Bilateral eye motion mechanism with servo configuration maintained left/right vs. reflected..

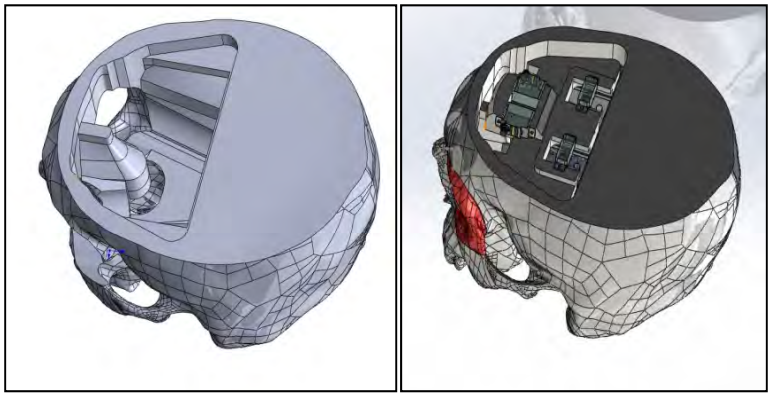

Figure 26: Partitioning of skull; skull component with motion cavity shown; assembled skull design with mechanism.

During Q7, some modifications were made following the work of our intern, Mr. Zivieri, mainly in terms of altering clearances to avoid binding of the proptosis motion, enclosing moving parts to protect them from damage and allow for later addition of lubricating grease, and simplifying fabrication by combining previously separate parts held together by screws, into monolithic components that take better advantage of the RP facilities available.

The new assembly was connected to our drive circuitry for testing and debugging of the code, mainly to ensure that all of the independent and linked motions behave correctly – blinking of both eyes occurs in the same direction (the servos are arranged opposite to each other, so inverse command signals must be sent to them for the output shafts to generate the same blinking motions).

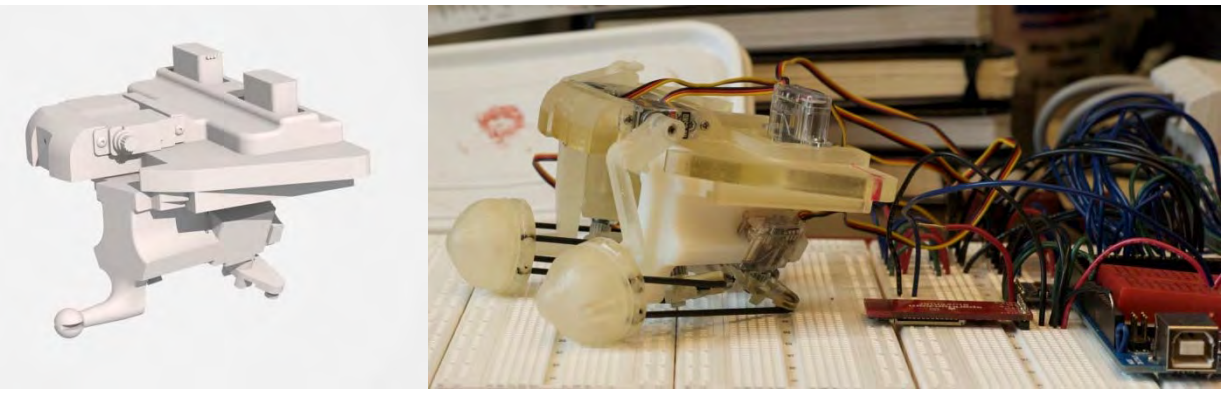

Eye motion kinematics

The eye mechanism can rotate in both the yaw (α) and pitch (β) directions, under the control of the two independent servos, with rotations θ_1 and θ_2. Because the elastic cables would physically interfere with rigid components of the system if the servos were oriented at 90 degrees to each other, the servos are rotated 50 degrees away from parallel, or +/- 25 degrees away from the vertical y-axis shown in Figure 27. In this configuration, rotation of the globe requires motions of both servos.

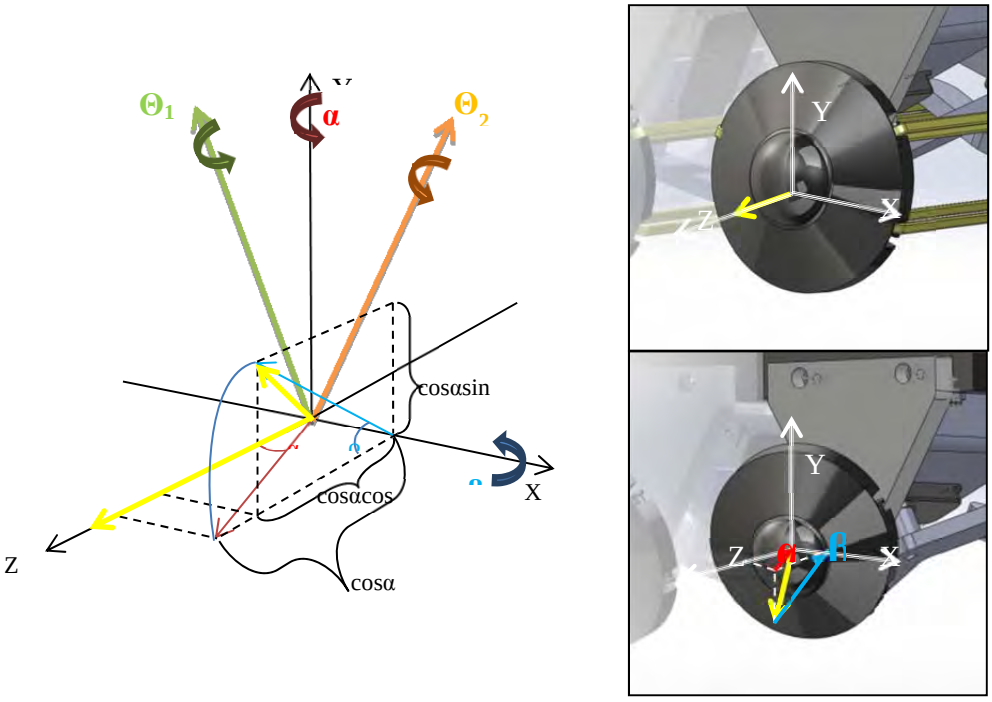

Figure 27: Eye motion polar coordinate system. Globe motion control is defined about the X and Y axes, while the servos rotate at offset axes, with motions θ_1 and θ_2.

To make the calculations more general, the servo offset angle is defined as γ (instead of using 25 degrees specifically) and the command positions sent to the servos for a given eye are determined by::

$$\theta_1 = \tan^{-1}\left[\frac{(\sin\alpha\cos\gamma + \cos\alpha\sin\beta\sin\gamma)}{\cos\alpha\cos\beta}\right]$$

and

$$\theta_2 = \tan^{-1}\left[\frac{(\sin\alpha\cos\gamma - \cos\alpha\sin\beta\sin\gamma)}{\cos\alpha\cos\beta}\right]$$

These equations have been implemented in the motion controller for testing the eye motion mechanism. A basic point-and-click interface was generated to control both eye orientation and proptosis position, as well as motion speed.

Motion controller test user interface

Using an Arduino 2009 microcontroller and a Processing graphical user interface, motion control of the mechanism was achieved. This formed the basis of a later, more comprehensive controller, described below. Examples of control entry and corresponding eye mechanism positions are shown.

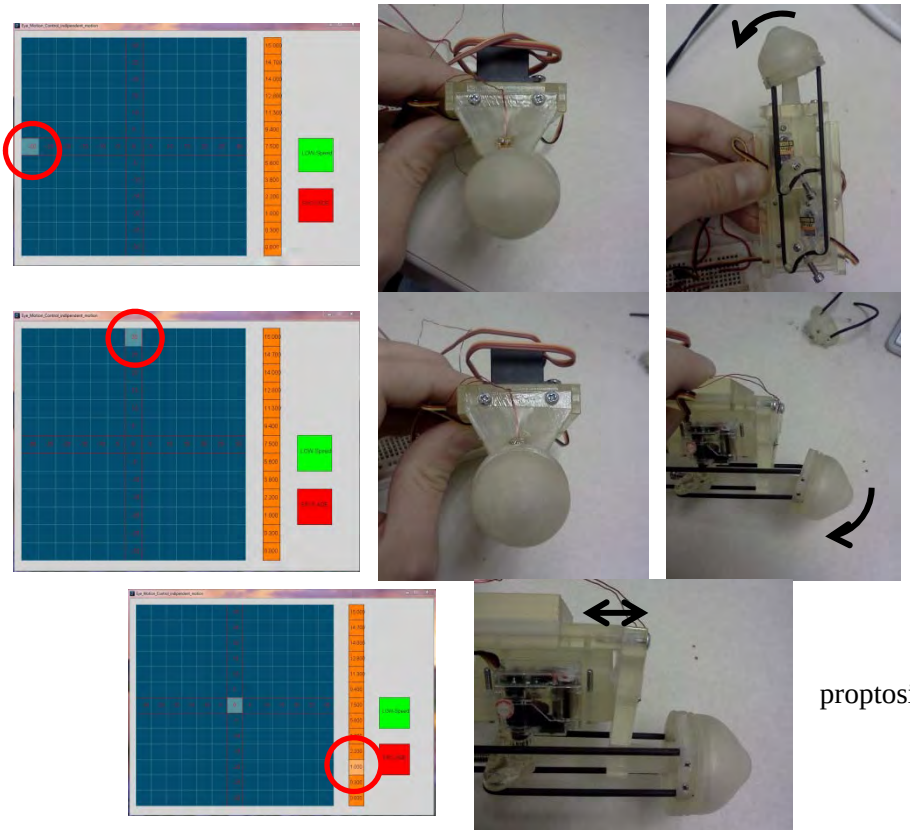

α=-30, β=0

α=0, β=+30

proptosis: +14mm

During Q7, we described a move from the Arduino 2009 platform for interfacing with the eye/head/neck control systems to the Arduino Mega 2560. The new board supports 40 more digital I/O lines and 10 additional analog input channels. Based on the restrictions of the central microprocessor and our needs for controlling multiple functions, we replaced a stock interface program available for the Arduino with one of our own, which optimizes the available I/O channels for our use. The board is now set up to run 8 different latching valves, 12 servos (primarily eye mechanism motion), I2C communications to the digital-to-analog modules for use with the electronic regulators we acquired earlier, one or two stepper

motors, two quadrature encoders, and unassigned I/O for 10 PWM or digital I/O lines (e.g. pump control, single acting valves), three serial communication ports, and all 16 analog input lines.

To test this system and provide control for the existing hardware elements, we prepared the GUI currently being used with the eye motion platform described above and the latching valves on the air muscle test bed developed in earlier quarters (see neck motion sections, below).

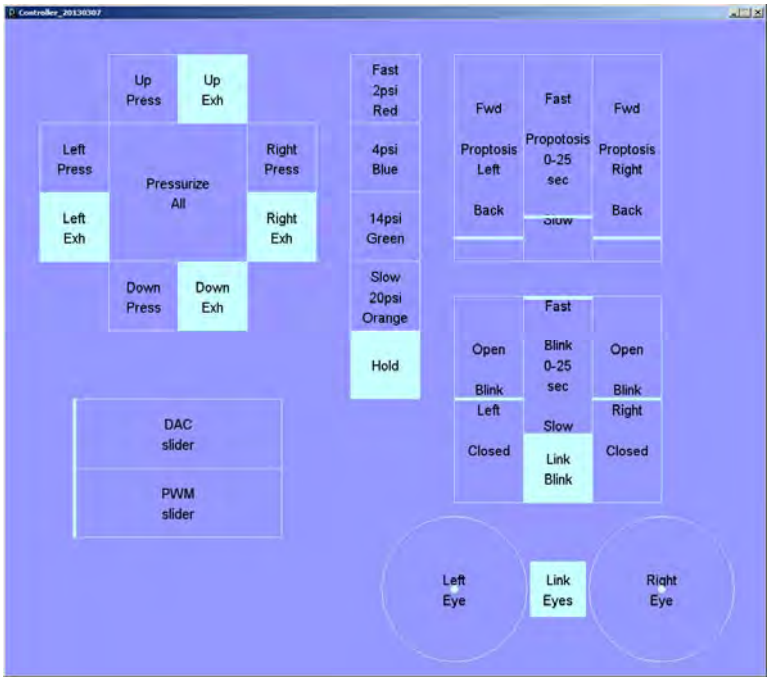

Figure 28:Comprehensive development graphical user interface, including pneumatic controls (upper left), proptosis position and speed for left and right eye (upper right), blinking servo position and speed and whether left/right eyes are linked (middle right), and independent or linked eye orientation control

The control circuitry was unified as well, shifting from an initial version with discrete transistors to a smaller number of ICs. A Bluetooth module was added to the circuit, which allows the Instructor Tablet computer associated with the mannequin to control the new components wirelessly. When connected to the mannequin's power supply, we have achieved a state where the new components require no external wired connections.

Testing of the valves in late Q7 showed that the 12V mannequin supply, when run through the earlier discrete transistor circuit or the new version, did not produce sufficiently high voltage at the valve inputs, which are also rated at 12V. Voltage drops across the transistors result in insufficient voltage at the valves, so we have observed that some of the valves are not reliably actuated. To solve this issue, we ordered, installed and tested a DC/DC converter, which boost the 12V supply from the mannequin to 15V output of the converter. This comes at the cost of a higher current draw from the mannequin, so we are limited to running two valves at a time at most (mannequin current limit is 1A). Since the valves would generally be activated one or two at a time during normal operation, this is not an issue – only during initialization of the system would numerous valves be activated in short order, but since the time

to pulse the valves to set their state is under 100ms, this does not present problems. Modifications to the custom interface code to support easy sequencing of multiple valves are in process.

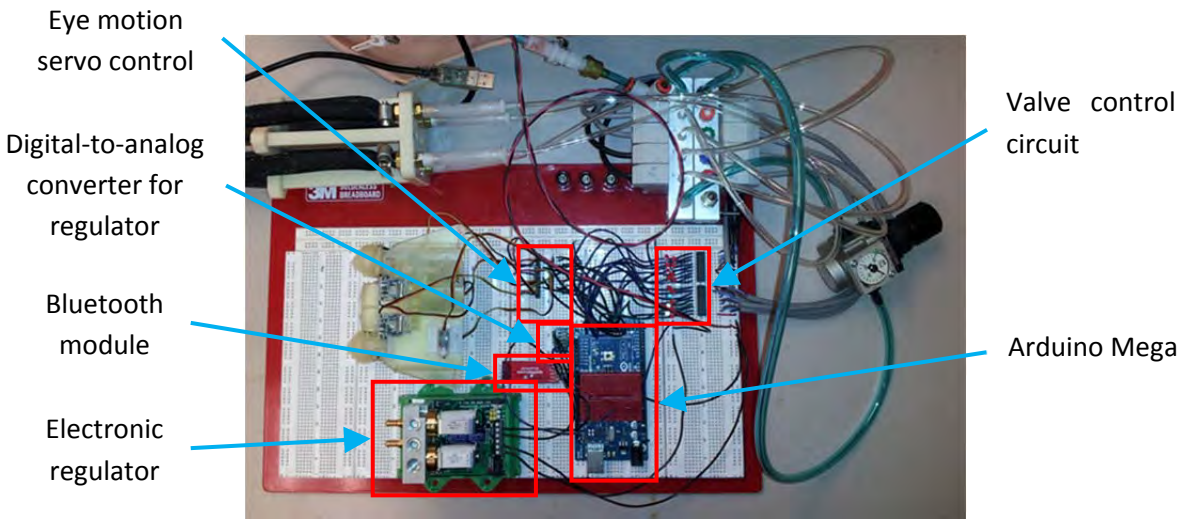

Figure 29: Protoboard for eye servo and neck pneumatic valve control

Eye globe design iteration

In Year 1, our earlier globe models provided the basis for the development of molding techniques and materials selection, including the use of the nylon mesh to enhance suture retention and rip-stop characteristics in the silicone. During Q5, we modified the globe design for compatibility with the mobile eye platform (the earlier versions were fixed in location) and to add the bulbar conjunctiva, which was previously not a feature. Taking advantage of the capabilities of the rapid prototyping system, we created a one-piece design to test fabrication, attachment and retention concepts for the new globe. One of the two fluid channels enters the globe and then exits into the space between the globe and the conjunctiva, providing a means for filling the space with fake blood to simulate hemorrhagic chemosis. Future steps were envisioned as developing a fabrication sequence for silicone molding of this structure, addition of muscle insertions into the globe and refinement of the geometry of the conjunctiva component.

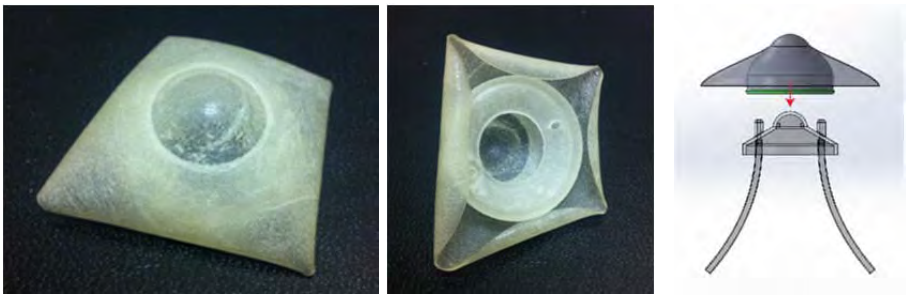

Figure 30: Front and back views of new globe concept showing conjunctival layer and fluid/retention ports. Concept of attachment to baseplate and fluid channels.

During Q6, this design evolved into a two part assembly: one for the eye lid and orbital rim, one for the globe. This approach will permit mixing and matching of different kinds of trauma modules, from simple lid laceration with no globe involvement, to lid avulsion and lacerated orbit. The globe component must be compatible with the symptoms of retrobulbar hemorrhage, one of which is hemorrhagic chemosis – bleeding underneath the bulbar conjunctiva layer. Shown below is the bony orbital rim described above overlying a multi-layer flexible conjunctiva structure. The blue layer is part of the globe module, bonded to the globe at the margin of the cornea, extending to the seat in which the orbital rim is mounted. This would be semi-transparent, so simulated blood would be visible. The red layer is mounted to the skull and seals the fluid space between red and blue apart from the mechanical and electrical spaces within the skull. The tubes and ports that connect to the globe (described in previous reports) provide an inlet for simulated blood to enter this space. Removal of the eye lid and globe portals will provide access to the fluid space for ease of cleaning and inspection.

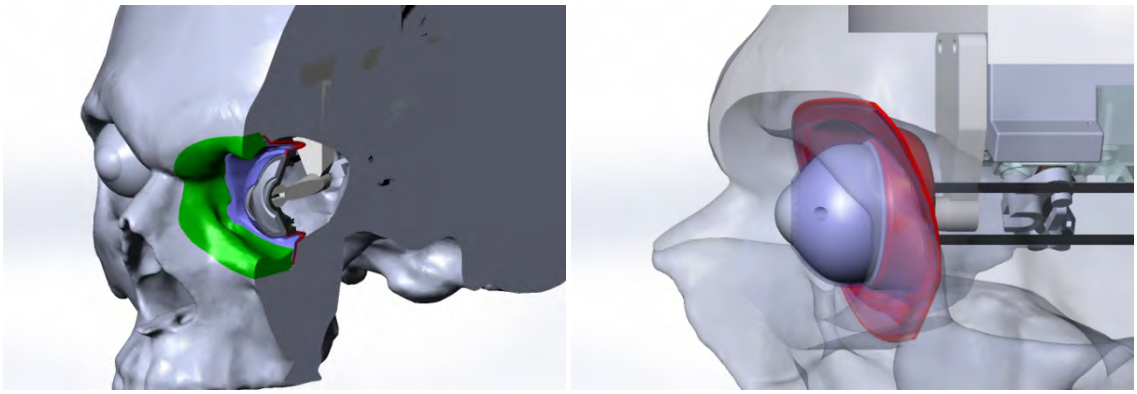

Figure 31: Concepts for flexible conjunctiva layers and sealing surface to protect mechanisms from fluid contact.

During Q8 we experimented with a technique for producing a conjunctival layer. The layer will consist of a hollow sphere of 0030 durometer silicone with a wall thickness no greater than .02”. The current methods for creating this part are 1) a dipping process around a hollow meltable core and 2) a glove mold. The benefits of the dipping process are speed and simplicity—the drawback being poor control over thickness. The advantage of the glove mold is that wall thickness and overall shape can be controlled to a very precise degree, but the castings must be produced at high pressure to ensure that the mold is filled without any air pockets. The extreme thinness of the part will result in many casting failures. The conjunctiva will be attached to the edge of the cornea with silicone glue and will also be attached to the inside of the eyelid with silicone glue. The opening of the eyelid will serve as a guide for the cut line of the conjunctiva.

Eyelid anatomy development

During Q5, we began to add silastic tubing into the margin of the eyelid model to provide the anatomy for performing canalicular repair, for more advanced eye lid laceration scenarios that the initial full-thickness marginal laceration. Dr. Mazzoli provided advice and detail on the relative sizes of the canaliculi and the punctum, the small opening that drains tears from the eye. We have acquired larger tubing than the initial 0.5mm ID version and are developing methods for properly retaining it in the molds.

In addition, we began to CT-derived skin surface models to generate new eye lid structures, vs. our earlier Phase I system that used the life-cast original. Shown below are surfaced CT data, CAD models of elements of the mold, partially molded lid structures, with the first mold lid removed prior to installation of the second lid with the cavity for the tarsal plate, and the front and back views of the new lid structures.

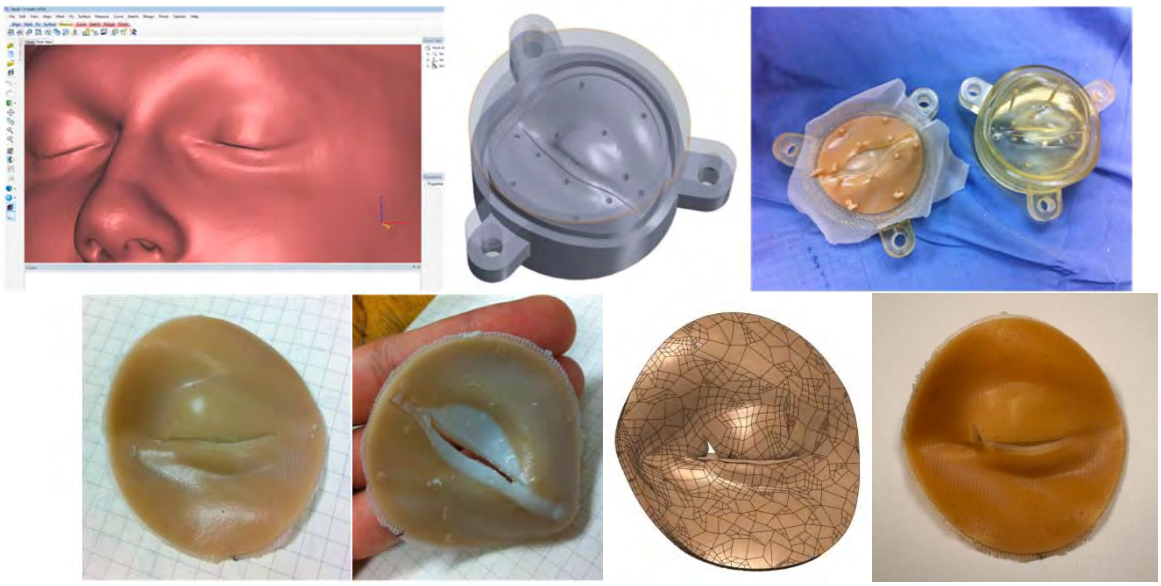

Figure 32: Eyelid based on CT-derived data: (top row) Mimics software view of anatomy, CAD model of mold, partially completed eye lid, prior to over-molding of tarsal plate. (bottom row) Front and back views of overmolded portal structure, CAD model with laceration, physical test model with defined laceration molded-in.

During Q6, we reported on the direct design of a laceration into the 3D printed molds, so that variation in the trauma modules due to artistic variation would not occur. Using the components that were produced at that time, we performed tests to determine how to create molded eye lids with multiple layers that would be compatible with the blinking mechanism described above.

The initial part of the test was to create incisions in the lids and attach threads to examine the likely motion during retraction. These tests suggest that an approach to the soft tissue components is to incise the skin layer, seat the molded soft tissue into a second mold with the lid in a hyper extended position and mold in additional silicone to create the redundant tissue that Dr. Mazzoli described for us in earlier conversations. This redundant tissue rolls over during the eye lid opening process, creating the fold of the eye lid. Using the 3D models extracted from the CT scans using Mimics and 3-matic an inner layer is designed that extends through a cutout above the upper eyelid and an extruded feature extending upward from the tarsal plate. Design of the hook-mate to the mechanism described above remains pending. Initial testing of a modified module demonstrating blinking under servo control is described in section 2.3.9.

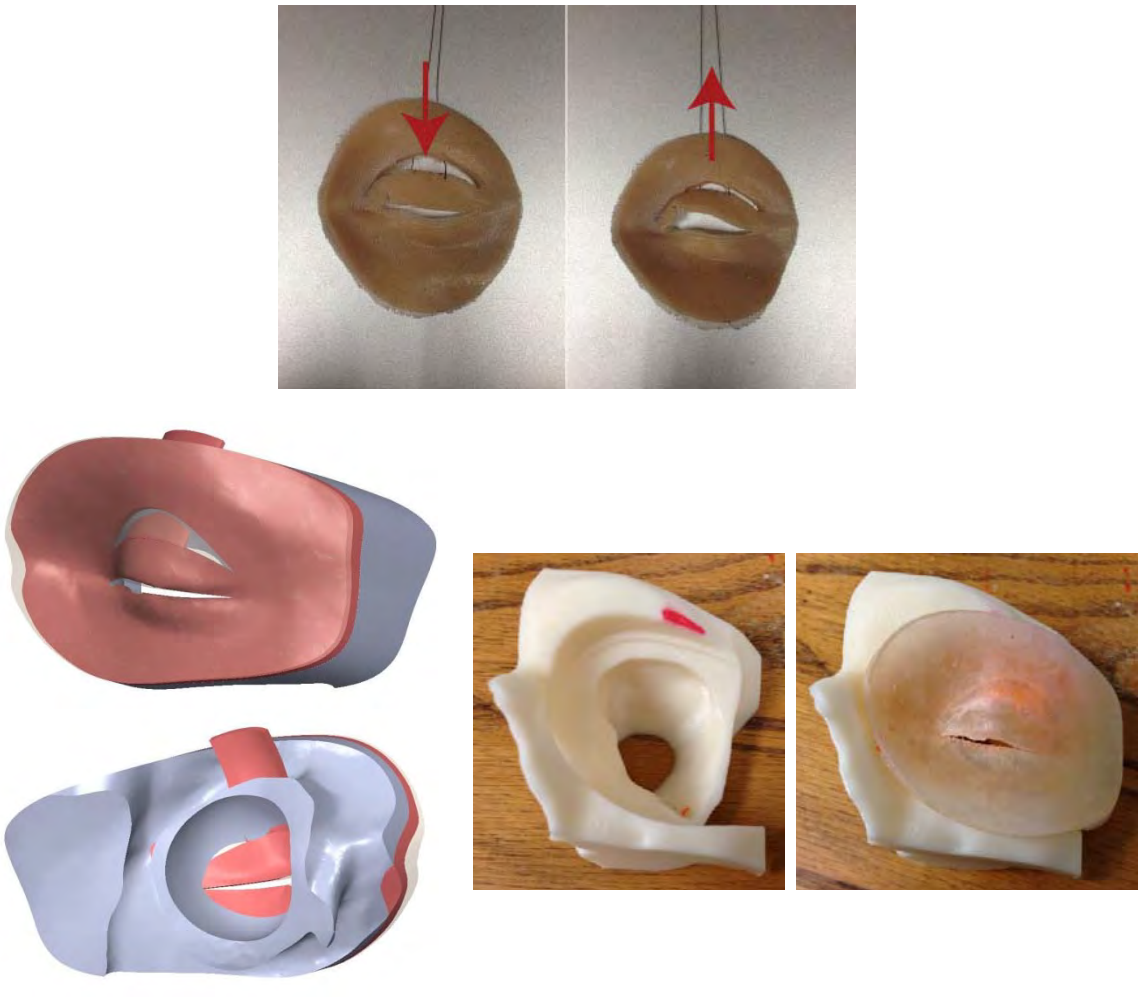

Figure 33: Blinking soft tissue test object; design for eye lid with levator muscle structure; test version installed in skull section, with orbital rim and assembled soft tissue layers.

During Q7, work on moving the lacrimal duct structures forward, necessary to complete development of an eye module for lacerated lid with canalicular repair, the second major eye trauma portal for this project.

The lacrimal assembly consists of the canalicular ducts and the nasolacrimal sac/duct. With the ducts running through the margin of the upper and lower eyelids, the portal mold now includes alignment slots for the canalicular/tarsal assembly. The ducts consist of silastic tubing of an appropriate diameter, bonded and sealed with silicone glue. The assembly is then attached to the tarsal plate using nylon string. The whole assembly is then plugged into the revised mold using the new alignment slots. Sprues, which are a by-product of the molding process and are normally discarded, are preserved to serve as alignments pegs. The mold revision ensures proper placement of the assembly in the mold prior to injection. The entire assembly is then encapsulated by silicone during the casting of the portal, resulting in a lifelike, multilayered object.

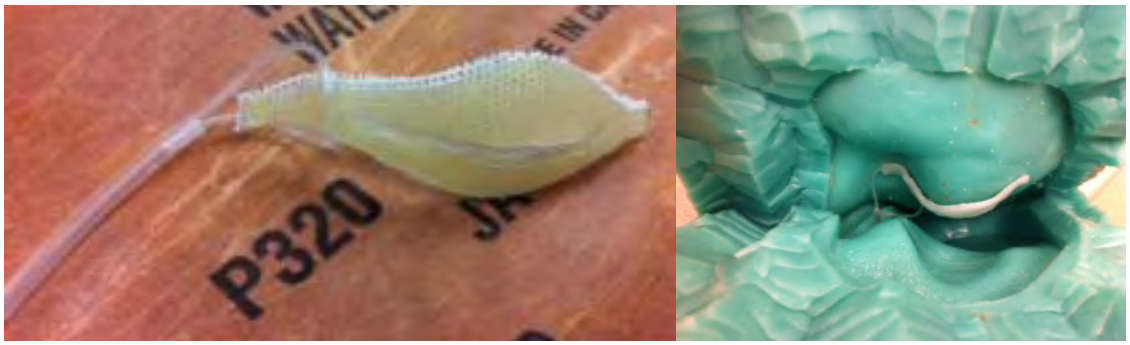

Figure 34:(Left) eye tarsal plate, with attached lacrimal, nasolacrimal duct tubing, reinforcing mesh (as per previous versions of the portal) (Right) Mold for eyelid portal, with tarsal plate, ducts in place for over-molding with softer durometer silicone for eyelid/skin structures. Sprues from tarsal plate molding process hold the plate and duct structure in place for overmolding process.

During Q8 we implemented and improved upon the canalicular structures. The overall size and position of the silastic tube was modified to more accurately reflect the anatomical structures. Small grooves, similar to the ones present in an actual lateral canthal ligament, have been replicated in the module and securely hold the canaliculus in place.

We have made a substantial redesign for the tarsal plate part for use in a second-generation module, which were shown to our SME(s) at the 2013 USUHS Ocular Training Course. Unlike the previous generation tarsal plate part, a one-piece, flat band that resembles a simplified version of the anatomical structure, the second-generation tarsal plate more closely resembles the real anatomy. It includes a well-defined medial canthal ligament which contains the aforementioned canalicular grooves in the superior and inferious crus, an anatomically accurate lateral canthal ligament, Whitnal's ligament, Lockwood's ligament, and the upper and lower tarsal plates.

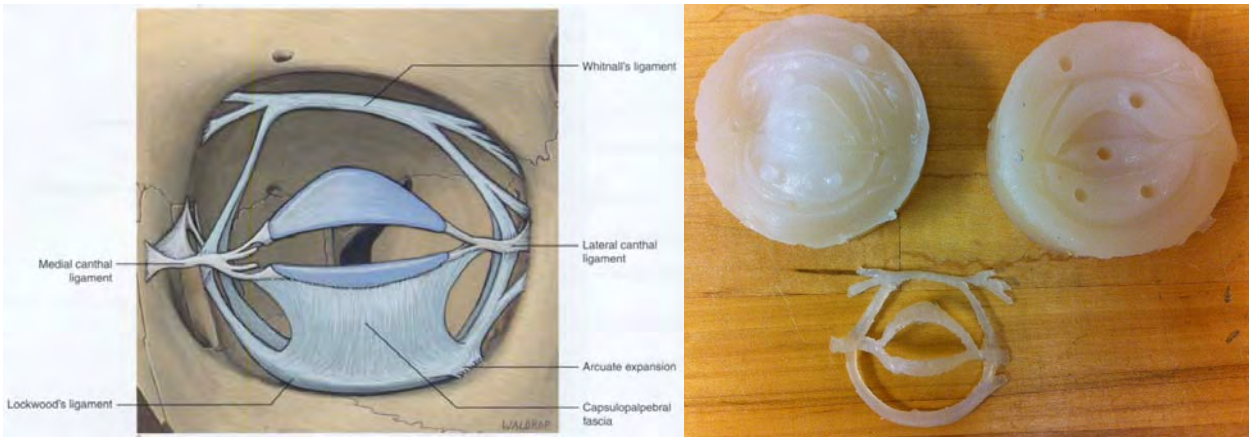

Figure 35:(Left) Textbook anatomy of tarsal plates, periorbital ligaments used as reference for advanced module design. (Right) Molds and cast version of new anatomy, fabricated in stiffer silicone than surrounding eyelid tissue.

All of these structures are cast as a single part. The part aids in providing a realistic surgical experience, strengthens the overall structure by providing more surface area for the module to bond with, and provides a robust framework for the attachment of the canalicular tubes. Furthermore, the lateral

canthal ligament together with the Lockwood's ligament have been outfitted with wires to serve a cut detectors during the proptosis procedure. During this procedure, a surgeon is required to cut through the lateral canthal ligaments, bisecting it until they reach the Lockwood's ligament. They then bisect the Lockwood's ligament until pressure on the orbit is released. We can now detect if these incisions have been properly executed by monitoring a voltage passed through the embedded wire.

The electronics for this detection circuit are deliberately simple; the wires through the ligaments tie a digital input channel on the Arduino microcontroller (or other later system) to ground (also providing electrical safety as there is little current passing through the wires at any time). When the wires are cut, the ground connection is lost and a pull-up resistor internal to the microcontroller raises the measured voltage, signaling the incision.

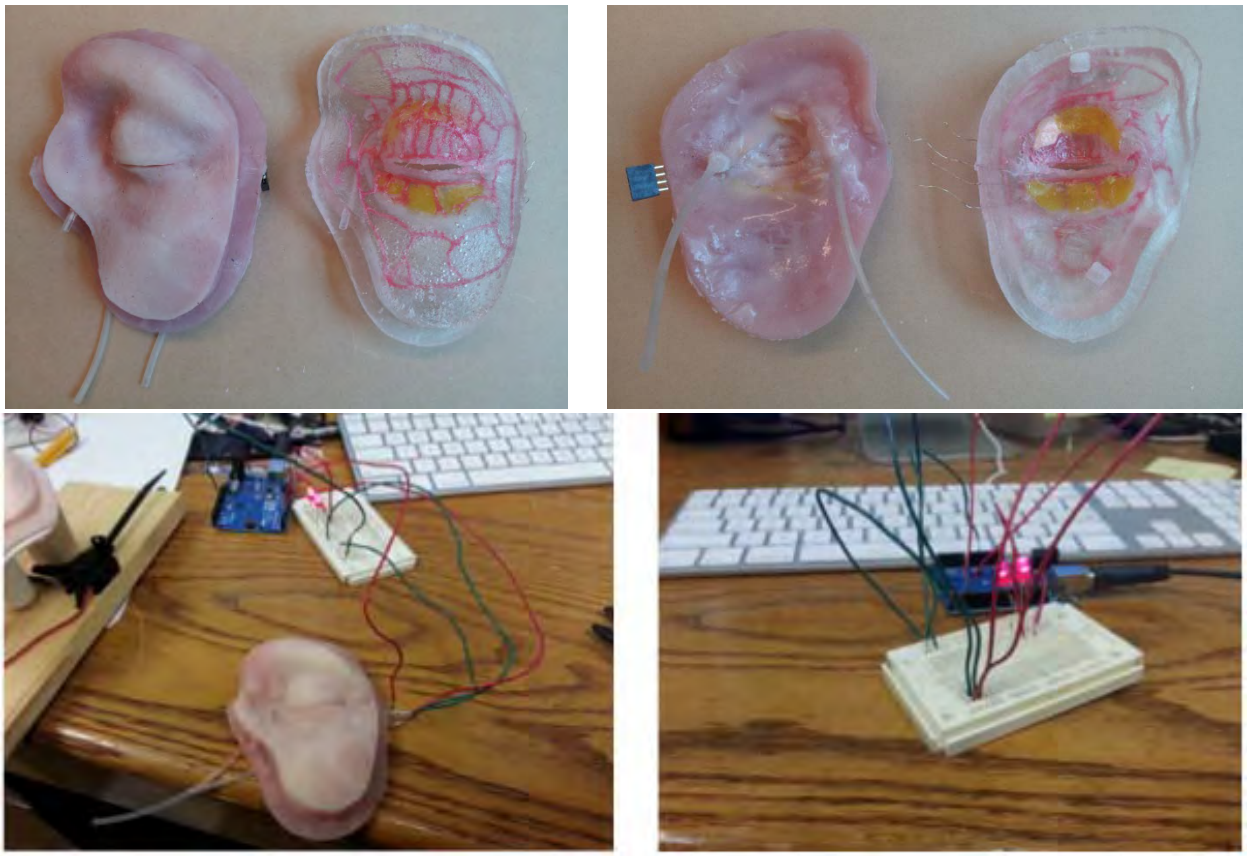

Figure 36: (upper row) Front and rear views of new-version trauma module (uninjured version). Soft, pigmented silicone and hard, clear version for illustration. Internal structures include tarsal plate with ligaments, periorbital fat deposits, arterial vasculature, canaliculi and naso-lacrimal duct. Canthal ligaments have fine wire embedded in them (visible in rear-view, bare wires and attached to temporary connector), arterial system has inlet and outlet ports for blood simulant flow and external pressure sensing. (lower row) Module connected to microprocessor showing illuminated LEDs that indicate un-cut anatomy.

The module has been further augmented by the inclusion of a layer of periorbital fat and a lacrimal gland. The fat adds to the overall realism of the module, creating a more lifelike feel. Additionally, the fat could be used to simulate a subconjuctival prolapse. It is possible to view the fat deposits as well as

the lacrimal gland by inverting the eyelid with a forceps. These structures add a level of realism that with previously unavailable.

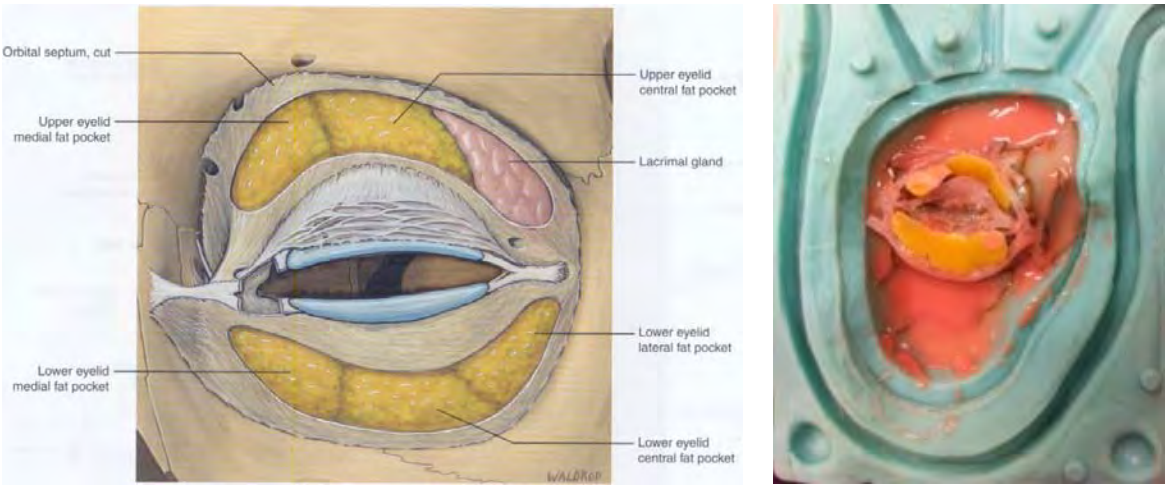

(Left) Textbook anatomy showing fat deposits, lacrimal gland. (Right) Intermediate step in advanced module casting, showing placement of periorbital fat deposits.

We have further augmented the module by the inclusion of a functional arterial system. An analog of the authentic orbital arterial system has been designed and created for the purpose of providing the option of a lifelike bleeding scenario. The arteries are filled with a synthetic blood which is fed from an IV bag. The pressure of the arterial system will be monitored by an external pressure sensor. When an artery is cut, causing a hemorrhage, the pressure drop can be detected by the pressure sensor. This data can be incorporated into the model at a future period. We can also detect when a hemorrhage is stopped by the user, opening up the possibility for different scenarios than were previously possible.

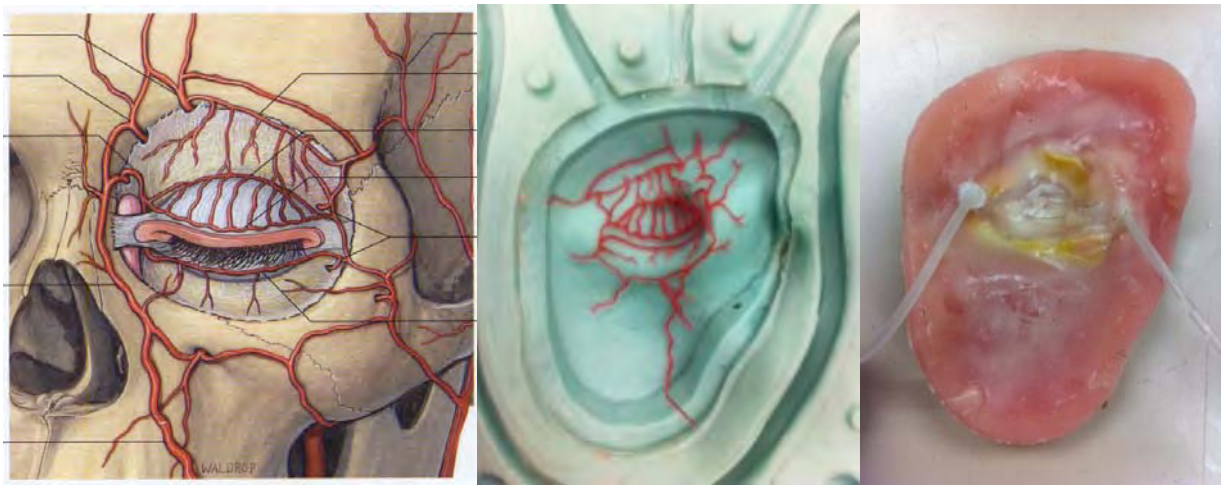

Figure 37:(Left) Textbook anatomy showing arterial network. (Center) Inlay of wax vessels to preserve vessel lumens – wax is melted/dissolved out after silicone cures to produce empty vessel lumens. (Right) fully assembled advanced module, with inlet and outlet taps for bleeding from eyelid laceration module.

After several discussion with SMEs, it was determined that it would be extremely difficult and not useful to excise the canaliculus from the surrounding tissue in an actual surgery, and that there is no reason for the simulator to be able to do this. Instead, the canaliculus is contained within the muscle and tissue that makes us the medial canthal tendon. Therefore, the simulated canaliculus need only be a channel that is capable of being located by a whitish color and is capable of being intubated. When lubricated with a small amount of silicone oil, the part pictured below fulfills this requirement.

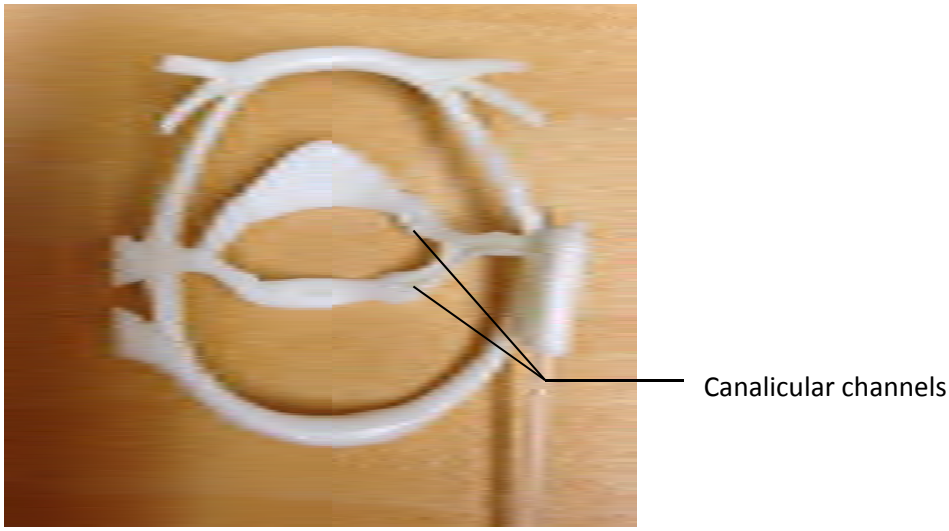

Figure 38, Canalicular channels

Neck mechanism design – air muscle improvements

During Q5, we began testing the neck actuation system, first assembled at the end of Q4. Early in the quarter, we performed initial testing of single elements of the pneumatic (McKibben) muscles that will generate neck motion and neck compliance. We then constructed a solenoid valve controller for simultaneous control of all of the muscles, contacted Dr. Yong-Lae Park at the Harvard Wyss Institute (Harvard Biorobotics Laboratory) for advice on optimizing the air muscle design and developed a controller to test the motion capabilities of the current system.

Dr. Park's advice led to selection of an alternate, looser weave braid material that allows for a larger expansion limit of the muscle and thus a larger contraction. In addition, a closer fit between the internal diameter of the braid and the external diameter of the inner pneumatic tube prevents a buckling phenomenon that we observed in our early testing.

The solenoid valve assembly, a modular system that we employed previously and a basic user interface, is shown below.

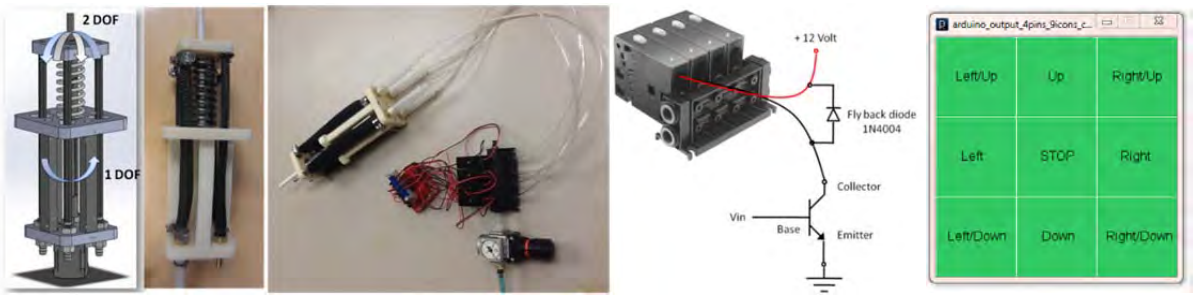

Figure 39: Neck motion test-bed design, initial structure fabrication, test system with enhanced muscle mesh, electrical control system, GUI for 8-direction motion control.

In Q6, we upgraded the pneumatic valving system for control the McKibben muscles that will drive neck motion (jerking motions to make intubation of a combative patient more realistic and difficult). This system makes use of one 3-way latching valve for each air muscle (supplies pressure or exhausts the air muscle), supplied from a common manifold. The air muscle exhausts are combined into a second common manifold which is in turn exhausted to atmospheric pressure through a series of relief valves, so that air the muscles are exhausted quickly or slowly depending on which relief valve is activated.

As described above in the context of the eye motion controller, earlier tests made use of an Arduino 2009 microcontroller. With four latching input valves and four latching exhaust valves in the pneumatic design, requiring two digital control lines each for a total of 16 digital outputs, we acquired an Arduino Mega microcontroller, which has 54 digital input/output connections. The neck motion control software was modified to make full use of the Mega's capabilities, and additional capabilities added for interfacing with the mannequin.

With this more capable system, we extended the basic function tests performed earlier to perform the same tests using the mannequin's power and pneumatic supplies, crucial in creating the mannequin-integrated system that is one of our primary goals.

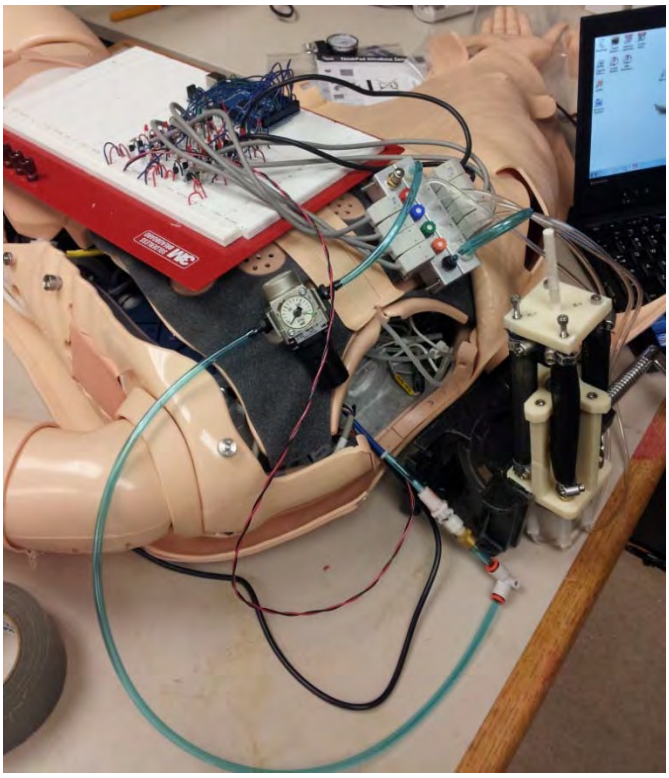

Figure 40: Pneumatic control system with fully enabled latching valves for four air muscles and four exhaust back-pressure valves. Arduino Mega and control circuitry in prototype form on mannequin's chest, valves and manifolds on right shoulder, pressure regulator on left shoulder, test platform for air muscles adjacent to neck-region.

Lastly in this section, we have begun investigations into optimizing the McKibben muscles for low-pressure supply air from the mannequin (rated at approximately 1 atmosphere by Laerdal), by sourcing thinner-wall elastic tubing for the muscles' internal bladders and changing the fitting diameters to minimize the pinching that distorts the muscle end geometry at present. Additional details are described in later sections of this report.

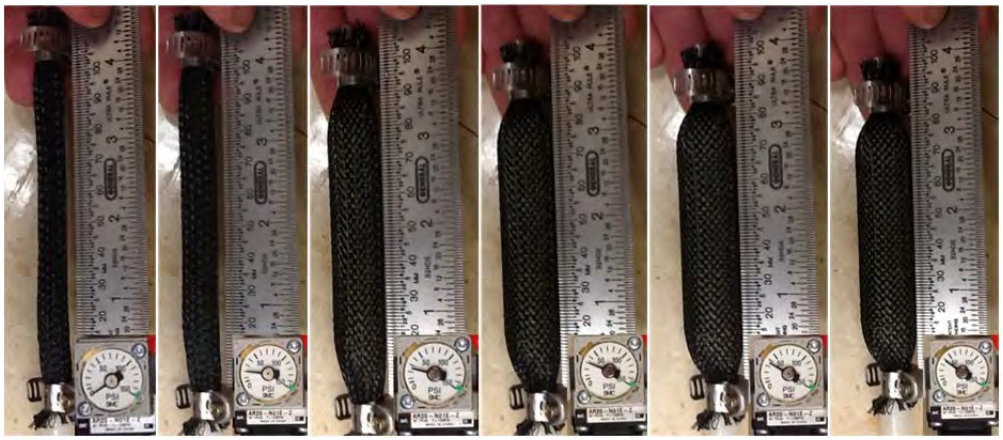

Figure 41: Air muscle images from Q5 showing pinching by hose clamps at muscle ends. Alternate design under development.

2.3.5.b. Start developing augmented reality training guidance system for enhanced eye trauma simulator.

Work towards creating the AR surgical microscope reached a substantial milestone during Q5, with the completion of the addition of a high brightness LCD monitor and optics into a commercial stereo microscope. We developed a graphical optics calculation tool using Solidworks, which was used to determine proper lens, mirror and beam splitter locations, optimizing lens choice and LCD image size based on maximizing the view factor between the LCD and the first lens of the system in light of available COTS optical components.

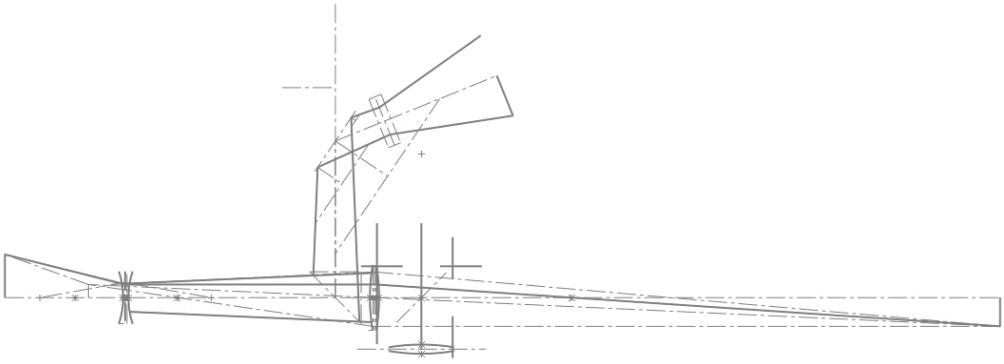

Figure 42: Graphical calculation tool for AR microscope design. Shows eyepiece image size at right, co-axially placed LCD panel image size at left and reconfigured, compact arrangement reflecting the image from an LCD placed above the original optics of the microscope.

This graphical tool allowed us to test LCD panel selection and provided dimensional parameters for designing the physical structure mounting the optics. The evolution of the system over the last quarter is shown below.

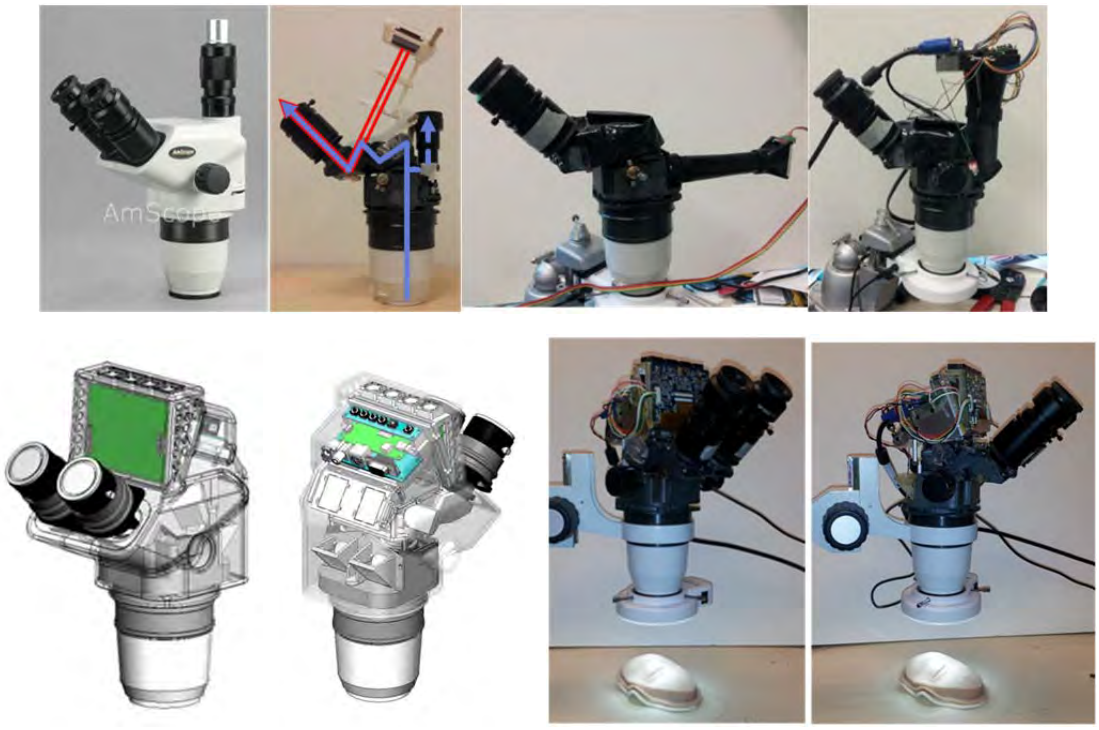

Figure 43: Sequential development of AR microscope. COTS trinocular microscope head. Early external display test. Initial inline test of small LCD display. Integration of high brightness LCD during Q5. CAD models of microscope with more compactly integrated display and optics. Internal structure of AR microscope awaiting external shell fabrication.

The second last version of the microscope was on display for the TATRC visitors at MHSRS/ATACCC. It was found that the heat generated by the high brightness display softened the plastic supporting components, which have been replaced with aluminum in certain positions and augmented by cooling fans driven by the LCD's power supply. Further developments of the AR system are described in section 2.3.7.

Gesture driven graphical UI

During Q5 we made progress in the gesture-driven sequencing of the instructional and feedback materials presented to participants. Rather than requiring that a user interact primarily with keyboard or mouse to advance the scenario, the various sensing elements provide the system with state and gesture information. For example, when setting up the system, it detects whether the proper instrument is connected, provides instructions for how to do so (training the user in how to use the system), and advances automatically when that step is complete. Later in the scenario, the system updates the instructional display tracking the placement of sutures, for example, advancing when it detects cutting corresponding with the trimming of sutures and replacement of the scissors in the instrument tray.

Figure 44: Examples of gesture driven scenario content. Simulator preparation instructions driven by correct sensor/instrument attachment. In-scenario feedback on completion of series of sutures.

We developed the underlying code structure so that each phase of the scenario and each element of instructional material have specific actions that will trigger the advance to the next phase. The structure also allows branching and return to earlier phases of a scenario, based on the description built into the instructional element.

The gesture recognition engine was consolidated into a single library for implementation as a DLL (Dynamic Link Library) with corresponding APIs. This last feature is important in order to export the whole gesture recognition engine in another different application and/or to implement and load a different one inside the data analysis software, making possible the use of the current software for different types of surgical specialties.

Developer interface improvements

In Q5, the developer interface, used for data collection and export of the data to the analysis tools continued to evolve. Features added were horizontal scrolling through the full data set and indications of the location of the current view is relative to the entire scenario, zoom functions, display of the details of manually entered event keystrokes, ability to change the rate of playback, from 4x normal to 1/64x normal speed, and selection tools to export only desired subsets of the acquired data.

The display of the virtual scene, showing graphical models of the instruments and the mannequin head were decluttered, showing only connected instruments rather than the whole available suite.

We added management tools for the AVI video files that correspond with the collected instrument data. We created a new software library that can access AVI streams in input and output, choose the proper compressor in order to save the AVI stream in the best format to optimize hard drive space consumption and the CPU overhead.

Quantitative scoring and data analysis

In Q5, the list of quantitative overall performance metrics included:

- Total Activity within ROI
- Total Duration within ROI
- Longest Run within ROI
- Total Transitions between ROIs
- ROI Containment
- Adaptive ROIs measures

as well as the beginning of a method for examining hand tremor.

Additional details on the AR system are covered in the sections below.

2.3.6. "Month 8" - Design of mandibular/maxillary trauma modules, upper airway model for use of airway devices, new cricothyroidotomy portal.

2.3.6.a. Cricothyroidotomy module cut sensing

In Q5, we made advances over Year 1's developments towards a cricothyroidotomy primary incision detection sensor. The earlier system, with strips of conductive material that indicated an incision only when completely transected, providing a yes/no signal, but not sufficient information for accurately locating the cut length or orientation, was replaced with an analog system similar in concept to resistive touch-screen technology. A 3-layer structure detects an incision through it with a conductive blade, when voltage from one of the "drive layers" is connected to the sensing layer by the conductive blade passing through them. A series of circuits was created to alternate rapidly between the x and y direction layers so that a near continuous output of cut position coordinates can be fed to the controller.

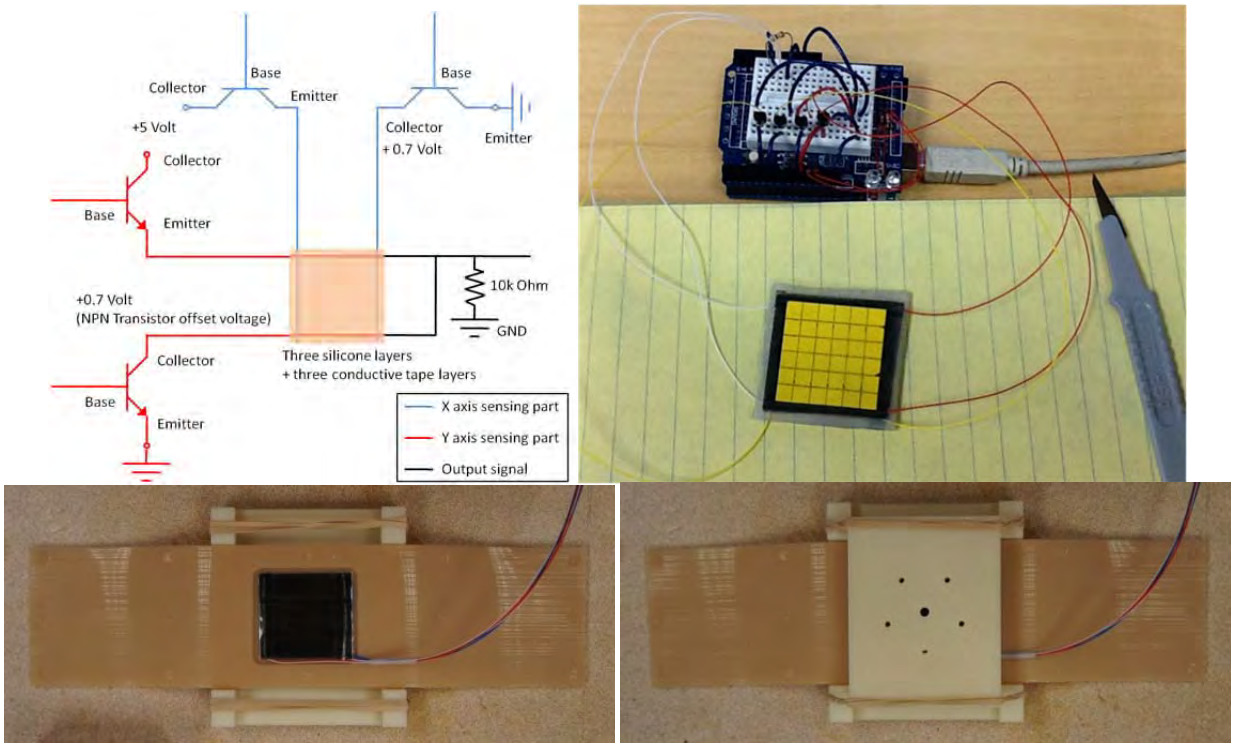

Figure 45: Drive circuit and sensor body for cricothyroidotomy incision sensor. Sensor in place on neck "skin" and over-molding assembly to encapsulate the sensor.

A concept for a simplified version that uses only two conductive layers and employs commercially available neoprene rubber with conductive surfaces (previously used in the original yes/no concept) was explored, however high and variable contact resistance between the thin surface layers and the incising blade made this solution unworkable at present.

2.3.6.b. Hemorrhage control sensing system

Also during Q5, we have developed a fluidic sensing circuit for hemorrhage control detection. Expanding on design concepts from our COMETS hemorrhage control design, work was conducted on the development of a simple, rugged, and intelligent system for detecting attempts at controlling hemorrhage from multiple sources. Specifically, we envision a network of simulated vasculature which spans the entire head and neck region of our simulator. Instead of placing flat pressure sensors underneath each “target zone” where a medic may apply pressure to stop bleeding, we investigated a method of detecting subtle signatures of treatment in the blood pressure feedback loop. By using a single, inline, pressure transducer we will be able to detect and respond to treatment in an *intervention independent* manner. It was our experience with the COMETS system that designs that rely on specific pressure thresholds to be exceeded tended to fail during actual usage. Therefore, we designed a system that uses higher-level event observation to evaluate treatment.

By monitoring the pressure signal from the inline transducer, we can observe changes in pressure of the overall system as well as spikes that correspond with treatment. Pictured below, the raw pressure signal (blue) from the sensor can be analyzed to extract the signatures (red) from applying or releasing direct

pressure on the hemorrhaging vessel. When combined with the average systemic pressure, we should be able to more reliably detect treatment of non-life threatening hemorrhage controls in areas such as the superficial face and eye orbit. While these are initial tests, they have resulted in promising data and warrant continued exploration.

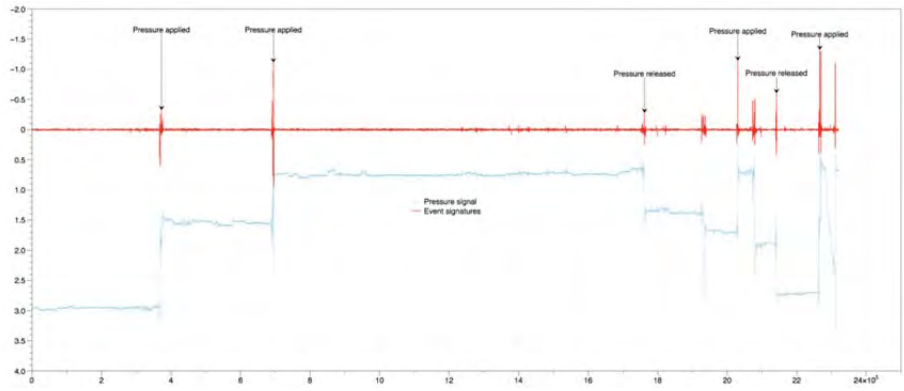

Figure 46: Raw hemorrhage back-pressure measured by restricting flow through one or more branches of the vasculature (blue). Derivative of pressure (dP/dt) for use to flag when significant changes occur, e.g. start or end of hemorrhage control (red).

We tested the Deltran DPT-100 pressure transducer from Utah Medical which is a clinical device used on actual patients. It is a cheap, 5VDC sensor that is capable of monitoring a pressure range of -30 mmHg to 300 mmHg without the chance of cavitation and without require a separate priming circuit.

The signal from the DPT-100 sensor is quite small and somewhat noisy, so amplification and signal filtering is required. We built an initial prototype that allows the DPT-100 to connect to an industry-standard instrument amplifier (INA125P) and on to a low-cost Arduino for data collection and analysis (Figure 47). A 15Ω resistor was used as a gain resistor for the INA125P, though this will be replaced with a 20Ω cermet trimmer potentiometer to allow for more accurate gain control.

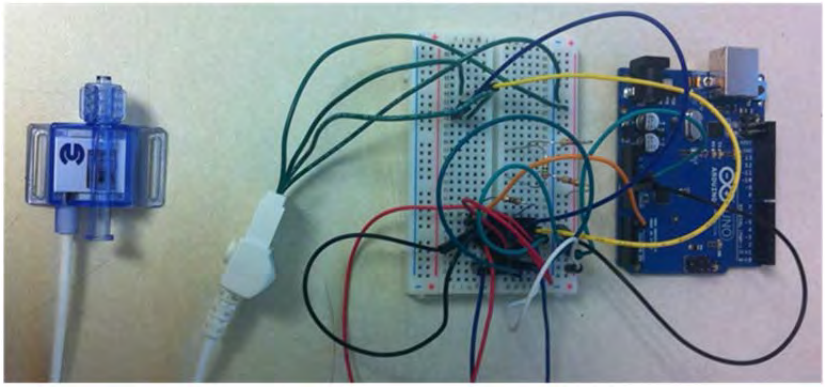

Figure 47: Test assembly for hemorrhage control pressure sensing. Clinical pressure sensor, signal amplifier chip, microcontroller kit for data acquisition.

During Q6, discussion with Dr. Troulis concerned the types of facial fractures that would be most relevant in the context of facial trauma and complications that would necessitate surgical cric. She recommended that bilateral mandibular fracture can allow the lower jaw to collapse, blocking the oral airway. We also discussed typical responses to jaw fracture, including wiring of the lower to the upper jaw to stabilize the bones, which in turn helps to reduce or stop ongoing oral hemorrhage. We will explore options for designing such features into the mandibular and non-ocular facial trauma elements.

Remaining developments in this section remain for the NCE period in Year 3.

2.3.7. "Month 10" –

2.3.7.a. User testing of enhanced eye trauma simulator at USUHS or Madigan Army Medical Center.

As described in the administrative sections above, we completed preparation of protocol, continuing review and amendments for the study protocol and received approvals from our IRB and ORP HRPO for a second data collection exercise and participation in the 2013 USUHS Ocular Trauma course. A new vendor agreement was prepared to bring the simulator onto the USUHS campus for the testing exercise.

During Q8, as with Year 1's testing, we had 25 lid laceration modules available for the students and faculty to use, all of which were used over the two-day wet-lab sessions of the course. As with Year 1, student availability was limited due to the primary requirements for their participation in the animal and lecture sessions. A software error resulted in certain demographic data being left out of the database, however we verified that at least ten PGY2 and PGY3 residents used the simulator. The remainder of the modules were used by faculty, of whom three were oculoplastics specialists.

All participants filled out a survey form which was requested by Dr. Marcus Colyer, course director, to provide feedback on participant impressions about the simulator. This survey (included in the Appendix) presented Likert scale-type questions, asking for agreement/disagreement or relative opinions and, on the following topics:

- User interface and teaching content
    - Teaching content was clear and understandable
    - Interface guidance was helpful in learning the technique
    - There was too much detail in the teaching content
- Eyelid laceration module
    - Tarsal plate hardness was too hard/too soft
    - Eyelid hardness was too hard/too soft
    - Resistance to needle puncture was too much/too little
    - Friction of passing the needle through the tissue was too much/too little
    - Friction of passing suture through the tissue
- Simulator stand and instruments
    - Structure of the stand interfered with interaction with the surgical field
    - Cables and connectors interfered with performing the procedure

- Cable management bracelets and attachments interfered with performing the procedure
- Instruments were easy to take from and return to the rack
- Sutures were easy to access
- Lights were in a suitable position
- Lighting brightness was too dim/too bright

For each section, and open ended comment/suggestion section was included.

During Q8, we performed preliminary analysis on the data compiling the results for the scored questions.

For the **interface and teaching content**, the experts and novices showed the same overall preferences. The majority agreed or strongly agreed that the content was clear and understandable and that it was helpful. Both groups however, disagreed that there was too much detail in the content. We interpret this to mean that there was insufficient detail and that more should be added. Among the comments, were requests for additional detail generally, more specific instructions regarding details of the knots and suture techniques to be used in the different phases of the procedure as well as acceptable alternative methods, and information on suture depth and tissues to approximate.

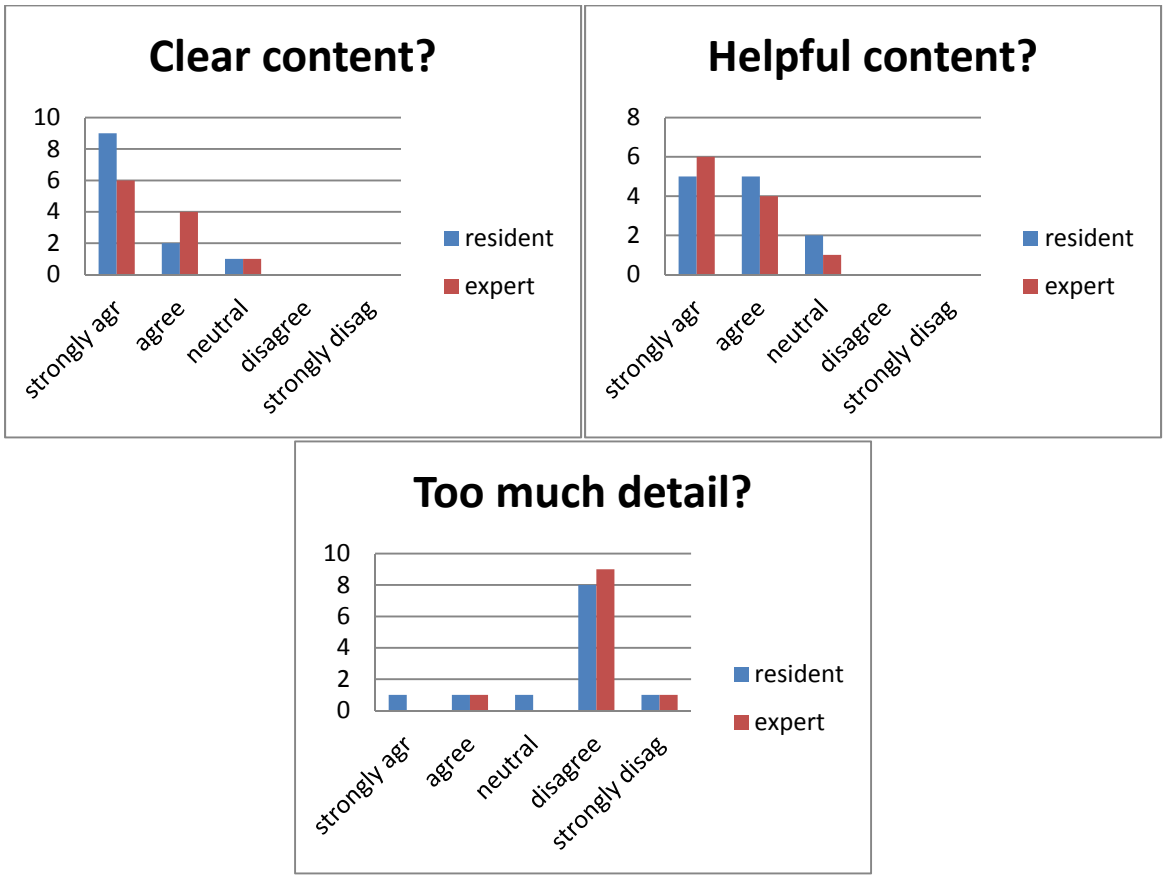

Figure 48: Simulator content responses between residents and experts

For the **eyelid laceration module** itself, experts and novices tended to have similar responses as well. Tarsal plate hardness was judged almost evenly split between about right or too soft; eyelid hardness was about right or too hard for most respondents; puncture resistance was about right for the majority of experts and residents; needle friction was about right for the majority, and suture friction was either about right or too much, evenly divided between experts and residents. Comments were fewer, however there were requests for additional and more obvious anatomical landmarks. These can be included through changes in pigment added to the future versions of the modules and alterations in the mold to include features such as the Meibomian gland pore, which were present, but not particularly deep.

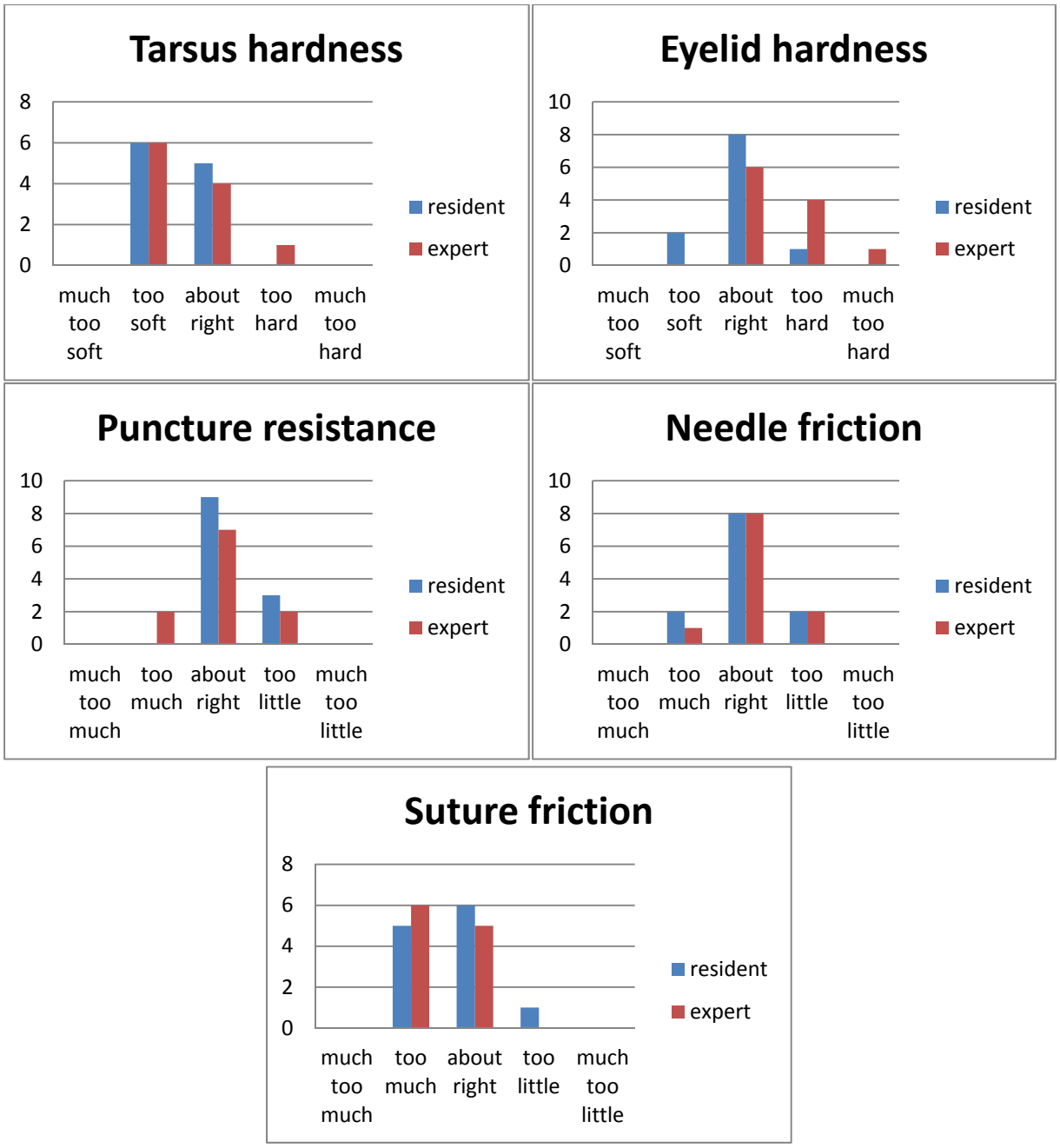

Figure 49: Lid laceration module physical characteristics responses

For the **simulator stand and instruments**, responses were in certain cases more broadly distributed. The median responded that the stand did not interfere, however there were some who felt that it interfered somewhat (possible that the agree/disagree statement was misunderstood and inverted). Cables and connectors clearly were troubling for some, but not for others. The cable management bracelets were roughly evenly distributed between those who were neutral, disagreed or strongly disagreed that they interfered with the task. The instrument access using the tray and the connection mechanism were found to be easy to use by nearly all participants. The lighting system was found to be

about right by most, although too dim for some users. The majority of the comments concerned the cabling attached to the instruments, with some requests for wireless instruments (which is not possible given current magnetic tracker state of the art technology and requirements on the size and mass of the component that would be attached to the instruments), others suggesting alternate cable management approaches.

Discussions with Dr. Colyer following the course indicated that we would be welcome to participate in the 2014 course as well.

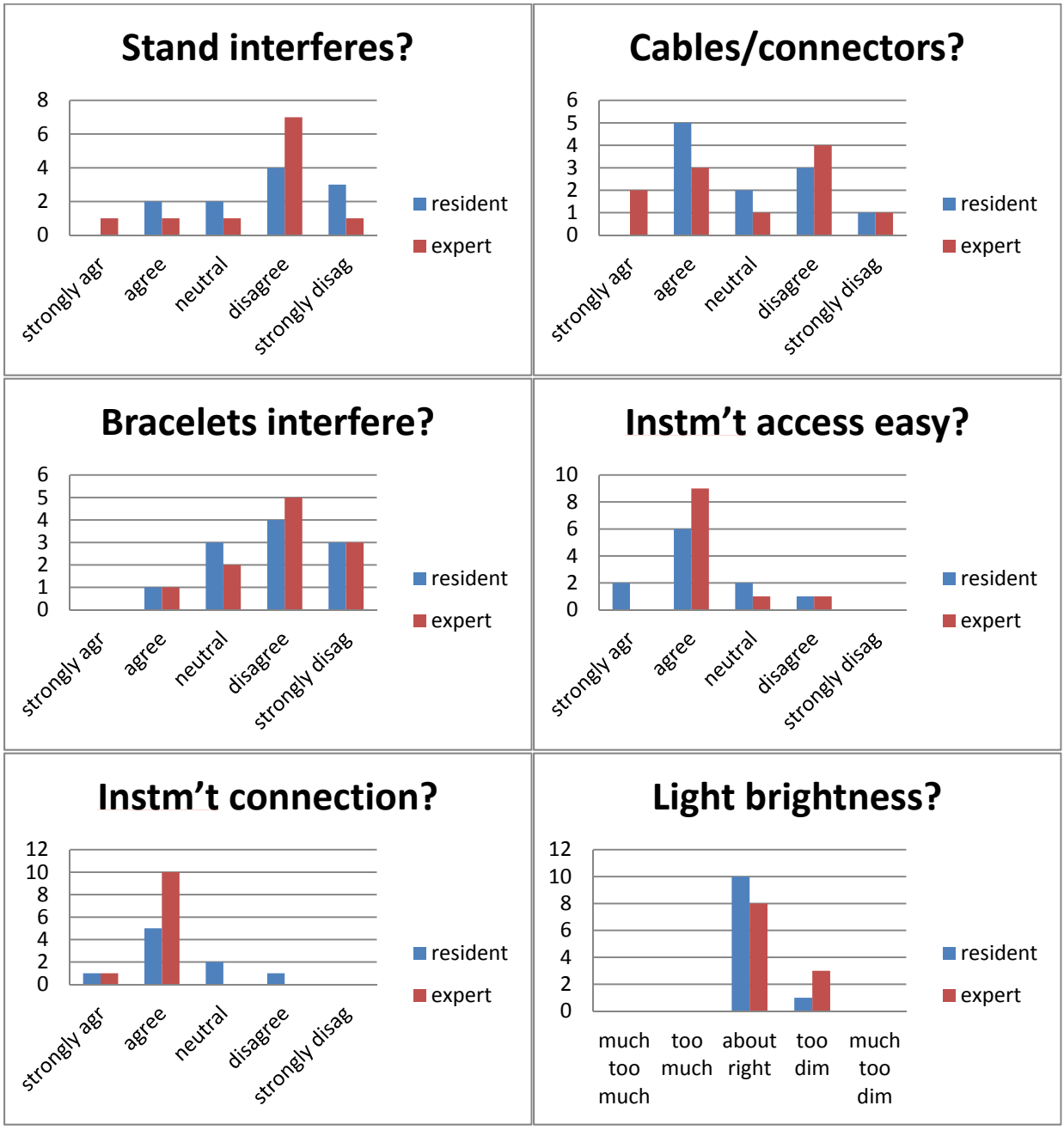

Figure 50: Standalone simulator characteristics responses.

2.3.7.b. Pass upgraded proof-of-concept simulator specifications onto commercial partner.

Year 2 was focused primarily on development of the simulator systems. We maintain the confidentiality agreement with Laerdal and were in periodic contact with them regarding interfacing our system with their mannequin operating system, however did not reapproach them for consideration of commercialization of the system.

As described above, we submitted three invention disclosures to our Research Ventures and Licensing office prior to the MMVR demo, which they converted into a provisional patent application. **During Q8** a subsequent invention disclosure was made covering the system as a whole, to be converted to a provisional patent prior to presentation of a poster at MHSRS 2013.

2.3.7.c. Continue working on augmented reality guidance system for enhanced eye trauma simulator.

AR Microscope

As described in the sections above, we continued to make progress towards developing the augmented reality components of the system. During Q6, the operating microscope reached the first useable state, with the optics for both left and right eye implemented, measurement of the zoom level available and power circuitry for the LCD, backlight and surgical light source, creation of software tools to display stereoscopic views and mounting of an Ascension position tracking sensor to the microscope to track its location relative to the mannequin head.

Following this early work, the software architecture has been modified to display a model of the microscope within the virtual environment of the data acquisition interface, and the same position tracking information is used to define the stereoscopic imagery shown to the user through the microscope. As the microscope is translated or rotated, the view changes to match. At this stage, test patterns were displayed; the next steps in this area include implementing views of the virtual environment for overlay onto the view of the real objects.

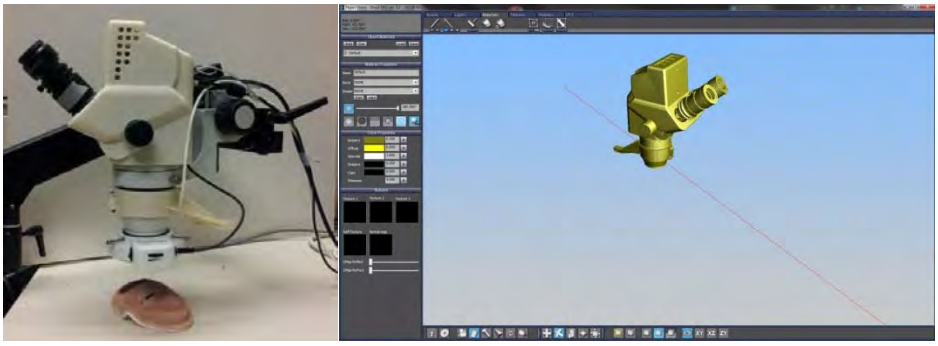

Figure 51: AR microscope with enclosure, internal LCD, ring light (at bottom), position sensor mounted to right of lower cowling. Graphical model of microscope in virtual environment for calculation of relevant display to be presented on LCD and viewed through eyepieces.

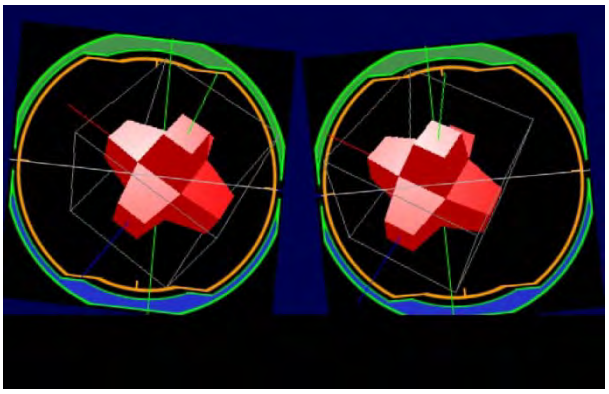

Figure 52: Early test patterns, one image for each eye piece.

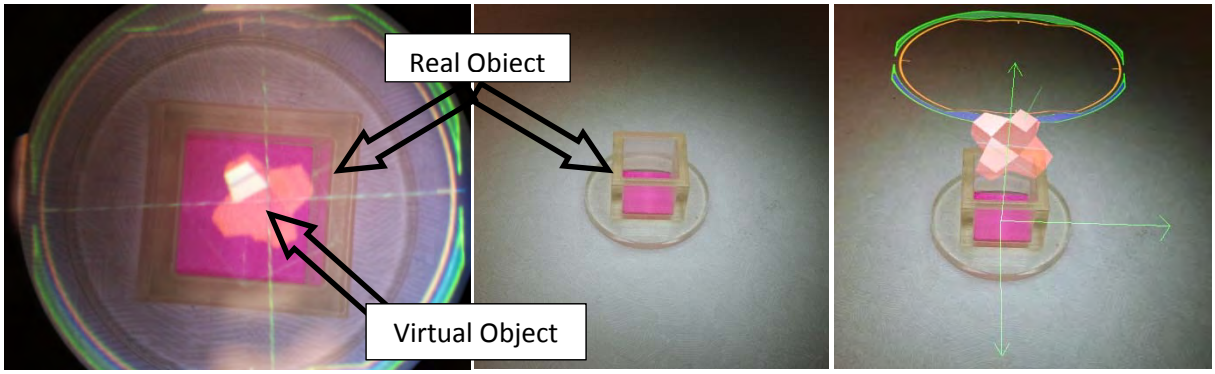

Figure 53: Monocular view of combined image (left) and external view of test object of known geometry (center). Simulated rendering of apparent relative positions of virtual and real objects.

Shown above it can be seen that the images are rotated with respect to each other (note colored rings around target object). This was necessary because the optical paths of the eye pieces diverge from each other by 10 degrees. To make the LCD image appear aligned through the eyepieces, the LCD image must be rotated by 5 degrees each in the opposite directions. Control panel elements were added to our primary data acquisition interface to allow for this rotation as well as providing offsets, skewing and scaling to the output images.

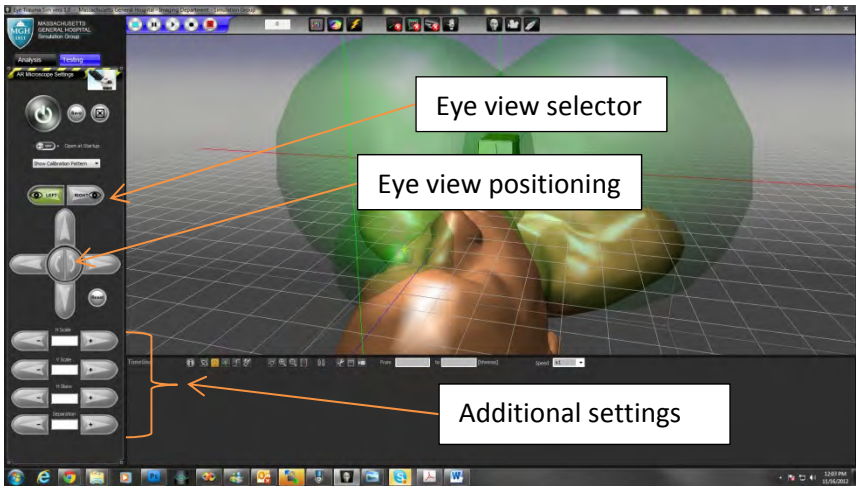

Figure 54: Control panel for microscope view positioning and alignment.

We observed that while the images are aligned, the pixels grids viewed through the eyepieces are still at angles with respect to each other. Image quality would be improved further if the pixel grids were aligned, which required modification of the optical path set up between display and eye piece lenses.

The earlier 2D graphical tool described above assumed that the path from display, through lenses and mirrors to the eyepiece lay on a plane. Relaxing this assumption and allowing a 3D path permits the generation of a path with chirality (rotation). The 3D calculation tool sets the LCD images to be aligned with the pixel array and the output optical axis aligned with the eyepiece. Four points defined on the LCD plane are projected through the series of lenses and mirrors to their image positions. The rotation of lines connecting pairs of image points shows the rotation of the image. By adjusting mirror locations and angles, the LCD image can be rotated optically (rather than graphically), resulting in the desired alignment. Once the mirror angles were calculated, the mirror holding components in the microscope were modified to match, and were installed, replacing the earlier versions.

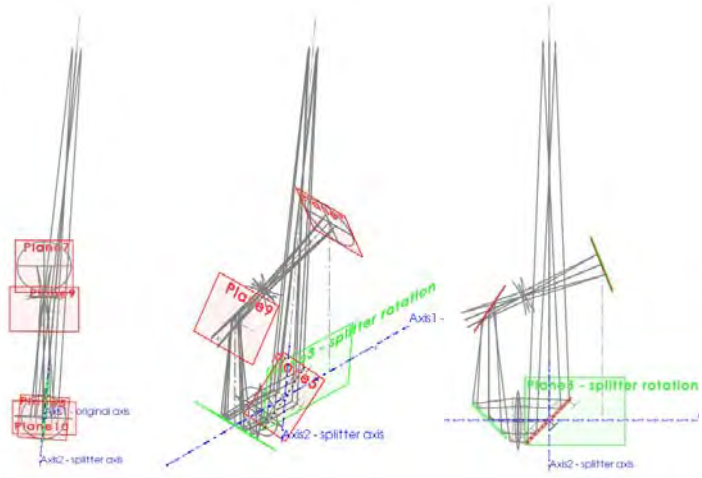

Figure 55: Front, isometric and side views of new 3D optical path calculator.

AV Recording and Compression

After the implementation of the different components required for the video acquisition, in Q5 all these software components were being combined in order to create the architecture to manage the video acquisition (webcam interface, that has required a manual decoding YUV filter implementation) a codec manager (for the video compression into the desired video format) and the AVI manager (already implemented in the previous months. Remaining for completion is synchronization between the instrument tracking data and the video so that the synthetic view playback corresponds with the video playback. This will enable scrolling through recorded data from a scenario and selection of sub-elements for more detailed review and analysis.

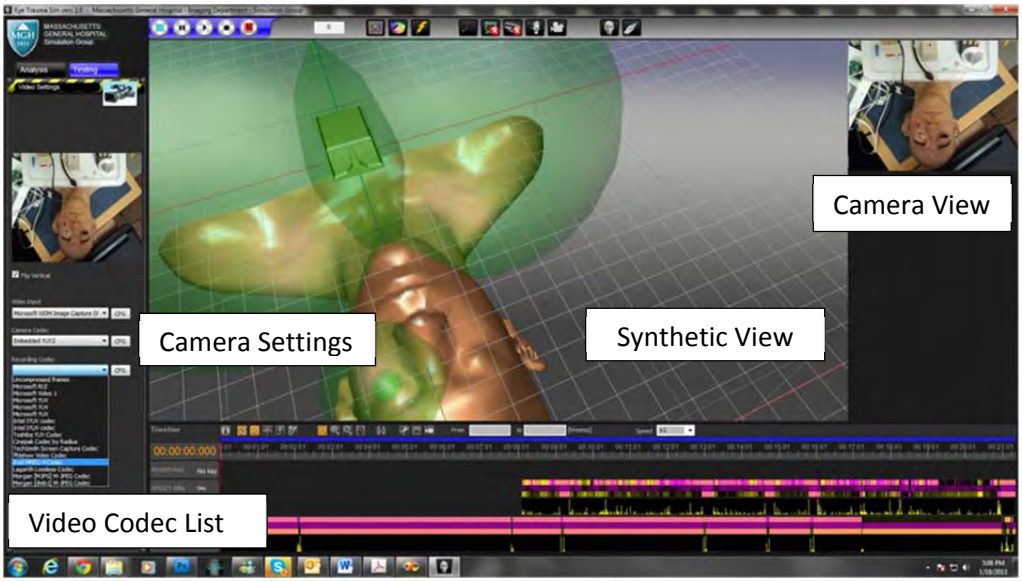

Figure 56: Updated data acquisition interface including new video capture elements. Available CODEC list and camera settings at left. Instrument tracking data streams shown in colored bars at bottom

Leap Motion Device

Our Year 1 tests of the Kinect system, which we are still evaluating, suggested that the tracking resolution was insufficient, in part because the minimum working distance between the Kinect and the surgical field is too large. A novel hand/finger tracking device called Leap Motion (www.leapmotion.com) has recently appeared on the market, and early release of development systems has been made available to developers with interesting applications, as determined by review of abstracts submitted to the company. In Q6, we obtained one Leap system and have began to evaluate its capabilities. At present, it is clear that it can detect up to 10 finger tips within its working space, a space approximately 24" on a side, and it appears that it is much better suited for hand/finger tracking than the Kinect. An additional intent of using hand/finger tracking is to make the user experience more comfortable, using the simulation platform for content management, through the use of the Leap.

Figure 57: Photo of Leap unit, with mini-USB connector. Product photo from Leap web site; demo application available with device shows only line segments for finger tips, not rendered hands.

In Q7, we began to study the possible uses of the Leap Motion finger/hand tracking system, through modification of the example programs included with the SDK, such as the Sample_VS2008 project, which

demonstrates access to the raw data coming from the sensor. The device performs similarly to videos displayed on the vendor website, as which we confirmed for ourselves through use of the example programs and software demos that it is possible to download from Internet.

The sensor provides multiple finger positions and orientations (each tracked finger in five degrees of freedom) and the code generates extra data (timestamp, number of fingers, frame ID). Mounted under a monitor positioned to the side of the simulation platform, the Leap could track surgical instruments (possibly out of range of the tracking system) or surgeon's gloved fingers and provide indications on the screen – sharp instruments and gloved fingers being incompatible with various touch screen technologies.

Event Driven Gesture Analysis

During Q6, we met with several of our subject matter experts to continue our framing of the educational goals of the upper eyelid laceration repair module. While very difficult to depict graphically, our state diagram of the entire procedure grew extensively. Based on input from the SMEs, we mapped the entire procedure from start to finish, including many actions we do not intent to simulate with this system. The purpose of this exercise being to understand what context the user is being placed in when using the simulator. States of the procedure such as requesting an x-ray of the patient would be carried out in software as a series of interactive steps in the GUI rather than an interaction with the simulator mannequin.

Several areas of the training module, when mapped, started to illustrate repetitive functions. We have captured these repetitive functions (actions, gestures, thresholds, etc.) and are using them to drive our software development processes. For example, our ability to detect a specific sequence of events associated with placing the needle through the eyelid and retrieving it through the other side forms a basic building block in our suturing gesture recognition system. If the system detects a second pattern of this type, we know that the user has taken two bites to pass the suture through the location in the wound. Should these events be followed by a knot tying gesture, we are then able to warn the user that it is advisable to leave the sutures untied until all of the sutures have been placed and the lid margin approximated. This is necessary for both real-time, in-context surgical

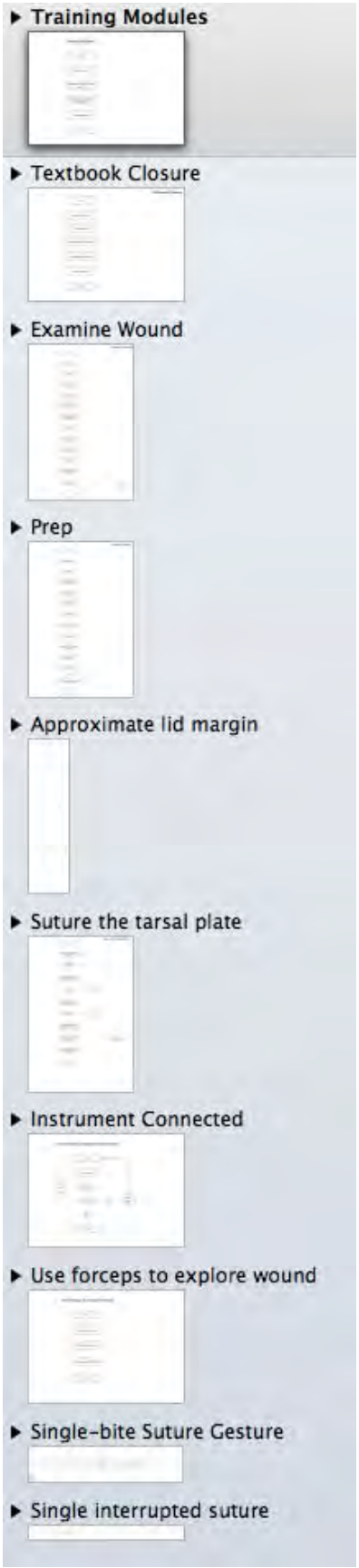

Figure 58

guidance for novices as well as forming the foundation of our gesture recognition framework.

As of Q6, the description hierarchy tree had 10 levels of description:

- Curriculum: 1 entry (eye trauma course)
- Module: 1 entry (marginal lid laceration)
- Styles: 1 entry ("textbook" sequence – later entries to include surgeon-specific techniques)
- Steps: 5 entries for current style (e.g. examination, suturing tarsal plate, incision closure) – different numbers of Steps will apply to alternate Styles
- Tasks: 52 defined across all Steps, with varying numbers for each Step – marginal suture through tarsal plate
- Gestures: may be simple (review X-ray) or compound, with further divisions (e.g. 2-1-1 suture gesture)
- Sub0-Gesture: optional –structure for capturing needle passages without knot tying
- Sub1-Gesture: high level components of gestures, e.g. single bite suture, 2-throw knot, 1-throw knot, cut suture
- Sub2-Gesture: mid level gesture component, e.g. tissue grasping, needle bites, repetitions of throws, suture grasping, knot tensioning
- Event: sensor-driven events that comprise the Sub2-Gestures: instrument jaw opening/closing, applied force level threshold transitions, passage across region of interest boundaries, focused path analysis

Sample elements of the hierarchy are depicted in the sidebar above.

Simulation Content Frame Structure

Extending the content frames described earlier, during Q7, the scripting language (XML-based) developed to manage the simulation content was been extended, introducing new functionalities and extending the syntax.

The new frame (underlying description of the content and functionality for a given node in the procedure) in the scripting language allows the positioning of the slide buttons and extends the type of buttons present in the simulation flow.

To support good coding practice and simplify development for future users, the capability to add comments in the frame structure has been added. Further replacement of the system condition index (numbers between the <system_Cond> tags) with a set of mnemonic labels is being implemented. A sample of the most recent version is shown below.

The source code was prepared to export the gesture recognition core into an external DLL. The ongoing work has been developed based on the specifications defined previously several months ago. The code has also been commented in order to make it more accessible to other members of the development team and it is still going ahead a cleaning of the entire software project.

In order to support the externalization of the gesture recognition core has been necessary to insulate the shared structures and library between the main program and the DLL, creating a common folder and moving inside specific shared files data structures, in order to keep the code consistent in both projects after modifications on the shared structures.

The changes have been made on the libraries that manage the simulation content slides and the event handlers used in between them. The different event handlers have been exported into the DLL library and the importing interface is about to be completed.

The scripting language used to code the simulation content (slide set) was extended incorporating the name of the proper DLL to use in order to handle the right events for the specific simulation.

Another new feature that is almost ready is the introduction of separate warning handlers that are currently coded in the same channels used for the event handlers, extending to 5 the total number of event handling channels for each slide.

```
// first slide with menu selection
 <Section>
  <ID>1</ID>

 <Slide>Contents\Simulations\MMVR\Slides\2013MMVROCFGUI.001.jpg</Slide>
  <Audio>none</Audio>
  <Light>0</Light> // no light on the mannequin
  <Events>
   <Button1>0,1,0.0000,0.4870</Button1>   // NO Button on the left side of the screen
   <Button2>3,23,0.8339,0.4870</Button2>  // Next Button on the right side of the screen
   <Button3>0,0,0.4169,0.9000</Button3>
   <Time>0,2</Time>
   <system_Cond>-1,0</system_Cond>
   <system_Cond>0,0</system_Cond>
   <system_Cond>0,0</system_Cond>
   <system_Cond>0,0</system_Cond>
   <system_Cond>0,0</system_Cond>
   <Warning_Cond>0,0</Warning_Cond>
   <Warning_Cond>0,0</Warning_Cond>
   <Warning_Cond>0,0</Warning_Cond>
  </Events>
 </Section>
```

The architecture has also been modified splitting in two different sections the content slides management and the gesture segmentation. These two last components now run independently.

Some of the Gesture recognition routines have been improved in order to make them more accurate and more tolerant to wrong movements into the workspace.

Some other time has been spent merging the last version of the source code, developed during the MMVR conference with the latest developments of the one on the workstation.

Gesture Detection Algorithm Development

The relatively simple early approach we developed to drive progression through the scenario content is being expanded with a richer set of algorithms have been created in order to recognize the different gestures performed by the surgeon during the procedure. This is based on a more extensive set of elemental states, listed below. This list is extended with an initial set of error conditions that will trigger warnings from audio cues to video instructions on correct technique.

ID	Routine Description
-2	Stop state machine
-1	restart state machine
0	NULL
1	Scissor is cutting inside a specified ROI
2	true if a forceps is connected
3	true if no forceps are connected
4	True if a needle holder is connected
5	True if no needle older are connected
6	True if an instrument is inside a specific ROI
7	True if a scissor enter inside a specific ROI, cut and after goes out
8	Record data for scoring
9	Plot scoring results
10	True if the spear is connected
11	True if the spear enter in a specific ROI and remains there for at least 3 seconds
12	True if the forceps enters into a specific ROI and remains there for at least 3 seconds
13	True if a double pass suture is performed (first pass)
14	True if a double pass suture is performed (second Pass)
15	True if 2-1-1 is performed (not complete)

ID	WARNING CHECKING
100	Check for too hard forceps grasping (A)
101	Check for too hard forceps grasping (B)
130	Check for single pass suture instead of a double one (A)
131	Check for single pass suture instead of a double one (B)

We are investigating possible extensions for the scripting language, namely including a numerical parameter for certain routines, in order to create different settings (e.g. trim length of sutures) allowing us to use the same algorithm but with different settings for different types of users.

A series of schematics of the state machine structure being implemented in code is shown below, now with the various links between states defined by the test functions that determine which threshold has been crossed.

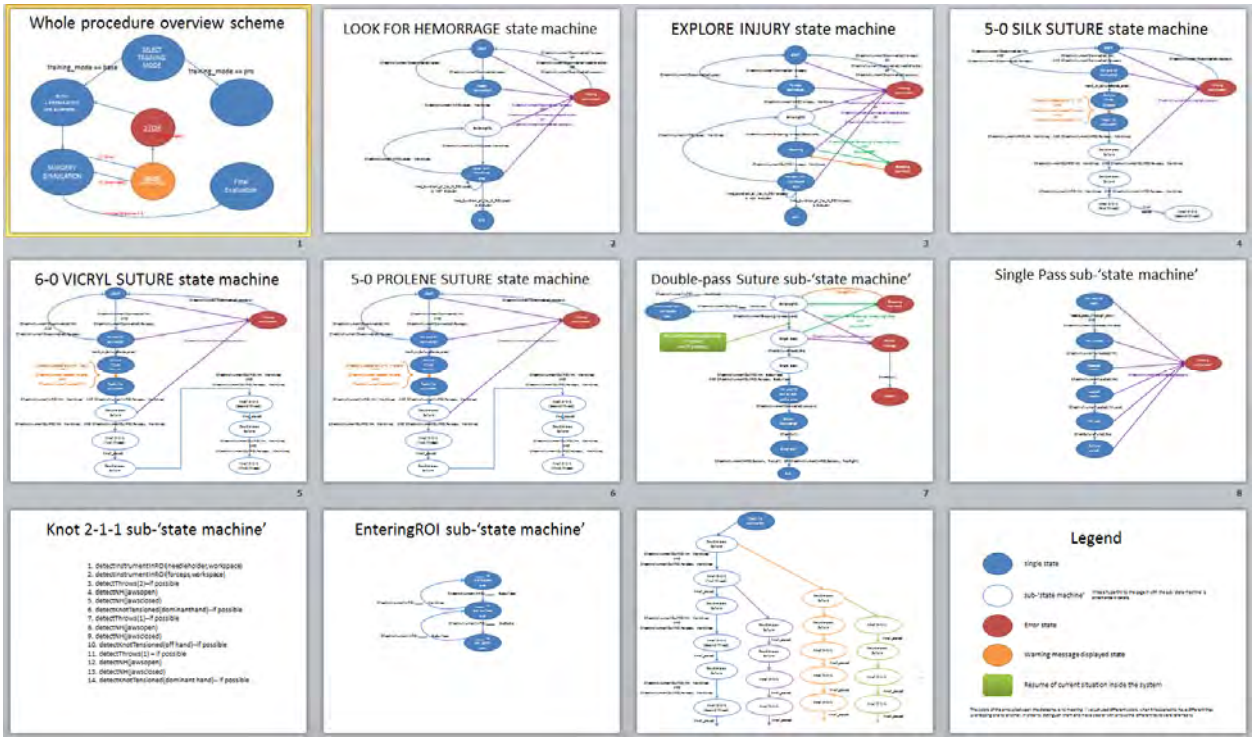

Figure 59: schematics of elements of state connections for different levels of gesture recognition heirarchy

Content Development for Scenarios

During Q7, the didactic content for the eyelid laceration module was fully-developed to incorporate the complete set of steps involved from a clinical point of view. These steps were established after reviewing existing training materials as well as from several meetings with our subject matter experts. While comprehensive and implemented on the simulator, we have not activated all of the steps in the setup for use at the 2013 USUHS Ocular Trauma Course. Rather, we have activated the steps that allow a user to be guided by an instructor and immediately begin suturing.

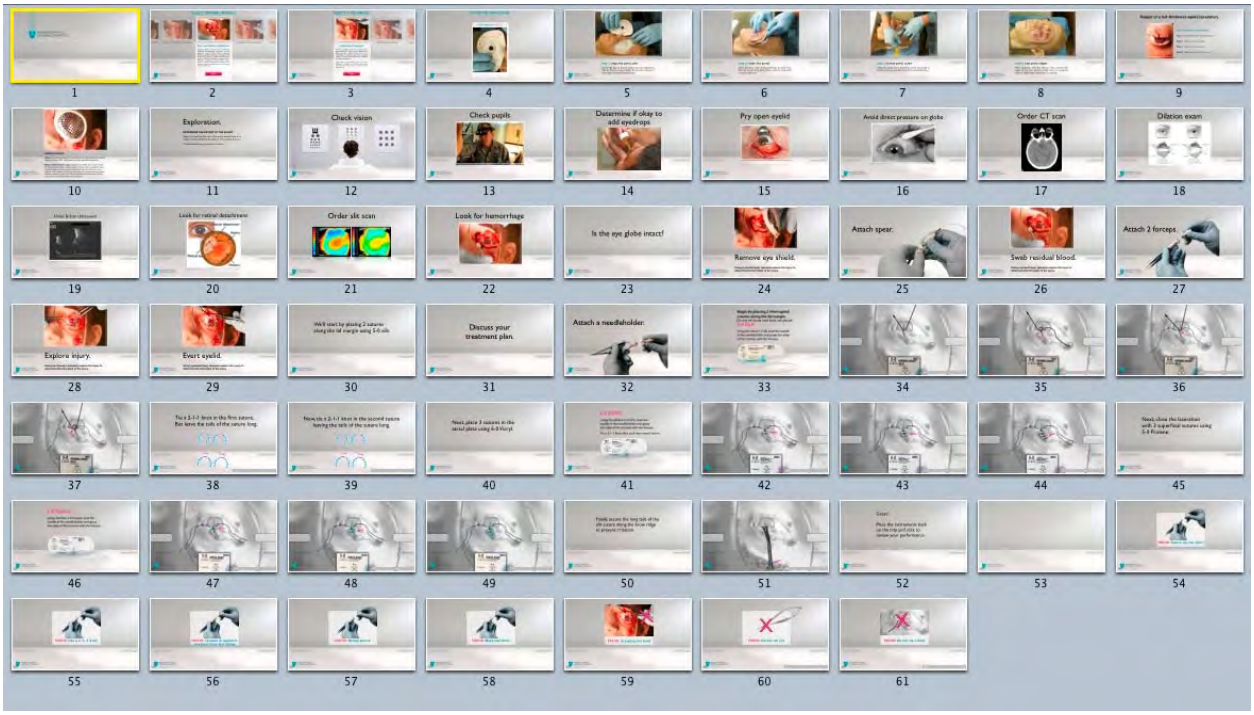

Figure 60: full sequence of available content and sequential guidance slides for lid laceration scenario.

Content, such as that pictured below, for steps that would typically be involved in patient prep and early diagnosis are currently set to "hidden." There are currently 61 screens implemented in our eyelid laceration training scenario.

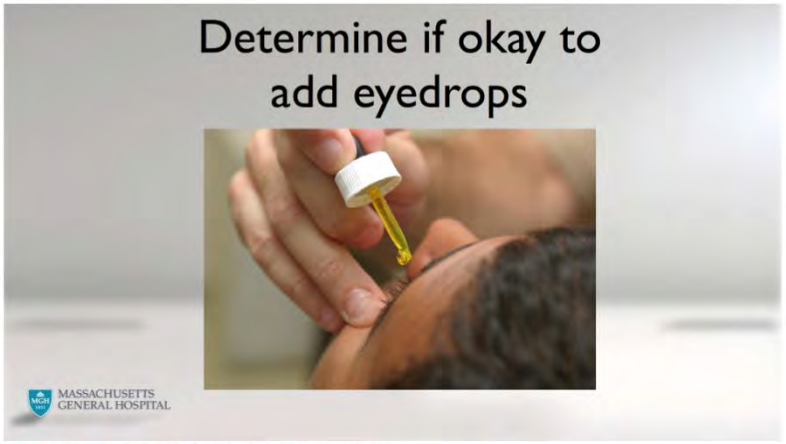

Figure 61: Pre-scenario preparation informational slide, available for full content use (hidden for 2013 Ocular Trauma Course use)

To better integrate with our underlying learning architecture, the eyelid laceration didactic content was organized as an individual module. There will be several modules developed for this simulator, providing an architecture that supports future content is important. The user begins by selecting the module

he/she wants to train on and clicks the *start* button in the center of the screen. Additional modules would be found by navigating to the left or right of the central area on the screen.

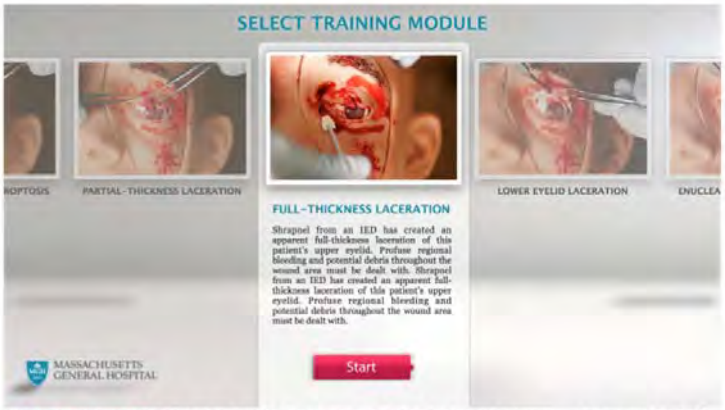

Figure 62: Scenario selection interface screen

Once a module is selected, the user is then presented with the ability to practice a specific *technique* to suturing the eyelid closed. We found that each surgeon and subject matter expert we consulted had strong opinions about the "right" way to provide guidance to the novice trainee. As they all referenced a "textbook" way of suturing as an underlying foundation to their personal approach, we began by implementing that basic version.

Figure 63: Selection among different techniques for given procedure

Our design allows a novice to learn the fundamental manner of suturing a laceration to the upper eyelid. Once completed, the user is then able to practice the individual techniques perfected by different surgeons. As they progress through the scenario, video and audio commentary accompany a custom-tailored set of didactic content in the interface to illustrate to the novice where they are deviating from the textbook procedure and why.

2.3.8. “Month 11” - Completion of prototype stand-alone ocular and craniofacial trauma training module, control software supporting sensing and response functionality.

This phase remains in progress. Description of progress towards completion are reported primarily in 2.3.4, the middle sections of 2.3.5 and 2.3.7a and 2.3.7c. Additional trauma module scenarios and content are slated for inclusion in the overall system.

2.3.9. “Month 12” - Testing of fit, function of sensors, actuators, replaceable components.

Air muscle and neck motion testing

Following early experiments to characterize our air muscle designs, described above, during Q5, we completed the test rig to allow testing of motion in all directions and reevaluate the capabilities of the new muscles (Figure 64). This system appears to be sufficient to generate neck motions that would be used in the mannequin-integrated version of the head (Phase III) to simulate a struggling/gagging casualty, a feature that does not appear to be present in the commercial market.

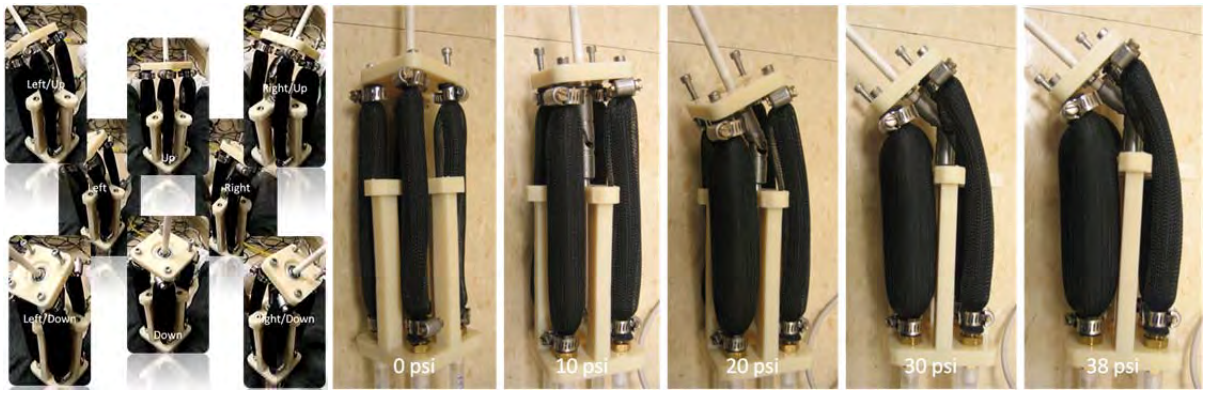

Figure 64: Motion control of neck using combinations of single or adjacent air muscles. Activation of single air muscle to illustrate range of motion. Base of "neck" at the bottom, "head" would be at the top.

Q6 and Q7 saw a hiatus in the neck development work, with changes in personnel,

In Q8 we continued this work in designing a more anatomically correct neck structure that integrates the neck pitching motions with head yaw. The mannequin-integrated version of the system will have the active motions, while the stand-alone version may make use of similar linkages to allow the surgeon to passively move the head with the same, normal range of neck motion, but without the actuation

components, thereby minimizing metallic elements that may distort the surgical instrument tracking system.

Using the anatomical models that were segmented during Year 1 and concepts developed during our earlier COMETS autonomous casualty simulation mannequin project, we created a flexible neck structure using a series of vertebral bodies and disks, each of which accommodates a fraction of the full flexing range of motion of the human neck.

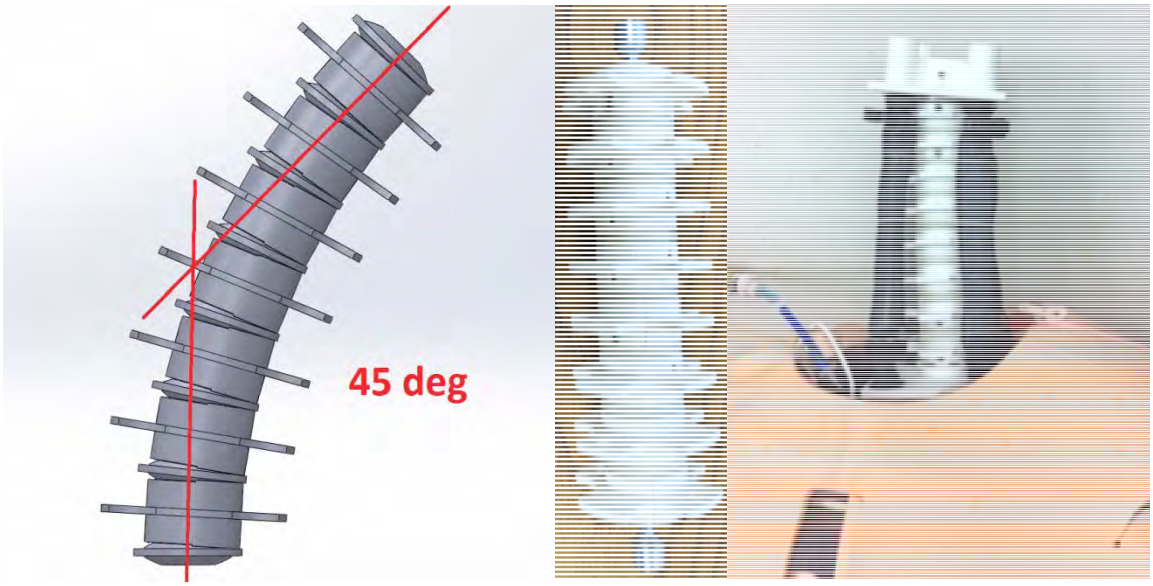

Figure 65: Anatomically inspired neck structure CAD model, physical implementation, and mounting to trauma mannequin.

The vertebral bodies have flanges extending away from their cores that mate with the McKibben muscles, so that they rotate with respect to each other when the head turns. A central flexible transmission shaft provides tensile strength and links the base of the neck to a head rotation motor that will be mounted in the head. Human neck range of motion is different in flexion/extension and lateral abduction, so the vertebral bodies are designed such that their surface contours allow for more motion before one body collides with the next at the front and back of the body than the left/right direction.

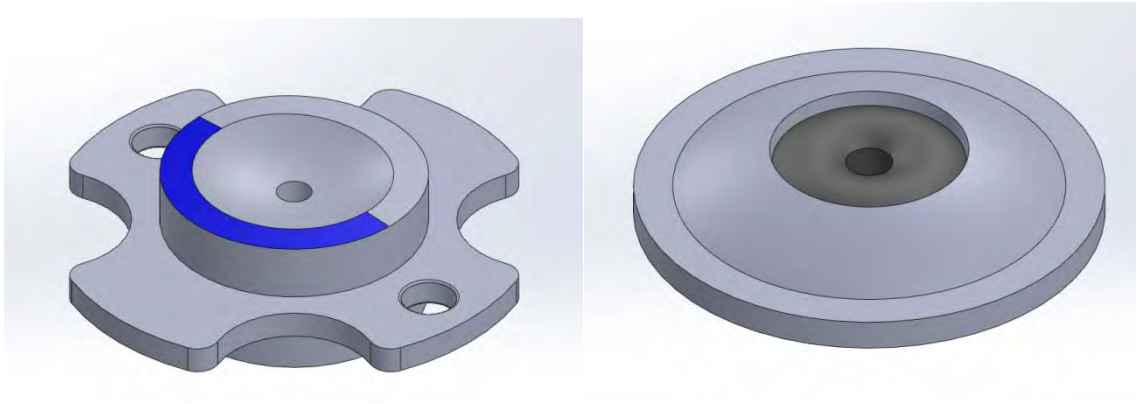

Figure 66: Vertebral body and disk designs

In the course of designing the neck mechanism, we reviewed the McKibben muscle design. The earlier work and inquiry showed that sparse mesh permits larger overall deformation. Thinner bladder walls, for a given material stiffness allow for greater deformation for a given supply pressure, as does a softer material for a given thickness. We identified both thinner wall silicone tubing and lower durometer rubing and redesigned the muscles to accommodate the new material. In addition, we found that the original tube fittings used as attachment points, which were smaller in diameter than the silicone and mesh tubing diameters resulted in pinching at the muscle ends, reducing the available amount of muscle contraction. Related to that, standard hose clamps that had been used were prone to pinch and puncture the silicone tubing walls. We replaced the fittings and hose clamps with larger diameter fittings and plastic snap-grip hose clamps without the hard, sharp edges.

With these design changes, we reexamined McKibben muscle performance, comparing the thin and two grades of soft rubber to determine the best available of materials sourced from industrial supply houses. The thin wall silicone was found to have the best performance of the materials tested.

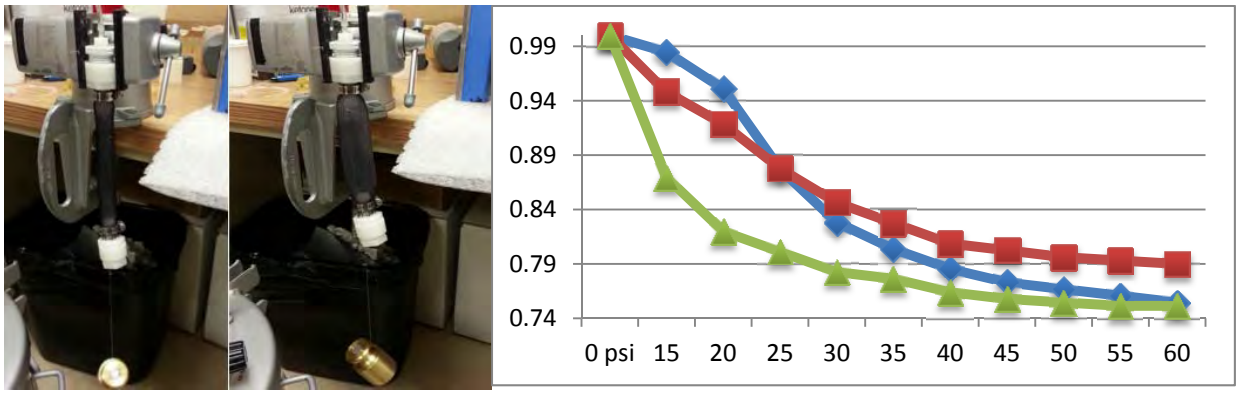

Figure 67: Retesting McKibben muscles with new materials, fittings. 500g load results shown: relative contraction for black latex (blue), amber latex (red) and thin wall silicone tubing (green)

A mating platform (described below) was designed to attach the neck design to the Laerdal SimMan Essential mannequin that we acquired in Q6. Using the pneumatic control system described above, we tested the range of neck motion. While the neck assembly is capable of the full human range of motion, when coupled to the air muscles, the available contraction appears to reduce the actual range delivered. In addition while the neck flexes quite far when the muscles contract, the platform shown (representing the mounting structure of the skull) may pitch by a lesser amount. Thus, at this stage, the mannequin will move less under its own control than can be generated by manual manipulation of the head/neck by a trainee. As we progress, we will endeavor to increase the controllable motion, however for the purposes of creating a system that can present autonomous motion that will indicate consciousness and present a simulation of a casualty resisting treatment (e.g. intubation/cric), this system will satisfy the basic goals.

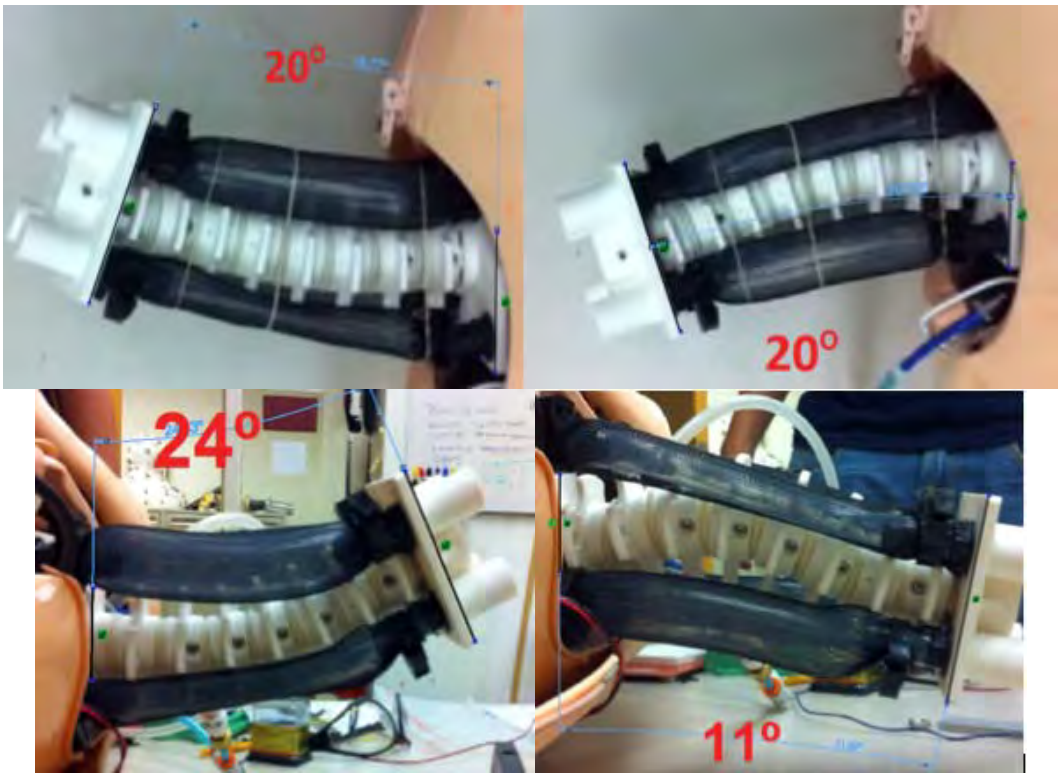

Figure 68:Initial range of motion of neck actuation system

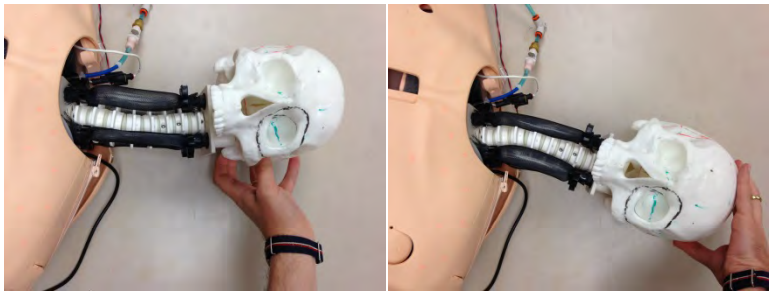

Figure 69: Manual manipulation of neck with attached skull model

Blink actuation testing

In Q7, much progress was made on the blinking mechanism. Based on developments described above, a prototype blinking portal was created which demonstrated an effective solution using embedded nylon string in the tarsal plate which can then be actuated by a servo. The string can be physically attached to the substrate in future iterations. This solution is consistent with the earlier developments of the servo-driven blink mechanism described in previous reports.

Changes to the portal were also necessary and consisted of incising relief flaps into the silicone. These flaps allow the silicone to bend more freely and control the way in which it deforms. In production, these flaps will be incorporated into the mold design. This feature addresses one of Dr. Mazzoli's principal suggestions regarding the eyelids, namely that redundant tissue should be present, permitting more realistic manipulation and proper creasing when the eyelid blinks.

Figure 70: Servo control of module eyelid blinking

2.3.10. "Month 14" - Design of modifications to trauma mannequin for integration of ocular and craniofacial simulator structure module.

During Q5 we made a final inquiry with CAE Healthcare regarding their Caesar mannequin, which previously was not expected to be available for purchase during our timeline. At the MHSRS 2012 conference, one of the mannequins was on display and the sales staff conveyed that they were available for distribution. Examination of the system, however, suggests that integration of a new head onto the mannequin would be more difficult than the options we had been examining with Laerdal. In addition, the Laerdal system that has sufficient capabilities for our purposes costs approximately half as much as Caesar, and further, the programming interface mentioned in Year 1 reports was not available for Caesar. As a result, we submitted a purchase requisition for a Laerdal SimMan Essential, which arrived during Q6.

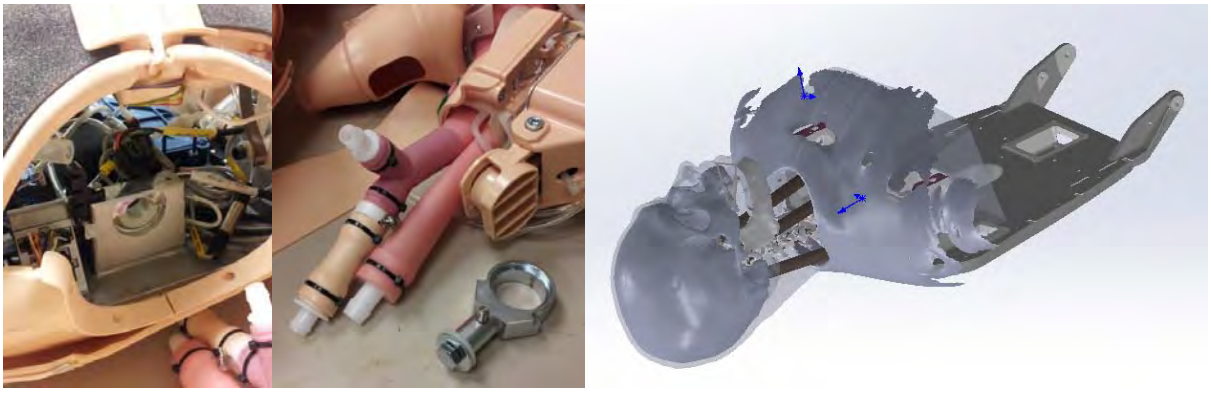

Figure 71: Disassembly and examination of Laerdal SimMan Essential mannequin in support of designing interface components to mate the new head/neck to the commercial body. Aligned CAD models in use for design of attachments between new head/neck and stock mannequin.

In Q6, the early work involved opening the mannequin to identify power and air pressure supplies, test its normal functionality under control of the Laerdal software, and begin to look into the SDK available for programming the mannequin beyond the compiled software provided. This lead to a series of technical queries that were provided to Laerdal.

Following our discussions with Laerdal, they provided us with limited technical details of the mannequin's structure, pneumatic supply and electrical and communications capabilities.

We combined the CAD models of the main internal structural plate from Laerdal with a 3D laser scan of the outer surfaces of the mannequin shoulders, using a long focal distance photo of the mannequin to aid in aligning the head/neck anatomy with the original mannequin head. This is serving as the basis for our structural design of the connection and mounting of our head to the mannequin's body.

As described earlier, we have begun to use the mannequin's air and power supply to drive the mechanisms for the head and neck. Immediately inside the mannequin's left shoulder are a series of electrical connectors, one of which is dedicated for head control. It includes terminals for 12V supply and a serial communications port that commands the mannequin's normal head. We have added our own connector in place of the original to access power and detect the pulse-control signals of the mannequin, so that our later hemorrhage system can be synchronized with the mannequin's pulse.

The 12V power is now supplying the Arduino Mega that was mentioned earlier and the series of 8 latching valves. As described earlier in this report, in addition to the control of the valves, the Arduino's software has been upgraded to control of up to 12 servos (8 are currently designed into the blinking/eye motion mechanism), two electronically controlled pressure regulators, up to 10 PWM-controlled devices (e.g. fluid or air pumps) or other digitally controlled devices (e.g. additional valves for hemorrhage), up to two stepper motors (possible for jaw control, head rotation, measurement of 16 analog sensors.

The pneumatic supply provides air pressure that varies from a peak of approximately 1 atmosphere and falls by approximately 25% before the mannequin's compressor turns on to restore pressure. This pressure drop is related to the mannequin's own breathing mechanism, which consumes air during each breath (small internal bladders push the main chest plate outwards), allowing the system pressure to fall since there is no regulated internal reservoir.

Our testing of the neck mechanism under this air supply shows that with the fall of system pressure, actuated air muscles lose force cyclically as the mannequin compressor cycles, with slowly changing neck position as pressure falls, and a return to the set position when the compressor runs. We are evaluating whether to add a separate reservoir that maintains the neck's position, or whether this motion provides the appearance of random motion beyond the deliberate actions controlled by our valving system.

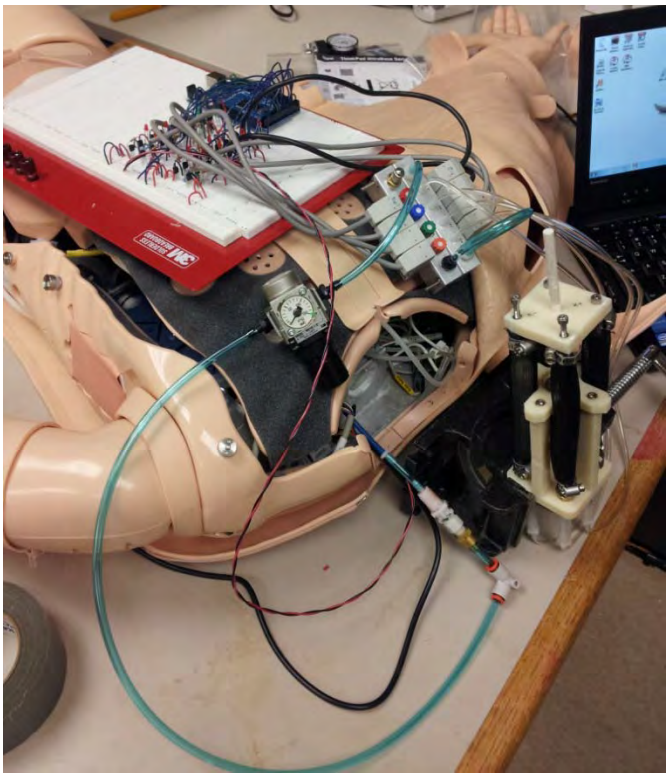

Figure 72: Air muscle system integrated with mannequin air and power supply. Blue tubing is connected in place of stock head air connector, twisted pair (black/red) wires supply mannequin power to the solenoid valve control circuitry and the Arduino Mega microcontroller.

During Q7, we isolated one of the problems that appeared during discrete component testing: while the air muscle valves are specified for use with 12V control signals, and the mannequin's supply voltage is also 12V, the transistors that switch the valves on and off have their own voltage drops in series with the valves. As a result, the voltage available to the valves is reduced below 12V, by an amount that makes valve activation unreliable. Two solutions were identified as of the preparation of the previous technical report: replace the 12V valves with their 6V equivalents, or use a voltage converter which boosts the 12V supply up to 15V (at the cost of drawing more current from the batteries), so after the transistor voltage drop, the valves still have enough driving force to reliably activate. A suitable voltage converter was ordered, received and tested to confirm that it functioned as planned. The code modification to properly sequence high current-draw components such as the valves is in progress.

During Q8 in conjunction with the neck mechanism developments described above, we used the CAD models provided by Laerdal for the main frame of the mannequin to create a mounting frame that mates the neck to the mannequin main body. The attached neck is shown in figures earlier in this section.

2.3.11. "Month 16" - Revision of physiology model software.

This work began substantially during Q7. In the first two months of the quarter, we began to examine the Laerdal SDK in detail, which provides a programming interface to the mannequin's control software, starting with familiarization with the programming language (C#) and with the layout of the VS (Visual Studio) C# project. To avoid potentially damaging the mannequin, when necessary we are doing preliminary testing of code using the Laerdal virtual mannequin system, which presents a system that responds to code written using the SDK the same way the real SimMan would.

The initial focus has been the LaerdalSimulatorAPI.dll dynamically linked library. The goal of the work was to find out a proper way to use the functions and methods provided by the dynamic library, in order to use them in a new C++ application. As the source code and documentation of the DLL is not provided, extrapolation of the content of the DLL is necessary. To help with that we used the "Object Browser" VS functionality and the free .NET decompiler and assembly browser "JetBrains dotPeek 1.0" [1].

Early approaches aimed at minimizing the number of additional files needed and retaining as much simplicity as possible in converting the functionality available in the SDK, written in C#, to functions compatible with our simulator, written in C++ were unsuccessful. A subsequent approach treating each component of the C# SDK separately, creating a library of files to form a bridge between the two languages was attempted by one of our interns next.

Developing the Wrapper for LaerdalSimulator.dll

The DLL wrapper works as a bridge, linking the C# DLL with the C++ client application. In order to create the linking, every member (classes, delegates, interfaces and enums) of the C# DLL, have to be re-declared inside the wrapper.

[1] Download and documentation available at www.jetbrains.com/decompiler

To create the wrapper we used an approach based on creating a different C++ file for every class implemented in the original DLL, and another single C++ file which contains enumerators and interface classes . Because of that, the wrapper project consists in the following files:

- **ExceptionData_Wrapper.h**, which contains the declaration of the class ExceptionData_Wrapper and its methods/constructors/destructors
- **ExceptionData_Wrapper.cpp** which contains the implementation of the methods of the class ExceptionData_Wrapper
- **ManikinException_Wrapper.h** which contains the declaration of the class ManikinException_Wrapper and its methods/constructors/destructors
- **ManikinException_Wrapper.cpp** which contains the implementation of the methods of the class ManikinException_Wrapper
- **ManikinFactory_Wrapper.h** which contains the declaration of the class ManikinFactory_Wrapper and its methods/constructors/destructors
- **ManikinFactory_Wrapper.cpp** which contains the implementation of the methods of the class ManikinFactory_Wrapper
- **LaerdalSimulatorAPI_Wrapper.h** which contains the declaration of interface classes, delegates and enumerators.
- **LaerdalSimulatorAPI_Wrapper.cpp** which contains the declaration of the enums (*as they are declare already in the .h file maybe I would delete them from here*) and would contain (*still to be done*) the implementation for some get/set methods for the interfaces.
- **LaerdalSimulatorAPI.h** header file of the original DLL created by me (*need some changes)*.

To test the wrapper our CS intern created a small Dialog application that shows the client a window and performs a series of functions based on which dialog button is pressed.

The first test performed was on the class ExceptionData_Wrapper. It contains a series of properties (data) that can be written and read. The test was very simple and did not need require a link to the virtual mannequin. The testing procedure was basically made of the following steps:

- calling the set method of the property (the one declare inside the wrapper). This is linked to the set method of the C# DLL, so whenever a new value is passed to the wrapper set function, the same value would be passed to the property of the LaerdalSimulator.dll.
- calling the get method declare inside the wrapper. Because of the linkage, this would go reading the value of the property contained in the C# DLL
- if the two value are the same, the linkage is verified

The test has demonstrated that a link was built, a first step towards establishing communication between our application and the mannequin.

Work on this element remained static during Q8 with a shift in emphasis towards assigning analysis of the USUHS data to the CS intern. It will continue during the extension period in Year 3.

2.3.12. “Month 18” –

2.3.12.a. Completion of prototype integrated ocular and craniofacial trauma system with mannequin.

Efforts towards this milestone has been commenced, as described above.

2.3.12.b. Completion of augmented reality system supporting stand-alone simulator.

Efforts towards this milestone has been commenced, as described above.

2.3.13. “Month 20” - User testing of combined system.

Efforts towards this milestone has not been commenced at this time

2.3.14. “Month 23” - Completion of revisions based on user testing.

Efforts towards this milestone has not been commenced at this time

2.3.15. “Month 24” - Final report submission.

Efforts towards this milestone has not been commenced at this time

3. Key Research Accomplishments

- Conversion of proof-of-principle demo system to final standalone eye trauma simulator
    - Design and fabrication of final standalone simulator main structure, including Kinect, projector, webcam and magnetic position tracker integration. Only minor revisions are anticipated
    - Redesign of surgical instrument connector and storage rack based on lessons learned in 2012 USUHS trials; improved robustness, intuitive usage, safer instrument storage (pointing away from user)
    - Addition of force sensors to needle holders and scissors to distinguish closure on tissue, needle, suture, etc. and algorithms for forceps, scissors and needle holders to distinguish contact between hard and soft tissues/objects
    - Upgrade and expansion of data acquisition and global scoring system to include video capture synchronized with data acquisition, tools for review and annotation of data sets, substantial progress in gesture recognition and state machine development
    - Creation of scenario content and integration with simulation elements of data acquisition architecture, creation of content frame structure allowing branching paths through scenario
    - Creation of augmented reality stereomicroscope hardware with sensing of microscope position relative to anatomical structures and zoom level sensing, creation of software libraries to generate graphical overlays combined with microscope views of anatomy
    - Testing of Leap Motion and Polhemus sensing systems for suitability of use with simulator system
- Development of improved anatomical models and sensing actuation systems for standalone and mannequin-integrated simulator components
    - Design and fabrication of eye motion systems with pitch/pan, proptosis and blinking actuation
    - Transition of anatomical designs from life-cast/molded version towards CT-derived skeletal and soft tissue structures, inclusion of laceration feature into CAD models
    - Creation of unified tarsal plate/ligament structures for improved realism, addition of vessels and canaliculi into eyelid models, sensing wires into canthal ligaments for detection of cantholysis
    - Initial work to create conjunctiva structure linking eyelid and globe models
- Integration of head/neck structures with commercial mannequin system
    - Acquired Laerdal SimMan Essential mannequin, access to Laerdal programming SDK, CAD models of key components of mannequin for physical mounting, details on electrical, data and pneumatic systems of mannequin
    - Designed & fabricated mounting structure for neck
    - Linked mannequin DC power supply to microcontroller and solenoid driver circuitry
    - Linked mannequin pneumatic supply to neck motion solenoid valve and air muscle systems
- Demonstration/data collection exercise at 2013 USUHS Ocular Trauma course

- Extension of human subjects research protocol
- Collection of 20 data sets for lid laceration repair from 12 attendings, 10 residents
- Collection of survey data for feedback on simulator, results showing areas for improvement of physical structure, anatomical models and presentation of content

4. Reportable Outcomes

Conference papers and oral presentations:

- Ottensmeyer MP. Ocular Trauma Training Simulator: Work in progress – system, gesture tracking, user trial. Oral presentation, MMVR 2013, San Diego, CA, 21 Feb 2013
- Ottensmeyer MP, De Novi G, Bardsley RS, Shah R, Moore JC, Ahn B. Ocular Trauma Training Simulator: System Description and Initial User Trials. Syllabus abstract, MMVR 2013, San Diego, CA, 21 Feb 2013

Conference & workshop posters:

- Ottensmeyer MP, De Novi G, Ahn B, Bardsley RS, Shah R, Munteanu E, Iorino S, Dawson SL. Development of an Ocular-Facial Trauma Treatment Training Simulator. Poster presentation, MHSRS 2012, Ft. Lauderdale, FL, 13-16 Aug 2012
- Ahn B, Moore JC, Zivieri S, De Novi G, Bardsley RS, Ottensmeyer MP. Ocular and Craniofacial Trauma Simulator Development: AR Surgical Microscope, CT-Derviced Physical Anatomy, Sensor & Actuator Systems. MGH Scientific Advisory Council Poster Session, Boston, MA, 20-21 March 2013
- De Novi G, Bardsley RS, Festi M, Ottensmeyer MP. Ocular and Craniofacial Trauma Simulator: Event Driven Gesture Recognition, Contextual Feedback Interface and User Trial Result. MGH Scientific Advisory Council Poster Session, Boston, MA, 20-21 March 2013

Invited presentations:

- Ottensmeyer MP. Eye trauma simulation: review and novel system development. 5th Military Vision Symposium on Ocular and Vision Injury, Boston, MA, 18 Sept 2012
- Ottensmeyer MP. Simulation – grand concepts & eye trauma example. Roadmap for Simulation in Eye Care Workshop, Boston, MA, 17-19 Oct 2012
- Ottensmeyer MP, De Novi G, Bardsley RS. Ocular and Craniofacial Trauma Treatment Training System: Program overview & work in progress. TATRC booth demo and poster, MMVR 2013, San Diego, CA, 21 Feb 2013
- Ottensmeyer MP. Development of an Ocular and Craniofacial Trauma Treatment Training System. JPC-1/TATRC CCTI In-Progress Review presentation, Ft. Detrick MD, 19 June 2013

Conference extended abstracts submitted for review

- Ottensmeyer MP. Development of an Ocular-Facial Trauma Treatment Training Simulator. MHSRS 2013, Ft. Lauderdale, FL, 11-15 Aug 2013
- De Novi G, Loan G, Festi M, Ottensmeyer MP. Events Driven Surgical Gesture Recognition Validation on Eyelid Laceration Surgery Simulation. IMSH 2014, San Francisco, CA, 25-29 January 2014
- Ottensmeyer MP, De Novi G. Conversion of stereo surgical microscope for augmented reality application in an eye trauma simulator. MMVR 2014, Manhattan Beach, CA, 19-22 Feb 2014

Graduate thesis manuscripts:

- Master's thesis, Stefano Iorino, Politecnico De Milano, Italy: "TrackSim: UN SIMULATORE DI INTERVENTI CHIRURGICI PER TRAUMI OCULARI E CRANIOFACCIALI" ("TrackSim: A simulator for eye trauma and craniofacial surgery")

Training experiences:

- Internship: Simone Zivieri, master's candidate, mechanical engineering, University of Modena and Reggio Emilia. 6-month work term learning mechanical design, CAD, control of servomechanisms, calibrating elastic response of transmission; working on the eye motion mechatronics. Graduated April 2013, cum laude.
- Internship: Martina Festi, master's candidate, computer science, University of Bologna, learning to use C# libraries, bridging methods between C# and C++, as applied to interfacing simulator to Laerdal mannequin SDK, assembly language coding as applied to simulator data acquisition microcontroller. Graduation expected towards end of 2013.
- Internship: Federico Pifferi, master's candidate, mechanical engineering, University of Modena and Regio Emilia, 6-month work term in progress, learning CAD, mechanical design, control of pneumatic actuators, design of pneumatic actuators. Working on design of animatronic neck of mannequin.
- Post-doctoral fellowship completed, promoted to Assistant in Research (MGH)/Instructor (Harvard Medical School): Gianluca De Novi, Ph.D. (U. Bologna) Robotics. Developing software architecture and implementation of simulator interface.
- Post-doctoral fellowship completed, accepted employment in industry: Bummo Ahn, Ph.D. (KAIST, Korea) Mechanical engineering. Developing mechatronic systems for simulator, instrument motion sensing, intervention sensing.
- Practical training in manufacturing by laser cutting: Mark P. Ottensmeyer, Ph.D., Ryan Bardsley.

Funding applications

- Proposal submitted: Open Architecture Virtual Autopsy/Anatomy Table (VAT), Gianluca de Novi, Ph.D., P.I. CIMIT Boston Simulation Consortium Innovation Award competition. Based on gesture recognition concept and graphical rendering techniques developed for and in parallel with craniofacial simulator
- Proposal submitted: Eye/Face Trauma Simulation Enhancements, Mark P. Ottensmeyer, Ph.D., P.I. Subaward proposal for CIMIT application to Joint Warfighter Medical Research Program, extending work previously supported by CIMIT. Proposal to develop mid-facial fracture module, adapt simulator to be compatible with CIMIT modular mannequin system under development.
- Proposal in preparation: Advanced Modular Manikin solicitation W81XWH-13-R-0032. James A. Gordon, M.D., P.I. Program to develop platform technology for a modular manikin systems, adapting ocular-craniofacial simulator for use as one possible head module for this system.

Invention disclosures and patent applications

- Invention disclosure MGH 22084: Includes simulator technological elements:
    - Augmented Reality Stereo Surgical Microscope
    - Animatronic eye motion mechanism for eye trauma simulator with pitch/yaw/blink/proptosis motions, replaceable eye lid and eye globe modules, treatment sensing and physiological response
    - Sensors for detection of incision creation and incision path for medical simulation
- Invention disclosure MGH 22275: "Training Simulator for Ocular Trauma and Other Domains Using Event-based Surgical Gesture Detection and Multiple Instrument and Hand Motion Tracking Systems", which described additional content presentation and use of reflected iR imaging using a Kinect-type device for hand tracking
- United States Provisional Patent Application, filed 02/20/2013, Serial Number 61/766,987, covering MGH 22084

5. Conclusion

This report presents the progress made in the second year of our program to create a novel eye and face trauma simulator for use by trainee surgeons and those new or returning to eye trauma practice as well as first responders facing eye trauma and likely coincident facial trauma in the field.

Based on lessons learned and user testing/demonstrations of Year 1, we created what is essentially the completed version of the standalone simulator platform for surgeons and surgical trainees. As a result of the first year's demonstration, we were invited to return to the 2013 USUHS Ocular Trauma course to serve as a demonstration of simulation-based training for eye trauma in parallel with our own testing and data collection needs. At this event, we were able to include improved content that was synchronized with the sequence of actions of the trainees. Based on this event, an invitation to participate again in 2014 was issued by the USUHS course director. Only minor alterations are expected to be made on the system hardware, and advances in the simulation, data collection and analysis software are expected to make the system more suitable as a teaching device (and potential commercial product).

Substantial work was performed towards the final goal of adapting the head and neck of the mannequin for use as a replacement for a commercial mannequin's head. We acquired a Laerdal SimMan Essential mannequin as a platform for modification, began the process of creating software links between our architecture and the mannequin's controls, developed prototype systems for integrating our actuators and sensors with the power and data systems of the mannequin, and fabricated a mounting structure to attach the work-in-progress neck to the mannequin's internal frame.

Improvements to the anatomical realism of the system, from the ligaments and tissues of the eyes to animatronic systems to animate the eyes to the inclusion of vessels and ducts in the eyelids have been accomplished. These will serve as the basis for the remaining eye trauma modules to be completed during Year 3.

The work has been presented to multiple experts, both our own SMEs and unrelated experts in eye surgery, and response has been positive. We anticipate that the future modules and improvements will continue to meet with approval. For the eye trauma elements contacts with some of these experts is likely to lead to additional opportunities for collecting user performance data to help develop the scoring and feedback system.

Implications of successful completion of this program lie in a number of directions.

The first is that a useful eye trauma training system will provide a new tool for teaching basic skills to young surgeons with limited trauma exposure. Such a tool will be versatile, in that the base platform will support multiple trauma scenarios, initially including simple and complex lid lacerations, lacerations and punctures of the anterior hemisphere of the globe, and retrobulbar hemorrhage. These will be more controllable, repeatable and predictable than the use of cadaver tissue or live animal materials for training.

The elements of the system that address the first responder will allow more comprehensive training scenarios beyond those available through current commercial mannequins, in which head and face trauma are represented typically by non-active, rubber masks or moulage placed on an otherwise healthy mannequin head/face. Realistic and responsive eye/face trauma will improve training by helping trainees to recognize that trauma is not limited to the extremities or torso of the casualty and remember to check for it in the field.

The tracking system and scoring methods that we are developing have application beyond eye trauma. The great majority of the research into measuring surgical performance produces global scores that may distinguish between expert and novice performance, but cannot guide improvement at the sub-task or gestural level – informing a trainee that they must increase overall speed or make their motions smaller is of limited utility, as it does not specify which elements of their performance is too slow and which are of acceptable speed, or where they need to make their motions more compact and efficient. We believe that the event-based gesture detection and tracking system will be suitable for quickly identifying where a trainee diverges in performance from that of an expert, and given a well-designed suite of tips and instructions based on experts' experience, can provide timely guidance to accelerate learning. This applies equally well to eye trauma as it would to many other types of surgery or tasks requiring manual dexterity together with cognitive skills required for a complex, multi-step process.